The Radio and Electronic Engineer

The University of Surrey's Satellite Project

A unique project is reaching its crucial stage at a British university: *UOSAT,* the educational satellite with facilities for radio amateurs and scientists which is being built in the Department of Electronic and Electrical Engineering at the University of Surrey, Guildford, is now at an advanced state of construction.

Due for launch by NASA during the summer, *UOSAT* possesses a number of important new features of special interest to school science groups and radio amateurs. It is the first satellite designed to transmit data, including pictures of the Earth's surface, in a form which can be readily displayed on a domestic television set. It will carry a voice synthesizer for 'speaking' (in English) information on telemetry, experimental data and spacecraft operations, and most standard amateur v.h.f. receivers will be able to listen in with a simple fixed aerial.

All previous radio amateur spacecraft launched either under the auspices of AMSAT, the Radio Amateur Satellite Corporation (the *OSCAR* series), or by the USSR (*RS 1* and *2*) have been primarily intended for relaying radio signals, thus increasing the v.h.f. and u.h.f. range of transmissions by radio amateurs. *UOSAT* has a different function: its purpose is to stimulate a greater practical interest in space science amongst schools, colleges and universities, to provide radio amateurs with a tool for studying the ionosphere through which their transmissions travel, and to establish an active body in the UK with the resources to contribute further to the amateur satellite programme.

In addition, the spacecraft carries a number of experiments intended for scientific research. These include beacons transmitting several different frequencies, two particle counters to provide information on solar activity and auroral events, and a magnetometer—identical to those used on the *Voyager* missions to Jupiter and Saturn—for measuring the Earth's magnetic field. These experiments will make possible a detailed study of how phenomena such as solar activity, affect the transmission of radio signals through the ionosphere.

UOSAT will be launched as a secondary pay load by a NASA Delta 2310 rocket from the Western Test Range at Vandenberg, California; the main pay load will be the NASA Solar Mesosphere Explorer (*SME*) spacecraft.
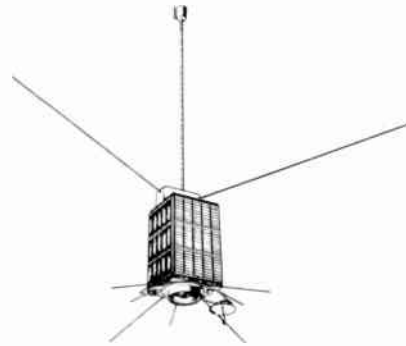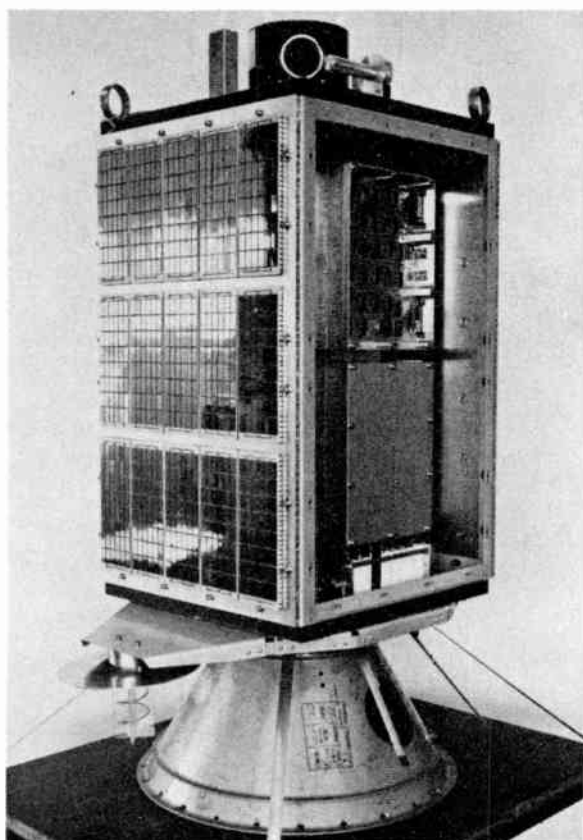

The launch, which is currently scheduled for September but may be advanced to late July, will place the spacecraft into a polar orbit with a period of 95 minutes, at a height of 530 km (about 330 miles). The expected life before re-entry is estimated at 4 to 5 years.

The spacecraft is controlled by a powerful on-board computer based around the RCA 1802 microprocessor. The computer's instructions will be loaded from the Surrey University Command Station, and can be changed during flight as desired.

One experiment of special interest to school and college science groups is an Earth-pointing camera, covering an area of the Earth's surface equivalent to most of England south of Newcastle, or the whole of Scotland. The image will be formed on a solid-state charge-coupled device and stored in the spacecraft computer until transmission to ground—a process taking 3 to 4 minutes. Unlike images from conventional weather satellites the picture will be transmitted in such a way that it may be readily received and stored by a simple receiver and can be displayed on any domestic television set. Experimental data in graphical form will also be available by the same link.

An electronic voice synthesizer, controlled by the on-board computer, will 'speak' details of telemetry, experimental data and spacecraft operations. Speech will be in English, and the vocabulary will be about 150 words. Transmissions will be on 145·825 MHz and any standard unmodified narrowband frequency modulation amateur receiver should be able to receive them by means of a small, fixed pair of crossed dipole aerials.

AMSAT Amateur scientific and experimental spacecraft (UOSAT) system diagram.

UOSAT is being built to a budget very different from that of the usual multimillion pound satellite. The primary sponsors of the project are the UK, USA and West German sections of AMSAT (Amateur Satellite Corporation); British Aerospace; British Telecom; Ferranti; MEL; Racal; and the Radio Society of Great Britain. Over twenty other companies have provided components, effort, test facilities and other support. Cash funds available amount to about £80,000 but the true cost is likely to be around £¼ million because of the gifts in kind and the loan of valuable facitities.

Any engineer with even a nodding acquaintance of space projects will probably view the *UOSAT* project with some incredulity, particularly when he learns that the full-time team of Project Manager Dr M. N. Sweeting numbers only four, while a further twenty engineers and scientists at the University and elsewhere contribute on a strictly 'part-time' basis, carrying responsibility for design or production of units in the spacecraft. But although this may seem on the face of things to be rather of the nature of 'cottage industry' space technology, the facts are very different. *UOSAT* has to meet the same stringent engineering criteria set by

NASA for a multimillion pound pay load: even though in some instances unorthodox components have been employed (often at a saving of thousands of pounds), their environmental testing (at British Aerospace's facility in Stevenage) has proved them to be adequate before the necessary permission for incorporation into the spacecraft.

In this era of financial cut-backs at universities, the construction of a spacecraft within a university department would have seemed completely impossible but Surrey have achieved it at an expenditure of nearly two orders of magnitude less than such projects usually cost. The emphasis of research and teaching within the Department does perhaps provide a clue to the initiatives and drive behind the project to date: it has closer ties with industry than are to be found in most university departments in this country and research and teaching projects have been and will continue to be linked with the satellite project. A successful launch and realization of the complex systems and experiments will surely boost the morale and prestige of the University of Surrey in particular and indeed, by example, that of university research generally.   F.W.S

SOME TECHNICAL DETAILS OF *UOSAT*

Power Systems

Four solar panels fabricated by Solarex (USA) will provide around 27 W each when illuminated. The total average power from the arrays, allowing for Sun angle and eclipse periods, will be around 17 W. The battery charge regulator regulates the solar array power to the 14V 6AH NiCd battery (90% efficiency) whilst the power conditioning module delivers regulated power supplies at +10V, −10V at an overall efficiency of around 87%. The average power thus available to the spacecraft electronics is around 11·5W.

In this view of the spacecraft structure, one of the solar cell panels has been removed to show four of sixteen boxes machined from solid aluminium; each box holds two printed circuit boards. The lid of one box is removed to show one board; the spacecraft contains about 400 integrated circuits.

Telecommand

Two modes of control over the spacecraft are available, with a command repertoire of 64 two-state commands:
(1) Direct real-time control of the spacecraft's functions by Ground Command Stations.
(2) Indirect, stored-program control executed by the on-board microcomputer according to a 'diary' loaded in advance from a Ground Command Station.

Any valid commands emanating from the Ground Stations will have over-riding precedence with any simultaneously issued by the on-board microcomputer. The telecommand uplink also carries a high data rate uplink to the on-board microcomputer for program loading.

Telemetry

To cater for a wide range of user Ground Station facilities, 60 analogue telemetry channels and 45 digital status points are available for transmission via the v.h.f. and u.h.f. Data Beacons in the following formats:

1200	baud ASCII	45·5 baud r.t.t.y. (Baudot)
600	"	"
300	"	10 or 20 words/min Morse code
110	"	"
75	"	synthesized voice

Any pair of the above formats can be available via the v.h.f. and u.h.f. Data Beacons simultaneously. The 1200 baud telemetry option also has channel dwell facility.

Data Beacons

Two v.h.f./u.h.f. beacons provide the primary engineering and experiment data links to the outside world and have been designed to provide a healthy satellite-to-ground transmission link to enable reliable and straightforward reception by the simplest of amateur ground stations. A standard unmodified n.b.f.m. amateur receiver and a small, fixed pair of crossed-dipoles should suffice for most orbit passes. The data sources available to these beacons are:

    Telemetry—ASCII—Baudot—Morse Code
    Spacecraft Computer—Primary Output Port
    Secondary Output Port—Speech Synthesizer
    Earth Imaging Experiment—Image Data

The General Data Beacon operates at 145·825 MHz with a power output of 450 mW and efficiency of 45%, while the Engineering Data Beacon operates on 435·025 MKz with a power output of 400 mW and an efficiency of 40%. Both use n.b.f.m./c.w. modulation and the data format is a.f.s.k. (n.b.f.m.)

Spacecraft Microcomputer

The powerful on-board computer is based around the RCA CDP 1802 microprocessor and has access to the spacecraft experiments, telemetry and command systems. These are: telemetry surveillance; command and status management; experiment data storage and processing; dissemination of orbital data, operating schedules and general news; and closed-loop attitude control using the magnetorquers. The computer has direct high-speed data links with the magnetometer and radiation experiments to allow rapid data acquisition yielding fine time-resolution data. The computer also has access to the Earth Imaging Experiment memory area thus allowing image processing.

The computer software is resident in dynamic r.a.m. loaded from ground via the telecommand link and can be modified or replaced during flight by a Ground Command Station in order to accommodate changes in the mission profile and to allow for the rectification of possible software or hardware failures.
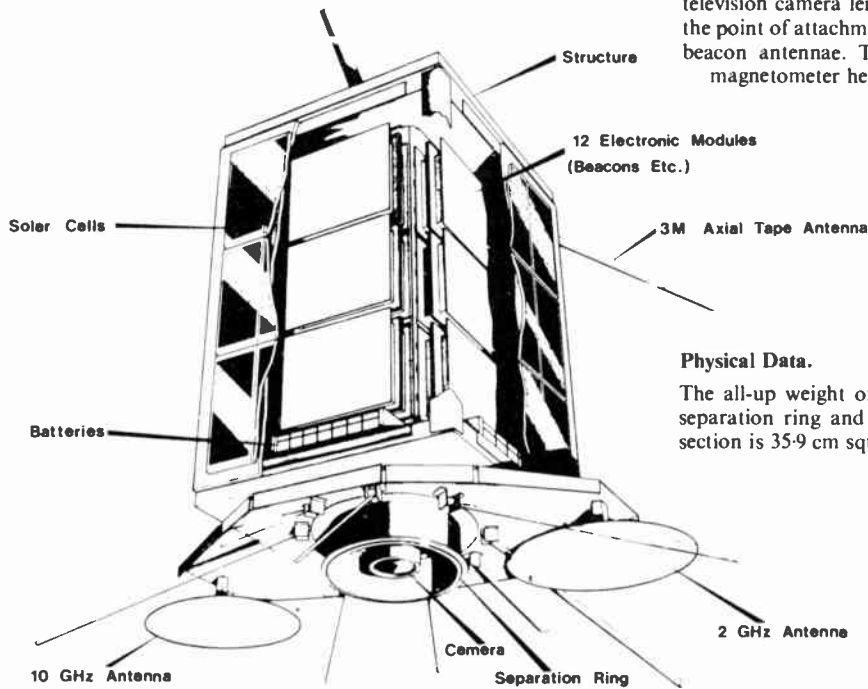
Propagation Studies Experiments

Phase-referenced beacons on 7·001, 14·001, 21·001 and 28·001 MHz will support a wide range of ionospheric experiments and observations, whilst two microwave beacons on 2·401 GHz and 10·470 GHz will encourage the study of s.h.f. propagation and the development of inexpensive microwave satellite ground stations.

The particle radiation counters (one detecting electrons of energies > 40 keV and the other detecting protons > 2 MeV) will provide real-time information on solar activity and auroral events. A three-axis, wide-range, flux-gate magnetometer will examine the fine structure of the Earth's magnetic field, any disturbances to it and their relationship to radio-wave propagation. The magnetometer is mounted at the end of a 15 m extended boom. The data from these experiments are routed to the spacecraft computer for detailed study and to the telemetry module for time-averaged, quick-look data, and subsequent transmission on the Data Beacons. The radiation experiments have been devised by the Appleton Laboratory and the magnetometer experiment by Dr M. Acunia of Goddard Space Center.

Education Experiments

An Earth-pointing, solid-state, charge-coupled-device, two-dimensional imaging array will provide land and sea image data for digital transmission via the General Data Beacon, using minimum-shift a.f.s.k.at 1200 bit/s line synchronous.

The image format is 256 × 256 pixels with 16 grey levels and is stored in an on-board 0·25 Mbit solid state memory. The camera optics are organized to cover a 500 km × 500 km area

Structure

12 Electronic Modules
(Beacons Etc.)

3M Axial Tape Antenna

Solar Cells

Batteries

10 GHz Antenna

Camera

Separation Ring

2 GHz Antenna

What the spacecraft will look like when in orbit. The down-pointing television camera lens is surrounded by the separation ring, which is the point of attachment to the launch rocket. Either side are two of the beacon antennae. The upper boom will be extended to place the magnetometer head about 15 m above the spacecraft structure.

Physical Data.

The all-up weight of the satellite is 47 kg; the height, including the separation ring and with upper boom stowed is 83·6 cm; the cross section is 35·9 cm square.

of the Earth's surface yielding a resolution of around 2 km. The response of the camera is optimized to enhance land features and land/sea boundaries. This experiment can also be used to display processed telemetry and experiment data in graphical form from the on-board computer. Circuits and full details for the necessary ground receiving and display equipment (using a domestic television receiver) will be published later this year, the component cost being estimated around £100.

A digitally synthesized speech experiment module under the control of the spacecraft computer will 'speak' telemetry, experiment data and spacecraft 'news' with a limited vocabulary for use with school demonstrations of space sciences. The 'speech' (in English) can be transmitted in n.b.f.m. on either of the Data Beacons.

Systems Experiments

Passive spacecraft stabilization employing gravity-gradient forces and active spacecraft attitude control using a two axis magnetorquer acting against the Earth's magnetic field will maintain the z-facet of the satellite aligned towards the centre of the Earth.

Letters to the Editor

From: E. Kentley, C. Eng., M.I.E.R.E.
   A. J. Rogers
   R. B. Mitson, C. Eng., M.I.E.R.E.
   D. King, C.Eng., M.I.E.E., M.I.E.R.E., M.I.P.M.

Oscillator Design

The letter from Mr B. Priestley in the February issue of *The Radio and Electronic Engineer* (p. 52) raises a number of important points.

The cases he quotes of improper oscillator design both happen to be quartz-crystal-controlled oscillators. Whilst the basic design of oscillator circuits is usually covered in courses in communications and electronics, the design of quartz-crystal-controlled oscillators is highly specialized and is usually dealt with in the simplest manner if indeed at all. This is recognized by the manufacturers of quartz crystal units who invariably offer an oscillator design advisory service to their customers. Despite this, examples of improper crystal oscillator circuit design do occur for a number of reasons.

The examples quoted by Mr Priestley are probably quite different from each other in terms of the original design faults causing the improper operation of the oscillator, but without further details it is impossible to comment specifically.

In the case of overtone crystal oscillators, oscillation at the required overtone will only occur if the conditions for oscillation are satisfied at that frequency. If conditions are more favourable at other frequencies, including the fundamental frequency or other overtones, then oscillation can and will occur at these frequencies.

In the case of microprocessor clock oscillators many poorly designed oscillators are coming into use, basically because of a lack of liaison between the microprocessor i.c manufacturer and the quartz crystal manufacturer. This problem has been dealt with in detail by Holmbeck* in a recent paper.

The microprocessor clock oscillator uses digital devices whilst the quartz crystal unit is an analogue device and it does appear that a new generation of digital circuit designers is with us who lack a basic understanding of analogue techniques.

Many quartz crystal units used in microprocessor applications are purchased in volume from low cost off-shore suppliers and in these cases the 'applications service' available from UK manufacturers is either totally absent or much reduced.

Most quartz crystal manufacturers offer guidance to users of their products. An international publication, I.E.C document 122–2, 'Guide to the use of quartz oscillator crystals' is available. This publication is now close to twenty years old and therefore technically obsolescent but a new edition is in a late stage of preparation and should be available in about a year's time.

I doubt if the problems mentioned in Mr Priestley's letter can be overcome by action at the university or college level but information and help is available at the industrial level if only the people involved can be persuaded to seek it.

E. KENTLEY

40 Cambridge Road
Waterbeach
Cambridge
5th March 1981

* Holmbeck, J. D. 'Frequency tolerance limitations with logic gate clock oscillators,' Proceedings, 31st Annual Symposium on Frequency Control, U.S. Army, Fort Monmouth, NJ, 1977 (Doc. AD A088221 NTIS)

Referring to Mr B. Priestley's letter in the February issue, I wholeheartedly endorse his view concerning operational failure of crystal oscillators due to inadequate design. However, it is important to realize that the application of quartz crystals is a very complex subject and it is recommended that users seek the advice of manufacturers of quartz crystals, in order to achieve adequate performance.

The reason for failure of the examples quoted is likely to be due to the designer of the oscillator circuit failing to appreciate some of the more difficult aspects of crystal parameters and their interface with semiconductors. This is particularly relevant when dealing with digital circuits where the specified parameters bear no relation to analogue oscillator circuits. Most of the published articles on crystal oscillators assume the conventional equivalent circuit of a series LCR network in parallel with self-capacitance, when in fact, due to the mechanical vibratory nature of the crystal, the actual circuit is far more complex. It is these additional complexities which gives rise to the problems referred to.

In specialized applications where a specific characteristic is vitally important (e.g. good short-term stability or low power consumption), the use of the same basic oscillator circuit is not advisable, and each requirement must be considered on its own merits. Quartz crystal manufacturers, of course, have the necessary skills to do this in cases where volume production will result.

In cases where the commercial aspects do not permit the quartz crystal manufacturers to offer anything more than a standard crystal, application notes for the common requirements are normally available. Should the requirement be for a specific 'one-off' requirement the design engineer must resort to purchasing a completed frequency source, often grossly overspecified but nevertheless more economic than designing his own oscillator circuit from first principles, especially when it fails to start, oscillates at random frequencies, and generally fails to perform as expected.

A. J. ROGERS
Engineering Manager

Cathodeon Crystals Limited,
Linton, Cambridge CB1 6JU
10th March 1981

Mr Priestley's letter about oscillator design in the February issue provided too much negative feedback to your readers. His so-called engineers were in fact biologists, striving to carry out their research work by making radio tags for attachment, in the main, to small animals. The constraints on these people are acute shortage of funds, lack of interest of British manufacturers, the need to meet stringent regulations, but perhaps the most critical is the tag specification in terms of size, weight and length of life which must be achieved. Just how difficult the latter problem is can be judged shortly when a resumé of progress in this field is published in *The Radio and Electronic Engineer*. One purpose of the meeting was to bring the biologists into contact with engineers who could explain the regulatory rules and the basis of good electronic design. There is already some evidence that the meeting was fruitful in this sense.

RON MITSON

Fisheries Laboratory
Lowestoft
Suffolk
18th March 1981

A New Service to Members

I write with regard to the article* entitled 'A New Service to Members' in which the impression is given that MSL Engineering will provide a unique career guidance and selection service. I am sure that the article has been written and published with naivety rather than an intent to mislead. There are many other points which should have been made, including the following:—

● MSL is just one of many competent recruitment agencies with good knowledge of the electronic engineering industry.
● Candidates with MSL would only be considered against the vacancies of those employers who happen to be clients of MSL—and not all companies are.
● Although there is no charge to the Institution or the candidate, there *is* a charge to the employer, usually between 10% and 20% of the offered annual starting salary. In the case where there are two identical acceptable candidates for one post, some employers will, inevitably, choose the one who did *not* come through an agency.
● Some employers do give extra credit to those candidates

---

* *The Radio and Electronic Engineer*, 51, No. 2. p. 52, February 1981.

who have sufficient initiative to contact a company directly rather than use an agent to act on their behalf.
● In seeking employment via agencies, there is some risk that the selection may be made initially on a series of set criteria. A direct approach to a company may well result in one of those criteria being over-ridden or indeed, in the candidate being offered an alternative post of which an agent may be unaware.

These are some of the issues involved from the candidate's point of view. From the Institution's standpoint, to advocate the use of agencies reduces the market of potential advertisers, the revenue from which ought not to be insignificant.

D. KING

8 Mayfield Close
Old Harlow
Essex CM17 0LH
26th February 1981

[Needless to say, there was no intention to mislead or to exaggerate the benefits of the new service. However Mr King's observations, writing as he does with some experience in the field of personnel management, will doubtless be helpful to any members or organizations contemplating making use of the MSL File or the services of any other agency—EDITOR.]

Human Factors of V.D.U.s

The possible health hazards associated with the operation of visual display units are reviewed in a recent research paper* published by the Health and Safety Executive. Its general conclusions are that although, for most people, v.d.u.s pose no risk to health, closer attention should be given to some aspects of their use if discomfort is to be avoided.

The study, undertaken by Colin Mackay, a senior psychologist with HSE's Employment Medical Advisory Service, is a contribution to the debate that has grown up with the widespread introduction of v.d.u.s into business and industry during the last decade. It presents a review of the scientific and medical studies on the subject and provides both background and recommendations. The views the paper contains are those of the author and not necessarily those of HSE.

Most concern, the paper says, has been expressed over direct effects of v.d.u. operations on the individual, particularly risks from radiation and the likelihood of the v.d.u. eliciting an epileptic attack. The paper concludes from surveys commissioned by HSE and from other investigations that the low levels of radiation emitted from v.d.u.s are far below the most stringent permissible for continuous occupational exposure. It also concludes that whilst v.d.u.s have the facility to induce seizures in sufferers from photosensitive epilepsy, the likelihood of an individual suffering a first attack while operating a v.d.u. is extremely remote. Potential operators who suffer from photosensitive epilepsy are, nevertheless, urged to seek expert medical advice before working with a v.d.u.

The paper explains that v.d.u. operators complain of a number of symptoms many of which are the result of visual fatigue ('eyestrain') and discomfort related to posture. These

indirect consequences of v.d.u. operation have occurred, it says, because of insufficient attention to ergonomic principles. Emphasis is placed in the paper upon the need to present a clear and stable image to the operator. Careful consideration should be given to the design of lighting in rooms in which v.d.u.s are sited. This applies both to the quantity and quality of the lighting, particularly the need to reduce reflections in the screen and off other equipment and furniture and direct glare from bright lights and windows. Attention to the operator's environment should also encompass the requirement for low levels of noise, and the need for comfortable levels of temperature and humidity.

The paper explains that the design of the workplace should take account both of the operator's comfort and the requirements of the task. Particular emphasis is placed on the use of adjustable seating, detachable keyboards and the provision of document holders. A conclusion of the paper is that while pre-employment screening of eyesight and subsequent re-testing of operators is unnecessary, some individuals may continue to experience visual fatigue even after attention to ergonomic considerations. These individuals should be referred to an ophthalmic optician for an eye examination.

Further scientific studies need to be undertaken on the question of fatigue and rest pauses before any firm guidance can be given, the paper says. It suggests that the most satisfactory length of pause can only be determined by considering the individual operator's job, but short, frequently occurring pauses would seem to be preferable to longer pauses taken occasionally.

Other problems associated with v.d.u. operation examined in the paper are those caused by the repetitive and routine nature of the work particularly when the operator has little control over its pace or feels that his performance is excessively controlled by the machine. These job characteristics should be minimized, it says. Participation of potential v.d.u. users during the planning stage will also aid in the successful introduction of a new system.

Members' Appointments

FELLOWSHIP OF ENGINEERING

At the Annual General Meeting of the Fellowship of Engineering held at St James's Palace on February 17th with HRH The Duke of Edinburgh, the Senior Fellow, in the chair, 58 new Fellows were elected and these included four members of the IERE:–

Francis Kenneth Chorley (Fellow 1979, Member 1956) Deputy Chairman and Managing Director, Plessey Electronic Systems. For his development work in the sonar field and his contributions to electronics in radar, avionics and communications.

Professor Jeffrey Hamilton Collins, B.Sc., M.Sc. (Fellow 1973) Professor of Electrical Engineering, Edinburgh University. For his wide ranging research contributions to electronics, particularly in spread spectrum communications, s.a.w. oscillators in mobile radio, and spectrum and cepstrum analysers.

Colin Crook (Member 1977) Managing Director, Rank Precision Industries. For his design of integrated circuits, particularly for his leadership in the development of v.l.s.i. microcomputers.

Thomas Bryce McCrirrick (Fellow 1962, Member 1954, Graduate 1953) Director of Engineering of The British Broadcasting Corporation. For his engineering achievements in broadcasting.

CORPORATE MEMBERS

Professor W. Gosling, D.Sc., B.Sc., ARCS (Fellow 1968) has been appointed Director of Technology with the Plessey Company. Professor Gosling was for six years at the University of Bath and before that he was Head of the School of Engineering at University College Swansea; he was recently awarded the degree of D.Sc. by the University of Bath. President of the Institution for 1979–80, he is now Acting President for the remainder of the year of office of the late Mr John Powell.

Colonel M. J. Hales (Fellow 1980, Member 1969) is now with the Ministry of Defence, leading the Saudi Arabian National Guard Communications Project Team at Riyadh. For the past four years he was General Staff Officer for Plans Division of the Combat Development Wing at the School of Signals, Blandford Camp.

Brigadier R. W. A. Lonsdale, C.B.E., B.Sc. (Fellow 1971, Member 1953) has recently taken up the appointment of Systems Quality Manager with the Plessey Company. He has been for the past six years Director, Quality Assurance (Technical) in the Procurement Executive of the Ministry of Defence. Brigadier Lonsdale who is a Vice President, is a former Chairman and member of the Institution's Membership Committee and he has recently succeeded the late Mr John Powell as the Institution's representative on the CEI Standing Committee for Internal Affairs.

Professor H. W. Shipton (Fellow 1963, Member 1949, Associate 1948) has moved to Washington University St Louis, Missouri, to become Professor of Biomedical Engineering and Director of the Interdepartmental Program in Biomedical Engineering. Since 1957 he has been at the University of Iowa, initially as head of the Department of Medical Electronics and more recently as Professor of Bioengineering and Director of Bioengineering Resources. Professor Shipton has contributed several papers to the Journal; these included a joint contribution with Dr Grey Walter on EEG Toposcopic Display when he was working at the Burden Neurological Institute, Bristol.

C. F. H. Teed, B.Sc. (Fellow 1971) has been appointed Marketing Director with the Plessey Defence Systems and is concerned with overseas sales of the *Ptarmigan* and *Wavell* battlefield trunk communications and data processing systems. He was previously for some ten years with Marconi Communication Systems, latterly as Director responsible for marketing overseas.

Lt Cdr S. H. Brooks, B.Sc. (Member 1979, Associate Member 1972) has been appointed to the staff of the Director General of Naval Aircraft at the Ministry of Defence following two years at RNAS Yeovilton.

Commodore W. J. Crossley, RAN (Member 1980) who was formerly Director General Naval Manpower with the Department of Defence (Navy Office) Canberra, has been appointed Chief Superintendent Technical of the Royal Australian Navy Support Command Sydney.

T. E. Downing (Member 1975, Graduate 1970) has taken up a new appointment as Field Manager of the Coast Radio Station Maintenance Unit for British Telecom International. He was formerly an Executive Engineer, planning international exchange switching and signalling systems.

P. Forestal (Member 1963) has been appointed General Manager of Bahrain International Communications for Cable and Wireless. His previous post was that of Divisional Manager International Engineering for the company in Hong Kong.

T. P. Grogan (Member 1970, Graduate 1964) is now Manufacturing Manager of P&B Metal Components, Whitstable. He was previously Production Manager with Allen-Bradley Electronics, Jarrow.

Sqn Ldr R. G. Hatcher RAF (Member 1973, Graduate 1967) has relinquished his post as OC Electrical Engineering Squadron at RAF Cottishall and is now at the Ministry of Defence (RAF) as Air Eng 12c.

S. Jugessur, M.Sc., D.Sc. (Member 1975), Head of the Physics and Electronic Engineering Division at the University of Mauritius since 1974, has been appointed to the Chair of Industrial Technology.

A. W. Jury (Member 1973, Graduate 1969) who has been with the Coal Research Establishment of the National Coal Board since 1967, is now Physicist (New Developments) in the Physics Branch.

K. R. Lowe, B.Sc. (Member 1979), formerly a Senior Design Engineer with Philips Croydon, has taken up an appointment with Electrohome Electronics in Ottawa as a Development Specialist in the Data Display Section, OEM Marketing.

F. J. McCarthy (Member 1979, Graduate 1967) has been appointed Supervising Engineer in the microprocessor applications and customer services section of the New Zealand Post Office's HQ in Wellington. Formerly with the British Post Office, he has since 1974 been an engineer on telephone and telex exchange installation in the Regional Engineer's Office in Wellington.

Cdr C. L. Salmon, O.B.E., M.Tech. (Member 1969, Graduate 1956) has retired from the Royal Navy and joined Y-ARD as a Senior Consultant at their recently opened Branch Office in Chippenham, Wilts. From 1975 until his retirement, Cdr Salmon was Project Manager of the Naval Weapons Department's Design to Life Cost Study which developed methods of reducing the total cost of ownership of DGW(N) equipments.

S. W. Soysa (Member 1974, Graduate 1969) who held the position of Manager, Pye Audio Plant No. 4 in Hamilton, New Zealand, has now taken up a post as Assistant Development Manager/Projects with Gallagher Electronics in Hamilton.

T. Vudali (Member 1974, Graduate 1972), for three years a Principal Scientist with the Allen Clark Research Centre at Caswell, has taken up a post as Electronics Engineer at the European Space Agency, ESTEC in the Space Communications Division in Noordwijk, The Netherlands.

NON-CORPORATE MEMBERS

A. M. M. Aabad, B.Sc. (Companion 1979) has been appointed Director of the Technical Centre of the Asian Broadcasting Union at Kuala Lumpur. He was previously Additional Chief Engineer of Radio Bangladesh.

G. D. Brown (Graduate 1970) who has been with Geophysical Service International since 1971, latterly as Boat Manager, has taken up a post in Singapore as South East Asia Marine Data Collection Manager for GSI.

Obituary

The Institution has learned with regret of the deaths of the following members.

Peter John Adams (Associate Member 1973, Associate 1970), of Stanmore, was killed in a motor accident on 21st March 1980, aged 47 years. Mr Adams was Sales Manager with Ronian Packaging of Bedford. He had previously been a Radio Officer in the Merchant Navy and had held Design Engineer appointments with Hilger and Watts and Racal-BCC. In 1970 he joined Hunting Engineering as Sales Engineer.

William James Battell, B.Sc. (Member 1966) died 18th October, aged 56.

Mr Battell graduated in physics from Imperial College, University of London in 1944, and for the next two years he was a Junior Scientific Officer at the Telecommunication Research Establishment, Malvern. He then spent a year at the Atomic Energy Research Establishment before moving for a short time to Standard Telecommunications Laboratories. In 1948 he went to Canada, working for five years with Atomic Energy of Canada as a Scientific Officer and for a further three years as a Senior Engineer with the Canadian Marconi Company.

In 1956 he returned to the United Kingdom and was appointed to the Leading Scientific Staff of the General Electric Company at the Applied Electronics Laboratories, Stanmore. For most of his subsequent career he was concerned with research and development of advanced communication systems.

Mr Battell contributed two papers to the Journal on Digital Data Links for Aircraft Communication, one of which gained him the Leslie McMichael Premium in 1965. He was a founder member of the Institution's Beds and Herts Section and had served on the local section committee since its formation in 1974.

Cecil Edward Bottle (Fellow 1941) died in July 1979, aged 84.

Following service with the Royal Navy, latterly as a wireless instructor, Mr Bottle joined the British Broadcasting Company (subsequently the British Broadcasting Corporation) in 1924 as a Senior Control Room Engineer at Savoy Hill. He continued with the BBC holding a variety of positions including Assistant Engineer-in-Charge at Broadcasting House. In 1946 he was appointed a M.B.E. and he retired from the Corporation in 1957. Mr Bottle served on the Institution's Membership Committee from 1942 until 1956, and he was a member of the General Council from 1946 to 1949.

Albert William Arthur Fletcher (Associate Member 1973, Associate 1962), of Leicester, died on 9th April 1980, aged 59. Following service in the Royal Navy during the war as a Petty Officer Telegraphist, Mr Fletcher worked for two years as an Instrument Mechanic at Royal Ordnance Depots. In 1947 he joined the British Thomson Houston Company in Leicester as a Test Engineer on radar equipment and in 1956 he moved to the English Electric Company at Whetstone as Electronics Engineer working on instrumentation, control and measurement equipment.

Herbert Albert Henry Griffiths (Fellow 1944) of Essendon, Victoria, died on 9th August 1980, aged 75 years. Born and educated in London, Mr Griffiths gained his early technical training with the General Electric Company as a draughtsman and he subsequently worked for Burndept Wireless and H. W. Sullivan on progressively more senior posts. From 1933–1935 he was a Test Gear Designer with the Plessey Company and from 1935–40 he was Chief Designer with Muirhead & Company. In 1943 he was appointed Chief Designer with Scientific Acoustics, with whom he remained until 1952 when he went to Australia and joined the research section of the Post Master General's Department in Melbourne, where he designed specialized testing equipment. He retired from the Post Master General's Department in 1969. Mr Griffiths served on the Institution's Membership Committee from 1944–46.

Hickson James Hoult (Associate Member 1973, Associate 1959) died at Lowestoft in July 1980, aged 55. Mr Hoult served in the Royal Air Force as a radio mechanic during the war, and on demobilization worked for Marconi's Wireless Telegraph Company as an instrument assembler and tester. In 1947 he joined the Ministry of Transport and Civil Aviation as a Telecommunications Technical Officer. In 1956 he entered technical education as an Assistant Lecturer at the College of Further Education Slough and subsequently with the Suffolk Education Authority.

James Joseph Hunt, M.Sc. (Member 1969, Graduate 1963) of Dublin died in June 1980, aged 41. Mr Hunt undertook a student apprenticeship with the Ministry of Aviation from 1957–63 and soon after completion of his training received an appointment with the Ministry of Technology as an Engineer III in the Electrical Inspection Directorate concerned with r.f. and microwave standards and calibration. During this period he attended the University of Aston and obtained his Master's Degree. In 1968 he transferred to the grade of Senior Scientific Officer and worked on radio frequency power standards at the National Physical Laboratory. Since 1970 he had been working in Dublin.

Eric Jackson (Member 1973, Graduate 1955) of Leatherhead, died on 16th October 1980, aged 61. Following war service with the Royal Electrical and Mechanical Engineers, Mr Jackson was for two years a service engineer with the General Electric Company. In 1948 he joined the War Department as a Telecommunication Mechanic, subsequently becoming a Technical Assistant. In 1959 he transferred to the Ministry of Supply, eventually becoming a Professional and Technology Officer I; at the time of his death he was concerned with the production of publications on airborne electronic equipment.

Squadron Leader William McCann, BSc., RAF (Ret) (Member 1960) of Pangbourne, died in April 1980, aged 67. After graduating from the University of Manchester in 1935, William McCann worked up to the beginning of the war as an electrical engineer and in 1939 joined the RAF as a Signals Officer. He was demobilized in 1945 and was for the next four years director of a small manufacturing company. During this period he lectured on mathematics at the Northampton Polytechnic, London. In 1949 he returned to the RAF obtaining a permanent commission and for eight years held staff and lecturing appointments. Following a short period as assistant to the Chief Engineer of Burndept Radio, he was appointed as a Lecturer at the REME Training Centre, Arborfield, with whom he remained until he retired in 1978.

Mieczyslaw Pasik (Member 1957, Graduate 1955, Student 1948) died at Isleworth, Middlesex in August 1980, aged 62.

Born in Poland, Mr Pasik obtained qualifications in telecommunication engineering by study at the Northern Polytechnic. He subsequently obtained an appointment in the research department of Central Rediffusion Services.

Sydney Lloyd Robinson (Member 1941) of Wellington, Shropshire, died in October 1980, aged 73. He was for a number of years Works Manager of Hartley Baird, Shrewsbury.

John Edward, Lord Wall of Coombe, O.B.E., B.Com. (Companion 1968) died on 29th October, aged 67. John Wall graduated from the London School of Economics in 1933 and up to the outbreak of war was with O.T. Falk & Company. In 1939 he joined the Ministry of Food and rose to be Under Secretary from 1948–52. He then entered industry and was with Unilever from 1952–58, latterly as Head of the Organization Division. From 1958–66 he was with EMI initially as a Director and from 1960–66 as Managing Director. In 1966 he was appointed Deputy Chairman of the Post Office Board, a position he held for some two years until he moved to International Computers as Chairman. On his retirement from ICL in 1972 he joined the Board of the Grundy Teddington Group.

He was awarded the OBE in 1944, appointed an Officer of the Order of Orange Nassau in 1947 and was knighted in 1968; he was created a Life Peer in the New Year Honours of 1976. As Sir John Wall he served on the Institution's Council as representative of the classes of Honorary Members and Companions from 1970 to 1972. He also served on the National Electronics Council.

Membership Elections and Transfers

THE COUNCIL confirms the elections and transfers of the following members whose candidatures have been recommended by the Membership Committee and announced in Membership Approval Lists Nos. 276–280, published in issues of *The Electronics Engineer* dated 4th September, 3rd October, 6th November and 14th December 1980, and 8th January 1981.

GREAT BRITAIN AND IRELAND

CORPORATE MEMBERS

Transfer from Member to Fellow

GALLAGHER, Paul John. HORLOCK, Bertrand Albert.

STEPHENS, Stephen James.

DORMER, Donald Edward. HALES, Michael John.

BURTON, Thomas Jeffrey.

MOORE, Michael.

Transfer from Graduate to Member

CLAY, Stephen John. ROSSITER, Alan.

BALL, Kenneth Charles. BUNYARD, Ian Philip. HILLYER, Neville. STONEY, Stuart Douglas.

CHO-YOUNG, Christopher. CHU, Yu Kai. REES, Arthur Reuben.

BURROWS, William Henry. HARDING, Denis Arthur. NAPPIN, Donald. PHILLIPS, Terence John. WALTON, Christopher Rowland John.

Transfer from Student to Member

CASPERD, Alan Norman. DALE, David Richard.

Direct election to Member

HAMBLION, Rodney John S. JENNINGS, Terence John. LEWIS, Christopher. NORMAN, Laurence Charles. STUPPLES, David William. WHITE, David James.

BEALE, Michael Stanley. ELLIOT, John Stewart. FINLEY, Robert Stephen. SWAN, Michael John.

ANDREW, Peter John. CHAPMAN, James. FABRICANT, Michael Louis David. FU, Shu Leung. HAMES, Stephen William. HARDING, Wilfrid Brent. HARRIS, Neil. JENKINS, Desmond Edward. KOELLER, Anthony Martin. LIDBETTER, Paul Stephen. SHAKAIBA, Mohammad Ahsan.

BENSTER, Brian Mervyn. DAWE, David Frederick. FRENCH, Peter St. John Richard. GILLMOR, Alfred William. GREEN, Christopher Francis. RUSSELL, Robert William. SKIDMORE, William Marlin. THIRUCHELVARAJAH, Sittampalam. WALLER, Edmund Anthony.

CALLIS, Michael Raymond. COLLINS, Alan John. HADWICK, Frederick John.

NON-CORPORATE MEMBERS

Transfer from Student to Graduate

ISSAKHANIAN, Edmond. SMITHWICK, Mark Gerard.

AMMANN, Max James. CHIA, Kon Kwee. DA COSTA, Howard Scott.

FLETCHER, Robert William. SCOTT, John Richard. SMY, Clifford Martin.

Direct election to Graduate

BONNER, David Maxwell. BUCKING-HAM, John Richard.

QUANSAH, Issac. STEVENS, Mark William.

ABDUL-REDA, Abdul-Imam Jasim. ATHANASAKOS, Athanasios. HUNTER, Colin John Allan. MOTTERSHEAD, Duncan Paul Leigh. SPOONER, Cheryl Ann.

CLARK, Phillip John. GIBSON, Colin. REISCH, Richard Stanley. ROBERTS, Michael John. ROBERTS, Nicholas David. SANI, Suleiman Mohammed. SOLANKI, Jitendra Jayantilal. WICKENDEN, Cyril Albert.

HAWKER, David John. IBEKWE, Cyril Sunday N. JAYAWARDENA, Kattota Ralage A. JEYASEELAN, Sithamparapillai. JONES, Raymond. KHAN, Anwar Ali. PANG, Weng Fun. PATEL, Mansukh. RANAWEERA, Priyalaal Lakshman. RICHARDSON, Brian Albert. ST. JOHN-GREEN, Michael Ronald. TSANG, Raymond Yip Fai. VANN, Anthony John.

Direct election to Associate Member

EASTWOOD, Donald. VALENTINE, Mark.

BEARD, David Leslie. GUNSASINGHAM, Vilvan. JAGGER, David Stephen. TABE, Richard Tanyiabe. WHITTINGHAM, Robert Thomas.

BAVISTER, Roy Charles. BEDFORD, Michael Arnold. BRISCOE, Eric. HARMON, Henry Joseph M. JEWELL, Edward Richard. ODIAGBE, Emmanuel Useghe. PAGE, Andrew. PARK, Robert George. WYLD, David Keid.

FUDGE, Roy Charles. Twilley, John M.

GOODWIN, Steven Michael. GRAHAM, Earl Graham.

Transfer from Associate Member to Graduate

AZAGBA, Parkinson Jacob Ikpe.

Transfer from Student to Associate Member

DEVEY, Gary Alan.

Direct election to Associate

BAILEY, Robert Eugene.

OVERSEAS

CORPORATE MEMBERS

Transfer from Member to Fellow

McGREAL, David Edgar.

JACOBS, Jonathan Wolfe.

Transfer from Graduate to Member

AGBOGIDI, Godwin O.M. COOKE, Stuart James. PIPER, Stanley John. WAN, Tong Weng.

CRAWFORD, Ian Fergus. DONOHUE, Terence Henry. VARMA, Purushottam Parshad.

ADESEMOWO, Gbadebo Adeyemi. KADRI, Faisal Louay Tahsin.

BUSARI, Lateef Folorunsho. FRANCIS, John David. LEE, Ah-Nga. OGBOGOH, Fidelis Iweanya. POON, Albert Ka-Fat.

Transfer from Associate Member to Member

GOH, Teck Heng.

PONG, Kwok-Shu.

Direct election to Member

ABEYWARDANA, Botunga Arachchige. LAM, Hing Cheung H. LEUNG, Koon On Albert.

NANAYAKKARA, Chandrakumara S.

DO, Manh Anh. CHENG, Michael Ming-Ho. CHOUDHRY, Nasir Javed Saifi. JAYAWARDENA, Joseph Lashman. MOUSTAFA, Salah El-Deen.

FILIPPINI, Roger Bonafino. GRIEVE, Henry Frank. HO, Chi-Wah Raymond. KUM, Shiu Ming. MOHAMED, Mohamed Imptiaz. WONG, Sik Kei.

BYDDER, Evan Lloyd. HURST, Larry. KUMARASENA, Arya Keerthi. O'DRISCOLL, Robert Charles.

NON-CORPORATE MEMBERS

Direct election to Graduate

ADEBAYO, Wasiu Tunde.

CHAN, To Gary. KUNTIYA, Michael Fletcher. LAM, Sheung-Sung.

ACHAPA, Stephen. CHAN, Ming Wah. LEUNG, Man Yat. Kwun Tong. ONUNGA, John Ogutu. YIM, Yui Ming.

CHAN, Lai-lit. DIN, Abdul Saleem. HA, Yung Kuen. KWAN, Shu Wa. LEUNG, Kar Hung. LI, Kai-Yin. POON, Ming Cheong Vincent.

Transfer from Student to Graduate

CHEUNG, Shan Tai. LO, Hing Cheung. TONG, Chak Hong.

LAM, Shun Yuen. MAINA, Julius N. TANG, Chiu Kit. WONG, Siu Wah.

CHAN, Kin Fung. IP, Bo Cheung. LEUNG, Chung-yan Samuel. LEUNG, Kwok Yiu.

MAU, Chung Ming. PAU, Pok Kun Kenneth. WU, Kam-Wah.

Direct election to Associate Member

DOWNES, David Thomas.

ANG, Eng Wah. CHAN, Wan. LEUNG, Ka Yiu.

OGBUANI, Matthew Ogbude. ONG, Cheng Kiat. SINGH, Davendra. YIP, Hung Cheong.

LI, Ping-On Tom.

CHITTY, Annamalai. CHIU, Kai On. LAU, Wing Chiu.

Transfer from Associate Member to Graduate

METAXAS, Sotos.

YEE, Yew Choong, Seria.

Transfer from Student to Associate Member

YUEN, Tak-Sing.

Direct election to Associate

ALI, Syed Zahid.

Standard Spacecraft Microcomputer Module

A spacecraft microcomputer module (SMM) at Stevenage is being developed by British Aerospace Space and Communications Division as a standard unit suitable for general application in satellite systems requiring data processing capabilities. In addition to the hardware, the Division is also developing the necessary computer programs—the Software. This includes all the basic executive routines needed to control an SMM system.

Each SMM is a totally self-contained microcomputer comprising a microprocessor complete with information store and supporting logic circuitry. One of the design aspects of particular note is that of flexibility in choice of microprocessor used. The SMM development system at the Space and Communications Division currently comprises a Ferranti F100-L, three Texas Instrument 9900's and a DEC PDP11/34 mini computer, all running with compatible software and common hardware interfaces.

The F100-L which has been selected for use with SMM in the immediate future, is a bipolar microprocessor with low-power dissipation, manufactured by Ferranti as an l.s.i. circuit on a single chip encapsulated in a 40-pin dual-in-line package. Military standard F100-L microprocessors are subjected to additional special testing and screening before being nominated for service in space.

A method of interconnecting up to 64 SMMs has been developed whereby not only can their processing capabilities be shared for complex computations, but tasks may be transferred to other units should faults arise in individual devices. Input/output functions are performed by non-intelligent modules which are linked in an SMM System by a two-wire serial data bus designed by the Space and Communications Division. An addressable serial bus interface circuit (ASBIC) is used as the standard interface for connecting a module to the bus.

Data and control instructions are transferred as 32-bit long words via the bus at 500 kilobits per second. The ASBIC performs all data synchronization, module address detection and the serial-to-parallel and parallel-to-serial conversions necessary when transferring information between a module and the bus.

An ASBIC comprises a single 40-pin ceramic dual-in-line package. It is an l.s.i. circuit manufactured by Ferranti using collector diffusion isolation and the uncommitted logic array technology developed by that company. It is TTL-compatible and, importantly, operates at very low power levels from a single 5V source, an advance over similar circuits using hybrid and discrete technologies. It contains a 16-bit parallel data highway ideally suited to microprocessor applications and is manufactured to full military specifications. Utilizing ASBIC, non-intelligent terminals can be adapted for connection to the data bus with the minimum of additional circuitry.

The Space and Communications Division has established a Microcomputer Development Centre at Stevenage where SMM software is being written and tested. Concepts are being developed to ensure continued effective operation of spacecraft systems in the event of faults occurring after launch.

The configuration of the SMM and the selection of the military version of the Ferranti F100-L microprocessor is the outcome of an engineering study carried out over the last 18 months by the Space and Communications Division to assess the operational characteristics required of microprocessors for prolonged service in space aboard satellites. The F100-L was selected because its bipolar technology renders it inherently more resistant to radiation damage, with the added merit that it is the only 16-bit microprocessor wholly designed, developed and manufactured within Europe. Throughout the study, liaison was maintained with the European Space Agency (ESA) to ensure the technical solutions proposed were compatible with data handling requirements for satellites specified by ESA.

The Space and Communications Division will be incorporating SMMs in the next generation of satellite systems they build and have begun evaluating the device with its supporting components to qualify it for use in the space environment. It is envisaged that SMMs will also be eminently suited for a wide variety of data handling applications.

Techniques for utilization of hexagonal ferrites in radar absorbers

Part 1
Broadband planar coatings

M. B. AMIN, B.Sc., M.Eng., Ph.D., S.M.I.E.E.E., C.Eng., M.I.E.R.E.*

and

Professor J. R. JAMES, B.Sc., Ph.D., D.Sc., F.I.M.A., C.Eng., F.I.E.E., F.I.E.R.E.†

SUMMARY

The lack of suitable materials having permeabilities (μ_r) greater than unity at microwave frequencies has previously made it difficult to design thin coatings of broadband radar absorbers at this frequency range. A possible solution is to utilize the hexagonal ferrites that exhibit significant μ_r values (~ 5) over narrow frequency bands and this paper investigates methods of deploying this material to design thin broadband microwave absorbers. Several techniques are evolved involving layering of the materials and staggering of the material electrical parameters and dimensions to achieve a good match of the incident waves. The computed results are substantiated by measurements of the manufactured materials; measurement techniques and details of the materials used are given in appendices. It is established that a planar absorbent sheet having a reflection loss > 10 dB over 5–20 GHz is realizable within a practically acceptable thickness.

* Formerly at the Royal Military College of Science; now with the Independent Broadcasting Authority, Crawley Court, Winchester, Hants SO21 2QA
† Department of Electrical and Electronic Engineering, Royal Military College of Science, Shrivenham, Swindon, Wiltshire SN6 8LA

List of Symbols

μ_0, ε_0	permeability and permittivity of free space
μ_i, ε_i	permeability and permittivity of the ith layer
$\mu_{r_i}, \varepsilon_{r_i}$	relative permeability and permittivity of the ith layer
$\mu_{r_i} = \mu'_{r_i} - j\mu''_{r_i}$	
$\varepsilon_{r_i} = \varepsilon'_{r_i} - j\varepsilon''_{r_i}$	
$\tan \delta_\mu = \mu''_r/\mu'_r$	magnetic loss tangent
$\tan \delta_\varepsilon = \varepsilon''_r/\varepsilon'_r$	dielectric loss tangent
Z_m	intrinsic impedance in the material
Z_0, Z_{sc}, Z_{oc}	characteristic, short-circuited and open circuited impedance of a transmission line
λ_g, λ_c	guide and cut-off wavelength
λ_0, λ	free space and material wavelengths
α, β, γ	attenuation, phase and propagation constants
k	wave number
E_x, H_y	electric field parallel to x-axis and magnetic field parallel to y-axis
ψ	a field function
a_i, b_i	amplitudes of the incident and the reflected fields in the ith layer
n	number of layers
l_i, L	thickness of the ith layer, and total thickness
R	voltage reflection coefficient

1 Introduction

1.1 Basic problem

The concept of absorbing incident electromagnetic radiation by placing lossy material in the path of the waves is well known. The applications are numerous particularly at microwave frequencies and include the use of absorbent coatings on the walls of anechoic chambers[1,2] and on the exterior surfaces of military aircraft and vehicles to achieve radar invisibility.[3] When there is plenty of space available sufficient absorption of power over a wide bandwidth can generally be obtained by increasing the volume of the material and shaping its geometry. When the space is limited, it is a difficult design problem to ensure that the optimal bandwidth and reflectivity properties are achieved and this is the usual situation for most military applications. The electromagnetic reflectivity over a frequency range together with the material weight, depth, cost, durability etc. then determine the effectiveness of the absorber.

A thin coating of material can be theoretically designed to give any desired reflectivity over a specified bandwidth, but the realization of the material in practice imposes a severe constraint at microwave frequencies. Ideally the designer wants to have control over the material permittivity, permeability and loss constants, but the main fundamental problem concerns the dearth

of material having a relative permeability μ_r significantly greater than unity at frequencies in the microwave band. A class of materials, hexagonal ferrites, having significant permeability values over very narrow frequency ranges has been reported,[4-7] but it is not obvious how to deploy the material to obtain broadband absorption characteristics. The present paper describes a technique[21] of layering this narrowband material to increase the absorption bandwidth of a thin planar structure in the frequency range 2–20 GHz. The mathematical formulation of the problem and the design approach are given, together with sufficient details about the development and the measurement of the basic material. The reflectivity measurements on a layered block of material support the theoretical design and conclusions. A companion paper deals with the implementations of this type of material to cylindrical structures and the particular application considered concerns the development of a wire antenna that is to some extent 'invisible' to radar detection.[22]

1.2 Existing Techniques and Material Characteristics

If an absorber of electromagnetic radiation is to be efficient the materials must not only attenuate the waves penetrating its volume, but must also present a good match to the incident waves at the air/material interface. It is shown in Appendix 8.1 that a good absorption is obtained when μ_r', ε_r', $\tan \delta_\mu$ and $\tan \delta_\varepsilon$ are as large as possible while good matching at the interface requires $\mu_r' = \varepsilon_r'$ and $\tan \delta_\mu = \tan \delta_\varepsilon$; these material constants are defined in Appendix 8.1.

If there is sufficient space, broadband matching can be achieved by creating a gradual transition with cone-like protrusions of the material as in Fig. 1 where the cones are usually several free-space wavelengths long. A method for narrowband applications is discussed in Appendix 8.2, whereby the coating is comprised of lossy material a quarter of a wavelength thick; the space requirement is reduced considerably at the expense of bandwidth. A technique for increasing the bandwidth of this type of absorber using spinel type Ni–Zn ferrites dispersed in dielectric material has been described.[8] Attempts have been made to make broadband planar absorbers from lossy dielectric materials,[16-18] but the air/dielectric matching condition cannot be fulfilled

without creating a gradual transition of increasing permittivity values in the direction of the incident wave and this can lead to either thick bulky layers of materials or laminar structures that are complicated to manufacture.

The properties of hexagonal ferrites used in the present investigation are summarized in Appendix 8.3 together with some details about the frequency dispersive characteristics of the real part of the relative permeability μ_r' which can rise to about 5 at resonance. The various types of hexagonal ferrites have differing resonant frequencies ranging over microwave and millimetre wave band typically used by radar equipment. The relative permittivity ε_r remains fairly constant over a wide frequency range with ε_r' typically 10–30. A summary of the method used to measure these parameters is given in Appendix 8.4.

2 Theory

2.1 Reflection Loss due to a Multilayer Absorber

Figure 2 shows a metal-backed multilayer absorber having n homogeneous layers, with the thickness of the ith layer being l_i and its complex permeability and permittivity μ_i and ε_i respectively, $i = 0, 1, 2, 3 \ldots, n$. A transverse electromagnetic (TEM) wave propagating along the z-direction with its electric field (E_x) parallel to the x-axis and magnetic field parallel to the y-axis, is incident normally on the absorber and gives rise to a series of waves travelling in both the positive and negative z-directions within the layers. The electric and the magnetic field components E_x and H_y are constant in any x–y plane and satisfy the Helmholtz equation[14] $(\nabla_z^2 + k^2)\,\psi = 0$, where k is the wave number, ψ any field function (say, E_x in this case) and $\nabla_z = \partial/\partial z$. Both μ_i and
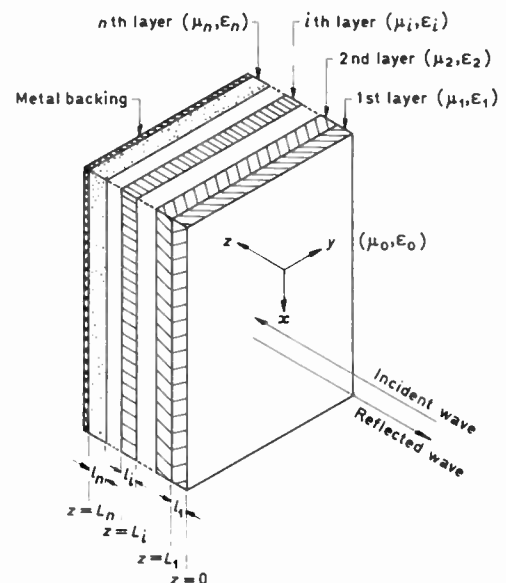

Fig. 1. Sectional diagram of a pyramidal type absorber.

Fig. 2. A multi-layer absorber showing different layer dimensions and the properties of the constituent materials.

ε_i are in general complex and frequency-dependent, and likewise $k = \omega\sqrt{\mu_i\varepsilon_i}$. The time variation $e^{-j\omega t}$ is suppressed in the following.

Electric fields in different regions can be written as:

$$\left.\begin{array}{l} E_{x_0} = a_0 e^{-jk_0 z} + b_0 e^{jk_0 z}, \qquad a_0 = 1, i = 0 \\ E_{x_i} = a_i e^{-jk_i z} + b_i e^{jk_i z}, \qquad i = 1, 2, \ldots, n \end{array}\right\} \quad (1)$$

where, a_i and b_i are the amplitudes of the incident and reflected waves respectively in the ith layer. b_0 is the amplitude of the resultant reflection of the electric field in free space due to an incident wave of unit amplitude.

The corresponding magnetic fields can be obtained[14] from equation (1) by using Maxwell's equation, $\nabla \times \mathbf{E} = -j\omega\mu\,\mathbf{H}$ thus

$$\left.\begin{array}{l} H_{y_0} = \dfrac{k_0}{\omega\mu_0} (e^{-jk_0 z} - b_0 e^{jk_0 z}), \qquad i = 0 \\[2mm] H_{y_i} = \dfrac{k_i}{\omega\mu_i} (a_i e^{-jk_i z} - b_i e^{jk_i z}), \qquad i = 1, 2, \ldots, n \end{array}\right\} \quad (2)$$

The coefficients a_i and b_i in equations (1) and (2) above can be obtained by involving the boundary conditions at the interfaces between adjacent layers and at the conducting surface at $z = L_n$. Using these conditions:

$$b_0 = \frac{1 - Q_1 - \tau_i(1 + Q_1)}{1 - Q_1 + \tau_i(1 + Q_1)} \quad (3)$$

where

$$\tau_i = \sqrt{(\varepsilon_{r_i}/\mu_{r_i})/(\varepsilon_{r_{i-1}}/\mu_{r_{i-1}})} \quad (4)$$
$$i = 1, 2, \ldots, n$$

Q_1 in equation (3) can be obtained through the following equations:

$$L_i = \sum_{m=1}^{i} l_m, \qquad i = 1, 2, \ldots, n \quad (5)$$

$$Q_n = e^{-j2k_n L_n} \quad (6)$$

$$P_i = \frac{e^{-j2k_i L_{i-1}} - Q_i}{\tau_i(e^{-j2k_i L_{i-1}} + Q_i)} \quad (7)$$

$$Q_{i-1} = \frac{(1 - P_i)}{(1 + P_i)} \cdot e^{-j2k_{i-1} L_{i-1}} \quad (8)$$

$$i = n, (n-1), (n-2), \ldots, 2$$

Q_1 is thus obtained by following the sequence of successively computing Q_n and P_n, then Q_{n-1} and P_{n-1} and so on in a descending order until Q_1 is reached. The coefficient b_0 is in general a complex function of frequency and the voltage reflection coefficient $R = |b_0|$. The power reflection loss $= -20\log_{10} R$.

2.2 Optimization of the Absorber Performance

The properties of the materials in different absorber layers and their thicknesses are to be chosen to create maximum absorption of the incident power over a desired bandwidth and under the constraint that the total thickness L of the n-layered slab should not exceed a stated limit.

The frequency at which the ferrimagnetic material exhibits maximum relative permeability μ_r' can be varied according to the amount of divalent and tetravalent atoms introduced by way of the added impurities (Appendix 8.3). The dispersive nature of the μ_r' resonance curves varies according to the chemical composition and μ_r'' is functionally related to μ_r' as noted in Appendix 8.3. The permittivity and permeability values can be reduced by diluting the material with a suitable binder material. In principle it is possible to carry out the design using well-known optimization[15] routines and we now illustrate the latter for three parameters: f_0, S (eqns (21) and (22)) and the layer thickness l_i. Since there are n layers there are $3n$ parameters to optimize and an existing[19] NAG subroutine E04UAF based on the Lagrangian method with constrained variables was implemented. This mathematical model represents a four-layer metal-backed structure constrained to give minimum reflectivity over a bandwidth of 1–15 GHz and L must not exceed 7·5 mm. The dispersive characteristics of μ_r' and μ_r'' are given by equations (21) and (22) and the maximum available permittivities ($\varepsilon_r' = 10$ and $\varepsilon_r'' = 1\cdot0$) are scaled accordingly to take account of the dilution of the permeabilities in individual layers. The optimal parameters arising from the computation are shown in Table 1 and the corresponding reflectivity performance in Fig. 3 where it is seen that the reflection loss varies

Table 1

Computer synthesized ferrite properties for a 4-layer optimized absorber. Parameters are defined in equation (21) and layer numbers refer to Fig. 2.

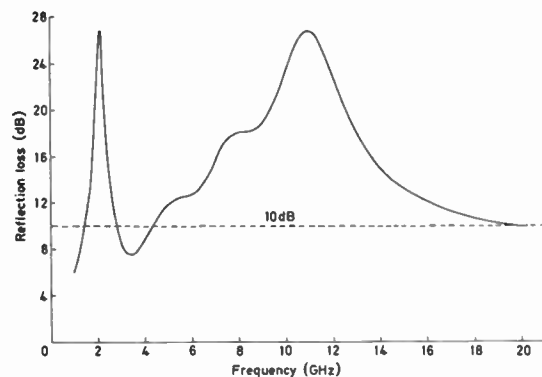| Layer No.	S	f_0 (GHz)	Layer thicknesses (mm)
1	3·27	10·35	0·85
2	2·91	7·56	1·43
3	2·10	5·23	2·22
4	1·0	3·50	3·00

Fig. 3. Reflection loss characteristics of an optimized absorber comprised of four layers of hexagonal ferrites specified in Table 1.

considerably over the design bandwidth; a reflection loss of > 10 dB is obtainable between 5 and 20 GHz.

3 Practical Design Methods

The above multivariable optimization method does not lead to a unique solution in practice because the bandwidth constraint is itself non-unique. That is the reflection loss is required to exceed a given level over the bandwidth but may fluctuate beyond that level in an unspecified manner. In practice the optimization routine would be run several times with different numerical weights so that a variety of possible solutions could be inspected. Since some degree of inspection is involved it is important to investigate whether the material parameters can be chosen entirely by inspection if further constraints are allowed and we describe two such design methods based on the layered computer model equations (3) to (8).

3.1 Tapered Impedance Transition

The additional constraint in this method is to arrange the layers so that they become progressively thicker and have higher permittivity and permeability values in the direction of the incident plane wave. The material resonances f_{oi} are spaced out across the desired bandwidth. So given L the designer then selects the tapered distribution of thicknesses and material constants by trial and error inspection of the computer simulated results given by equations (3) to (8). The number of layers will have some effect on the overall performance but the latter will ultimately be dictated by the allowable absorber thickness L.

3.2 Quarter-wavelength Technique

This method is based on the quarter-wavelength absorber described in Appendix 8.2. By constraining the material of each layer so that the resonant frequencies f_0 are again staggered over the bandwidth of interest it is possible for the entire absorber to exhibit quarter-wavelength action at several frequencies within the band.
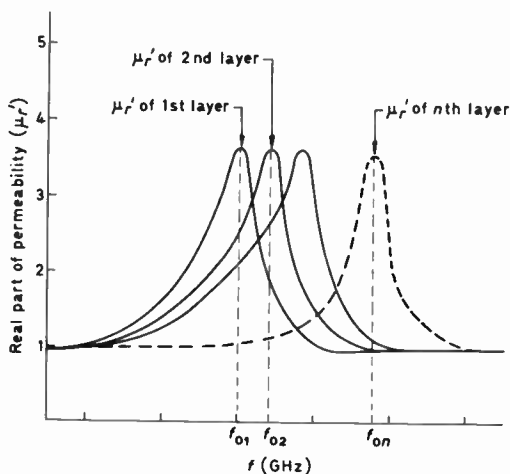
Let n layers have thicknesses $l_1, l_2 \ldots, l_n$ and material resonances at $f_{o1}, f_{o2} \ldots, f_{on}$ as illustrated in Fig. 4. If the $\mu_{r_i}(f)$ and $\varepsilon_{r_i}(f)$ are the relative permeability and permittivity respectively of the ith layer, then from equation (19), Appendix 8.2, the electrical length of the layer is

$$l_i \operatorname{Re} \sqrt{\mu_{r_i}(f)\, \varepsilon_{r_i}(f)}.$$

The electrical length of the n layers is the sum of the individual lengths, and is to be made equal to a quarter-wavelength, thus

$$\sum_{i=1}^{n} l_i \operatorname{Re} \sqrt{\mu_{r_i}(f)\, \varepsilon_{r_i}(f)} = \frac{300}{4f} \qquad (9)$$

where the frequency f is in GHz and thickness l_i in mm. If the number of frequencies where equation (9) is satisfied is n, then the solution of equation (9) is obtained by solving the resulting inhomogeneous equation for the unknown thickness l_i. This can sometimes lead to inconsistent results for some choices of n and f_{oi}; the process is to consider various distributions of f_{oi} and select the best reflectivity versus frequency curve by inspection of the computer simulated results of equations (3) to (8).

4 Computed and Experimental Results

4.1 Computed Results

The computed results of equations (3)–(8) are based on materials whose material constants are represented by equation (21) (Appendix 8.3) over a bandwidth of 1–20 GHz. It is evident from Section 3 that in the tapered impedance transition method the absorber thickness L must be initially specified whereas in the quarter-wavelength method there is no initial control of L but quarter-wavelength action is enforced. The methods are therefore distinguished only by the additional initial constraints imposed.

To illustrate the method of Section 3.1, L is specified as 7·5 mm and for the purpose of comparison we compute first an example that does not have a tapered thickness distribution. Figure 5 shows the performance
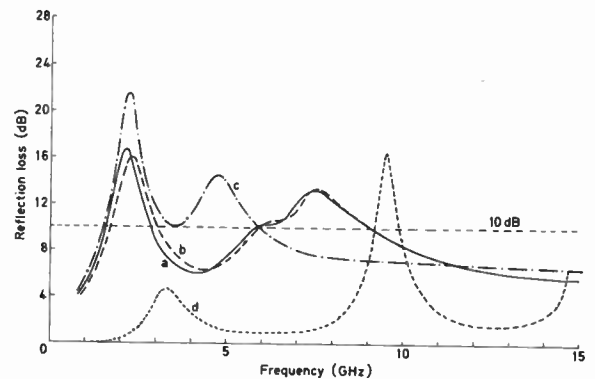

Fig. 4. Idealized magnetic properties of the materials at different layers.
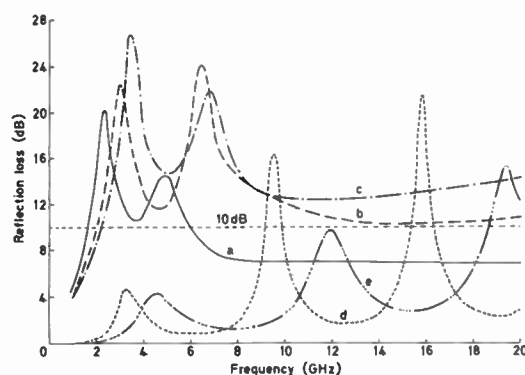

Fig. 5. Reflection loss characteristics of multilayer absorber without tapered transitions as specified in Table 2. (a) ——— single layer of ferrites; (b) – – – 2 layers of ferrites; (c) – · – · – 4 layers of ferrites; (d) ------- single layer of dielectrics.

Table 2

Specifications of single layer and multilayer absorbers with untapered transitions at the layer interfaces. Parameters are defined in equation (21).

Absorber sample	Number of layers	Thicknesses (mm)		f_0 (ferrites of successive layers)	S(ferrites of successive layers)	ε_r (frequency independent) (for successive layers)
		Total	Successive individual layers			
a	1	7·5	7·5	7·5	1·0	10−j1
b	2	7·5	3·75, 3·75	7·5, 9·0	1·0, 1·0	10−j1, 10−j1
c	4	7·5	1·875, 1·875, 1·875, 1·875	4·5, 6·0, 7·5, 9·0	1·0, 1·0 1·0, 1·0	10−j1, 10−j1, 10−j1, 10−j1
d	1	7·5	7·5	dielectric	dielectric	10−j1

obtained from cases (a), (b), (c) and (d) of Table 2 when the thicknesses of each layer is constant and only the material resonances f_{oi} are staggered. The single lossy dielectric layer is seen to be highly reflective compared to the other cases containing ferrite and this is due to the mismatch at the air/dielectric interface. In case (a) there are two peaks in the reflectivity curve; the first (lowest frequency) is due to the quarter-wavelength effect and the second due to ferromagnetic resonance in the material. The order of these peaks is set by the choice of material constants in the example. The results for case (b) are very similar to case (a) indicating that the incident wave never achieves significant penetration into the second layer, thus showing the need to taper the material composition in a progressive manner in the direction of the incident waves. In case (c) the two resonances, the first due to quarter-wavelength condition and the second due to the ferrimagnetic resonance of the front layer, merge together providing an improved reflection loss characteristic. For comparison purposes we take a reflection loss of > 10 dB as the criterion and case (c) thus has a bandwidth of about 1·2 to 5·8 GHz.

The effect of tapering both the layer thicknesses and the material constants is illustrated in Fig. 6 for the cases (b) and (c) specified in Table 3; the improvement over

Fig. 6. Reflection loss characteristics of multilayer absorbers having tapered transitions as specified in Table 3. (a) ——— 5 layers of ferrites without tapering transitions; (b) — — — 3 layers of ferrites having tapered transitions; (c) — · — · — 5 layers of ferrites having tapered transitions; (d) ------- single layer of dielectrics; (e) — ··· — 5 layers of dielectrics having tapered transitions.

the non-tapered case (a) in Table 3 is very marked. It is also important to note that the single dielectric layer case (d) shows little improvement when split up into five layers with tapered permittivity profile, thus endorsing the importance of the presence of ferrites in absorbers. Case (c) enables the 10 dB reflection loss to be achieved from 2–20 GHz due to use of five rather than three layers

Table 3

Specifications of single layer and multilayer absorbers having tapered transitions at the layer interfaces. Parameters are defined in equation (21).

Absorber sample	Number of layers	Thicknesses (mm)		f_0 (ferrites of successive layers)	S (ferrites of successive layers)	ε_r (frequency independent) (for successive layers)
		Total	Successive individual layers			
a	5	7·5	1·5, 1·5, 1·5, 1·5, 1·5	4·5, 6·0, 7·5, 9·0, 10·5	1·0, 1·0, 1·0, 1·0, 1·0	10−j1, 10−j1, 10−j1, 10−j1, 10−j1
b	3	7·5	1·0, 2·5, 4·0	6·0, 7·5, 9·0	3·0, 2·0, 1·0	3·3−j0·33, 6·7−j0·67, 10−j1
c	5	7·5	0·5, 1·0, 1·5, 2·0, 2·5	4·5, 6·0, 7·5, 9·0, 10·5	5·0, 4·0, 3·0, 2·0, 1·0	2−j0·2, 4−j0·4, 6−j0·6, 8−j0·8, 10−j1
d	1	7·5	7·5	dielectric	dielectric	10−j1
e	5	7·5	0·5, 1·0, 1·5, 2·0, 2·5	dielectric	dielectric	2−j0·2, 4−j0·4, 6−j0·6, 8−j0·8, 10−j1

Table 4

Specifications of multilayer ferrite absorbers having tapered transitions at the layer interfaces and showing the effects of the separation of resonances in adjacent layers. Parameters are defined in equation (21).

| Absorber sample | Number of layers | Thicknesses (mm) | | f_0 (ferrites of successive layers) | S (ferrites of successive layers) | ε_r (frequency independent) (for successive layers) |
		Total	Successive individual layers			
a	5	7·5	0·5, 1·0, 1·5, 2·0, 2·5	8·5, 9·0, 9·5, 10·0, 10·5	5·0, 4·0, 3·0, 2·0, 1·0	2 − j0·2, 4 − j0·4, 6 − j0·6, 8 − j0·8, 10 − j1·0
b	5	7·5	as above	4·5, 6·0, 7·5, 9·0, 10·5	as above	as above
c	5	7·5	as above	3·0, 5·5, 8·0, 10·5, 13·0	as above	as above
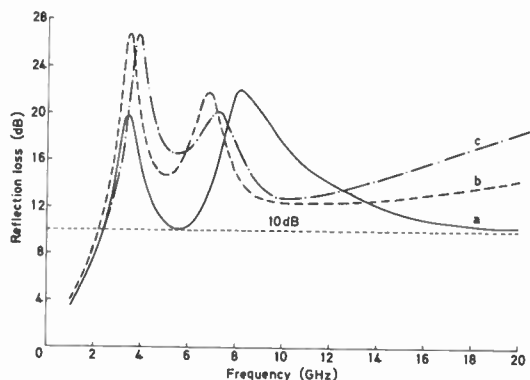
Fig. 7. Reflection loss characteristics of 5-layered ferrite absorbers for different separation of resonances in adjacent layers, as specified in Table 4. (a) ——— separation of resonances 0·5 GHz; (b) — — — separation of resonances 1·5 GHz; (c) — · — · separation of resonances 2·5 GHz.
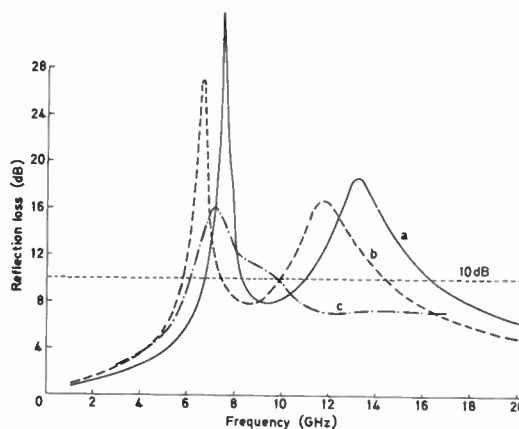
Fig. 8. Reflection loss characteristics of multifrequency quarter-wavelength absorbers as specified in Table 5. (a) ——— total thickness 1·6 mm; (b) — — — total thickness 1·79 mm; (c) — · — · total thickness 1·82 mm.

as in case (b) where the reflection loss is somewhat less throughout the bandwidth 2–20 GHz.

Some further improvement in reflection loss over the band can be obtained by selecting different resonant frequencies as shown in Fig. 7 and details are given in Table 4. Case (b) of Fig. 7 is case (c) of Fig. 6 and is included for comparison. Cases (a) and (c) of Fig. 7 have the same layer thicknesses as case (b) of Fig. 7 but different resonant frequencies.

The results for the quarter-wavelength method are shown in Fig. 8 and are detailed in Table 5. For this method no dilution of the material is required and $\varepsilon_r = 10 - j1$ for each layer while the ferrite resonances

f_{oi} are as shown in Table 5. The reflection loss has two pronounced peaks for cases (a) and (b) while in case (c) the peaks close together to give an inferior overall performance compared to cases (a) and (b) which in themselves are narrower in bandwidth, defined by 10 dB level of reflection loss, than the designs shown in Fig. 7. A compensating factor in this example is that quarter-wavelength design leads to a much thinner structure with L being at most 1·82 mm as opposed to 7·5 mm. Improved performance would result from utilizing more layers thus increasing L.

Table 5

Specifications of the materials of multi-frequency quarter-wavelength absorbers.

| Absorber sample | Number of layers | Resonant frequency of successive layers (assigned) GHz | $\lambda/4$ – frequencies (assigned) GHz, f_1, f_2, f_3 | Computed thicknesses (mm) | |
				Successive layers	Total L
a	3	13·0, 10·0, 8·5	11·5, 10·0, 8·5	0·37, 0·13, 1·1	1·60
b	3	11·5, 9·0, 7·5	10·2, 9·0, 7·5	0·41, 0·05, 1·33	1·79
c	3	7·5, 9·0, 11·0	7·5, 9·0, 11·0	1·41, 0·11, 0·30	1·82
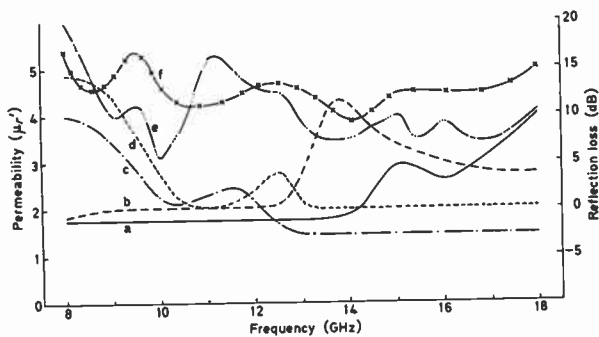
Fig. 9. Comparison of the experimental and theoretically predicted reflection losses of a 4-layered absorber and the measured permeability dispersion characteristics of the constituent ferrites. (a) ——— permeability dispersion of ferrite 1, i = 1; (b) – – – permeability dispersion of ferrite 2, i = 2; (c) – · – permeability dispersion of ferrite 3, i = 3; (d) ------- permeability dispersion of ferrite 4, i = 4; (e) – ··· – experimental reflection losses; (f) – × – predicted reflection losses.

4.2 Experimental Results

The materials were measured by the methods described in Appendix 8.4 and the dispersive behaviour of μ'_r is shown in Fig. 9 (curves a, b, c, d) for four types of hexagonal ferrite materials. The material was then arranged in four layers and pressed into a cylindrical disk 100 mm diameter; each layer was 5 mm thick, thus $L = 20$ mm. A polyvinyl alcohol (PVA) binder occupied 3% of the volume to provide additional mechanical strength and this applies to both the samples and the layered structure. The reflection loss was measured by the method of Appendix 8.4 and is shown in Fig. 9, curve (e) together with the computed result curve (f). The computed and measured reflection loss curves differed by about $\pm$ 2 dB in a way which shows little correlation and this is attributed to tolerance effects arising from material parameter measurement and material inhomogeneity. This completed absorber has a performance of about 7 to 16 dB reflection loss over 8 to 18 GHz. Utilization of material with slightly rearranged resonances f_{oi} will enable some of the dips in the response to be filled in and a general level of 10 dB reflection loss is considered to be realizable.

5 Conclusions

The computed results confirm that the presence of ferrite material in an absorber as opposed to just dielectric material considerably increases the reflection loss over a wide bandwidth even though the permeability of the hexagonal ferrites only achieves significant values over a relatively narrow bandwidth. The main contribution of this work has been to show that the use of the layers and controlled thicknesses of different materials gives improved reflection characteristics. Numerical optimization methods can be used to arrive at design data but the latter must generally be used as a basis for an additional iterative process which involves inspection of the results. There appears to be no simple design

equations that can be extracted from the theory of the wave interaction in the layered media; however, two practical approaches are noted and illustrated. These two practical design methods contain an element of trial and error inspection and are assisted by the computation of the reflection loss as a function of frequency. Measurements on a four-layer absorber substantiate the theoretical predictions to within $\pm$ 2 dB reflectivity and the difference is attributed to material variations and tolerance effects in both material and reflectivity measurements. It is concluded that hexagonal ferrites can be used to create more effective microwave absorbers and that the choice of material parameters and thicknesses can be greatly assisted by computer simulation. Ways of manufacturing the layered ferrite absorbers so that they conform to physical constraints have not been considered and depend entirely on the particular application. It is anticipated that in some applications it will be necessary to sinter the ferrite material which will necessitate remeasuring its electrical constants.

6 Acknowledgment

7 References

1 Microwave Materials, Plessey Connectors Limited, Wood Burcote Way, Towcester, Publication no. 4966.
2 Emerson, W. H., 'Electromagnetic wave absorbers and anechoic chambers through the years', *IEEE Trans on Antennas and Progagation*, AP-21, no. 4, pp. 484-90, July 1973.
3 Stepanov, Y. G., 'Antiradar Camouflage Techniques', Soviet Radio Publishing House, Moscow, 1968; English Translation: JPRS47734, March 27th, 1969.
4 Severin, H. and Stoll, P. J., *Z Angew. Phys*, 23, no. 3, pp. 209–12, 1967.
5 Heck, C., 'Magnetic Materials and their Applications' (Butterworths, London, 1974).
6 Tebble, R. S. and Craik, D. J., 'Magnetic Materials' (Wiley-Interscience, New York, 1969).
7 Loyd, R. A. and Porter, G. B., Royal Military College of Science, Shrivenham, unpublished report.
8 Wickenden, B. V. A. and Howell, W. G., 'Ferrite quarter wave type absorber', Proc. Military Microwaves Conference, Wembley, London, October 1978, pp. 310–17.
9 Von Hippel, A. R. (Ed), 'Dielectric Materials and Applications' (M.I.T. Press, Cambridge, Massachusetts, 1961).
10 Knott, E. F., 'The thickness criterion for single-layer radar absorbents', *IEEE Trans on Antennas and Propagation*, AP-27, no. 5, pp. 698–701, September 1979.
11 Wartenberg, B., 'Measurements of the electromagnetic material constants μ and ε of ferrites in the mm-wave range', *Z. Angew. Phys* 24, no. 4, pp. 211–17, 1968.
12 Birks, J. B., 'The measurement of permeability of low conductivity ferrimagnetic materials at centimetre wavelengths', *Proc. Phys. Soc. (London)*, 60, pp. 282–92, March 1948.

215

13 Hollis, J. S., Lyon, T. J. and Clayton, L. (Ed.), 'Microwave Antenna Measurements' (Scientific Atlanta, Atlanta, Georgia, USA, 1970).

14 Stratton, J. A., 'Electromagnetic Theory' (McGraw-Hill, New York, 1941).

15 Adby, P. R. and Dempster, M. A. H., 'Introduction to Optimization Methods', (Chapman and Hall, London, 1974).

16 Salisbury, W. W., 'Absorbent body for electromagnetic waves', US Patent 2,599,944, June 10th, 1952.

17 MacFarlane, G. G., 'Radar Camouflage, Research and Development by the Germans', unpublished notes.

18 Wright, R. W. and Wright, J. W., 'Thin, lightweight electromagnetic wave absorber', US Patent 3,887,920, June 3rd, 1975.

19 'E04UAF, a Routine for minimization subject to nonlinear constraints', NAG Library: 1667/1512, Mark 7, December 1978.

20 Frohlich, H., 'Theory of Dielectrics' (Oxford University Press, 1949).

21 Amin, M. B., James, J. R., Lane, R., Loyd, R. A. and Porter, G. B., British Provisional Patent Application, 1980.

22 James, J. R., and Amin, M. B., 'Techniques for utilization of hexagonal ferrites in radar absorbers: Part 2. Reduction of radar cross-section of h.f. and v.h.f. wire antennas', *The Radio and Electronic Engineer*, **51**, no. 5, pp. 219–25, May 1981.

8 Appendices

8.1 Attenuation and Reflection Properties of an Absorber Layer

The propagation constant (γ) of an electromagnetic wave at a frequency, f in a medium having a permittivity $\varepsilon_0\varepsilon_r$ and a permeability $\mu_0\mu_r$ is given by[9]

$$\gamma = \alpha + j\beta = j2\pi f\sqrt{\mu_0\varepsilon_0\mu_r\varepsilon_r} \tag{10}$$

where $\mu_r = \mu_r' - j\mu_r''$ and $\varepsilon_r = \varepsilon_r' - j\varepsilon_r''$, α is the attenuation constant and β the phase constant. On equating the real and imaginary parts of equation (10):

$$\alpha = 2\pi f\sqrt{\mu_0\varepsilon_0}\sqrt{\frac{\varepsilon_r'\mu_r'}{2}}\Bigg[(\tan\delta_\mu\tan\delta_\varepsilon - 1) +$$
$$+ \{1 + \tan^2\delta_\mu\tan^2\delta_\varepsilon + \tan^2\delta_\mu + \tan^2\delta_\varepsilon\}^{\frac{1}{2}}\Bigg]^{\frac{1}{2}} \tag{11}$$

$$\tan\delta_\varepsilon = \frac{\varepsilon_r''}{\varepsilon_r'}; \tan\delta_\mu = \frac{\mu_r''}{\mu_r'}. \tag{12}$$

To satisfy the condition of high attenuation it is seen from equation (11) that the values of $\mu_r'\varepsilon_r'$, $\tan\delta_\mu$ and $\tan\delta_\varepsilon$ of the coating material should be as high as possible. The reflection coefficient R due to the discontinuity at the interface between the free space and the absorber coating is:[14]

$$R = (Z_m - 1)/(Z_m + 1) \tag{13}$$

$$Z_m = (\mu_r/\varepsilon_r)^{\frac{1}{2}}. \tag{14}$$

The reflection at the front surface will be zero and all the incident energy will enter the coating when $Z_m = 1$. Using the complex values of μ_r and ε_r,

$$Z_m = \left(\frac{\mu_r'}{\varepsilon_r'}\right)^{\frac{1}{2}} \frac{\{1 + j\tan\delta_\varepsilon - j\tan\delta_\mu + \tan\delta_\mu\tan\delta_\varepsilon\}^{\frac{1}{2}}}{\sqrt{1 + \tan^2\delta_\varepsilon}} \tag{15}$$

So, the coating will be perfectly matched with free space when

$$\left.\begin{array}{l} \mu_r'/\varepsilon_r' = 1 \\ \tan\delta_\mu = \tan\delta_\varepsilon \end{array}\right\} \tag{16}$$

8.2 Quarter-wavelength Resonant Absorber

A technique used in narrow band applications is to cancel the reflected wave from the front surface of the absorber with those originating from the back surface by making the thickness a quarter-wavelength (or an odd multiple of a quarter-wavelength). If the absorber is backed by a perfect conducting plane, an incident electromagnetic wave will give rise to a primary reflection from the front surface, and a series of secondary transmissions in the free space due to multiple bouncing of the waves within the absorber between the front and the back surfaces. The effective reflection in the free space will be the vector summation of the multiple reflections and the reflection coefficient R for normal incidence is

$$R = \frac{1 - e^{j2kL} + \sqrt{\varepsilon_r/\mu_r} + \sqrt{\varepsilon_r/\mu_r}\, e^{j2kL}}{1 - e^{j2kL} - \sqrt{\varepsilon_r/\mu_r} - \sqrt{\varepsilon_r/\mu_r}\, e^{j2kL}} \tag{17}$$

where ε_r, μ_r, k and L are respectively the relative permittivity, relative permeability, wave number and the thickness of the constituent materials. When both μ_r and ε_r are real (i.e. both the magnetic and dielectric loss tangents zero), k is real and the magnitude of R (eqn. (17)) will be unity resulting in total reflection irrespective of the thickness, L. When μ_r and ε_r are complex (lossy medium), so is k; the magnitude of R will vary as a function of L for any given values of μ_r and ε_r.
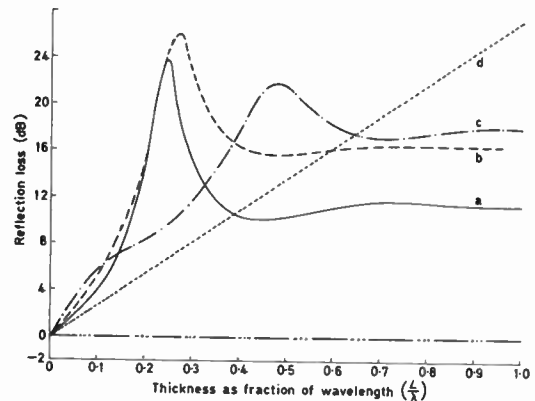

Fig. 10. Reflection loss versus absorber thickness as a fraction of the wavelength. (a) ——— $\varepsilon_r = 9 - j4\cdot5$, $\mu_r = 3 - j1\cdot5$; (b) – – – $\varepsilon_r = 6 - j5$, $\mu_r = 4 - j2$; (c) – · – $\varepsilon_r = 3 - j1\cdot5$, $\mu_r = 5 - j2\cdot5$; (d) ······· $\varepsilon_r = 10 - j2\cdot5$, $\mu_r = 10 - j2\cdot5$; (e) – ··· – $\varepsilon_r = 10 - j0$, $\mu_r = 10 - j0$.

Figure 10 shows the reflection loss of a single layer absorber as a function of its thickness and material compositions. It is observed for lossy materials having $|\varepsilon_r| > |\mu_r|$, which is often the case for ferrites at microwave frequencies, that the maximum reflection loss occurs around a quarter-wavelength thickness of the material (curves a and b), a fact which gives rise to the term quarter-wavelength resonant absorber. The thickness for such an absorber can be written as[10]

$$L = \frac{\lambda_0}{4(\sqrt{\mu_r \varepsilon_r})'} \qquad (18)$$

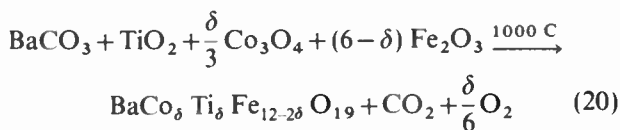where λ_0 = free space wavelength at the frequency of operation

$$(\sqrt{\mu_r \varepsilon_r})' = \text{real part of } \sqrt{\mu_r \varepsilon_r}$$
$$= \sqrt{\frac{\mu_r' \varepsilon_r'}{2}} \left[(1 - \tan \delta_\mu \tan \delta_\varepsilon) + \right.$$
$$\left. + \{1 + \tan^2 \delta_\mu \tan^2 \delta_\varepsilon + \tan^2 \delta_\mu + \tan^2 \delta_\varepsilon\}^{\frac{1}{2}} \right]^{\frac{1}{2}} \quad (19)$$

When $|\mu_r| > |\varepsilon_r|$ the maximum reflection loss occurs when the absorber thickness is greater than a quarter-wavelength. In the case of perfect matching condition (i.e. $\mu_r = \varepsilon_r$), $R = e^{-j2kL}$, thus diminishing exponentially with the thickness L (curve d). (c) and (e) are the conditions when $|\mu_r| > |\varepsilon_r|$ and there are no losses in the constituent materials respectively.

8.3 Hexagonal Ferrites

The basic structure of a hexagonal ferrite is $A\,Fe_{12}O_{19}$, where A is a divalent metal ion (e.g. Ba, Sr or Pb); an example is 'barium ferrite' $Ba\,Fe_{12}O_{19}$. The peaks in the losses of unbiased ferrites, corresponding to spin resonances, occur at frequencies which can be reasonably accounted for as the precessional frequencies in the anisotropy fields. Barium hexagonal ferrites have an unbiased anisotropy field of $17.0\,kOe$ (kilo-oersteds) which gives a ferrimagnetic resonance frequency of about $46\,GHz$. Severin et al.[4] observed that the anisotropy field, and hence the natural ferrimagnetic resonant frequency of the hexagonal ferrites $Ba\,Fe_{12}O_{19}$ can be varied between 2 to $100\,kOe$ by the substitution of a portion of Fe^{+3} ions in the lattice by some suitable divalent and tetravalent metal ions such as Co^{+2} and Ti^{+4} (e.g. $Ba\,Co_\delta^{II}\,Ti_\delta^{IV}\,Fe_{12-2\delta}O_{19}$). Hexagonal ferrites with a considerable range of compositions have been prepared and examined and the ferrimagnetic properties of a few of them are given in Fig. 11.

The method of preparation is straightforward, the ferrite structure being produced by firing an appropriate mixture of the oxides and carbonates of the constituent metals. The general formulae for the reaction is given by,

$$BaCO_3 + TiO_2 + \frac{\delta}{3}Co_3O_4 + (6-\delta)\,Fe_2O_3 \xrightarrow{1000\,C}$$
$$BaCo_\delta\,Ti_\delta\,Fe_{12-2\delta}O_{19} + CO_2 + \frac{\delta}{6}O_2 \qquad (20)$$

δ is between 0 and 1.5 and controls the ferrimagnetic resonant frequency f_0, (eqn. (21)).

Intimate mixing of the oxides and some control of the particle sizes are achieved by prolonged ball milling.

The following expressions have been used to represent the frequency dispersive characteristics of $\mu_r'(f)$ and $\mu_r''(f)$ for the hexagonal ferrites in the computer simulation studies.
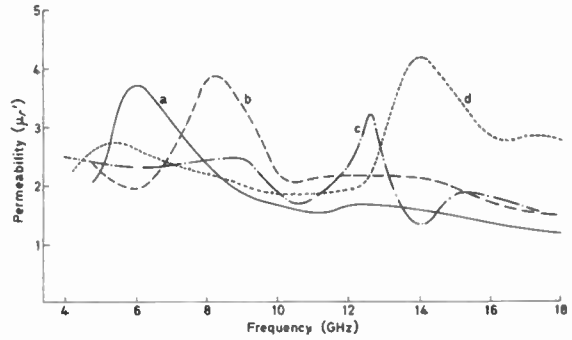
Fig. 11. Measured permeability dispersion characteristics of four hexagonal ferrites. (a) ——— ferrite 4; (b) – – – ferrite 3; (c) – · – ferrite 5; (d) ········ ferrite 2.

$$\mu_r'(f) = \frac{4}{\sqrt{S + (f_0 - f)^2}} \cosh \frac{2(f - f_0)}{f_0 + f/2} \qquad (21)$$

$$\mu_r''(f) = \mu_r'(f - 1.0) \qquad (22)$$

Where S controls the peak value of the permeability at the resonant frequency, and varies between 1 and 16 depending on the proportion of the binder added into the ferrite; f_0 is the resonant frequency; both f and f_0 are in GHz. These parameters were chosen so that equations (21) and (22) gave a realistic simulation of the material properties actually observed.

In theory the real and imaginary parts of the complex permeabilities are related through the following Hilbert transform[20]:

$$\mu'(f_1) - \mu_\infty = \frac{2}{\pi} \int_0^\infty \mu''(f) \frac{f}{f^2 - f_1^2} \, df$$

$$\mu''(f_1) = \frac{2}{\pi} \int_0^\infty \{\mu'(f) - \mu_\infty\} \frac{f_1}{f_1^2 - f^2} \, df$$

where f is the frequency used as a variable of integration. $\mu'(f_1)$ and $\mu''(f_1)$ are respectively the real and the imaginary parts of μ at a frequency f_1. μ_∞ is $\mu'(f)$ at $f = \infty$. Although checking of the above relationships against actual measurements is made difficult because of the measurement errors and insufficient available data, the general dispersive behaviour is verified.

8.4 Measurements
8.4.1 Ferrite properties

The complex permeabilities and the permittivities of the hexagonal ferrites were obtained from the measurements of the short-circuited and the open-circuited input
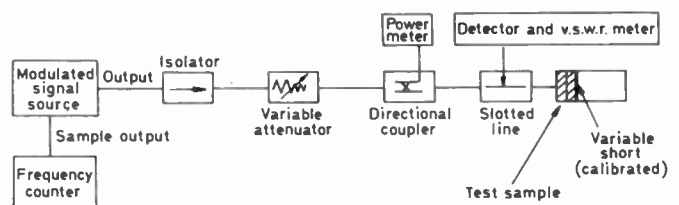

Fig. 12. Block diagram of the test rig for the measurement of the electromagnetic properties of ferrite.
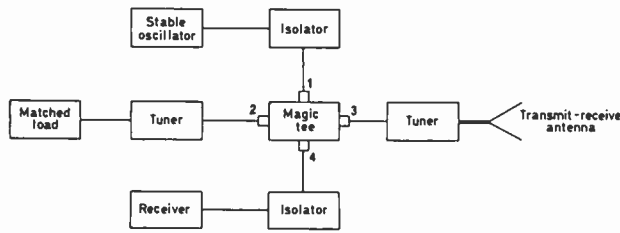
Fig. 13. Block diagram for the reflection loss measurements using magic-tee.

impedances (Z_{sc} and Z_{oc}) of a section of a transmission line (either coaxial or waveguide) completely filled with the test material.[11,12] The measurement procedure is somewhat lengthy and the circuit arrangement is given in Fig. 12.

The complex μ_r and ε_r were computed from the following equations:

$$Z_0 = (Z_{sc} \cdot Z_{oc})^{\frac{1}{2}} \tag{23}$$

$$\tanh(\gamma_0 d) = (Z_{sc}/Z_{oc})^{\frac{1}{2}} \tag{24}$$

$$\mu_r = \frac{jZ_0\gamma_0}{\{1 - (\lambda_0/\lambda_c)^2\}^{\frac{1}{2}}} \cdot \frac{\lambda}{2\pi} \tag{25}$$

$$\varepsilon_r = \left\{ \left(\frac{\lambda_0}{\lambda_c}\right)^2 - \frac{\gamma_0\lambda_0}{2\pi} \right\} \Big/ \mu_r \tag{26}$$

where Z_{sc} = short-circuited input impedance (normalized to that of free space) of the ferrite-filled transmission line (measured).

Z_{oc} = open-circuited input impedance as above (measured).

Z_0 = characteristic impedance of the ferrite-filled transmission line (computed).

γ_0 = propagation constant (computed).

λ_0 = free space wavelength at the frequency of operation.

λ_c = cut-off wavelength ($= 2a$ for waveguide and infinity for coaxial line).

d = thickness of the ferrite sample.

Equations (23) to (26) do not, however, yield unique values for μ_r and ε_r as the term $\tanh(\gamma_0 d)$ in equation (24) is periodic with a periodicity of $(jn\pi)$ (i.e. $\tanh \gamma_0 d = \tanh(\gamma_0 d + jn\pi)$). μ_r and ε_r will thus vary with n. It is therefore necessary to measure at least two specimens of different thicknesses for the same material and accept only the coinciding values in both the cases.

8.4.2 Reflectivity measurements

The microwave reflecting properties of absorbers were measured in terms of the relative reflectivity with respect to a perfectly conducting body of identical shape and dimensions. A mono-static system[13] employed for the measurement is shown in Fig. 13. An r.f. signal entering at port 1 of the magic-tee is equally divided and propagates through the arms 2 and 3 which are match-terminated, while the port 4 remains isolated. However, a reflected signal from the target entering the horn is divided equally in the magic-tee and one half is detected in the receiver in arm 4, while the other half is dissipated in the matched load in arm 2.

Any spurious signal due to scattering from the background or any part of the measurement rig is cancelled by a nulling technique. The tuner in port 2 is adjusted so that any spurious reflection entering port 3 is cancelled in the magic-tee by the cancelling signal generated by the reflection in arm 2. This system requires excellent frequency stability of the r.f. signal source in order to maintain the null over a reasonable time interval.

The Authors

Banie Amin (Member 1979) was educated at Bangladesh University of Engineering and Technology, Dacca where he received the B.Sc.Eng. degree in electrical engineering in 1968. He was awarded the M.Eng. and Ph.D. degrees by the University of Sheffield in 1974 and 1977, respectively. After graduation, he spent a short time in industry before being appointed a Lecturer in Electrical Engineering at the Bangladesh Engineering University. From January 1978 to August 1980 he held the position of a Senior Research Scientist at the Royal Military College of Science, Shrivenham, where his research activities included investigations of radar absorbent materials and their applications in microwave absorbent coatings and radar invisible antenna. Dr Amin has been with the Automation and Control Section of the Independent Broadcasting Authority since August 1980.

Jim James (Fellow 1975, Member 1960, Graduate 1956) has been a member of the academic staff at the Royal Military College of Science since 1961. He has published widely on research and development work in the fields of microwaves, antennas and speech processing, including papers in the Institution's Journal, for one of which he received the Heinrich Hertz Premium for 1973, and he is currently working on electromagnetics and communication systems. He was appointed to a Research Chair in Electronics in 1976. Professor James was a member of the Papers Committee from 1970 to 1978 and its Chairman from 1972 to 1975; after completing a three-year period of service as an Ordinary Member of the Council he served as a Vice-President from 1975 to 1978 and also since 1979. He is also a member of the Executive Committee.

Techniques for utilization of hexagonal ferrites in radar absorbers

Part 2
Reduction of radar cross-section of h.f. and v.h.f. wire antennas

Professor J. R. JAMES, B.Sc., Ph.D., D.Sc., F.I.M.A., C.Eng, F.I.E.E., F.I.E.R.E*

and

M. B. AMIN, B.Sc., M.Eng., Ph.D., S.M.I.E.E.E., C.Eng., M.I.E.R.E.†

SUMMARY
Coatings of hexagonal ferrites on a wire antenna reduce its back-scattering radar cross-sections (r.c.s.) at microwave frequencies without causing significant deterioration of its radiation efficiency at the h.f. and v.h.f. communication bands. The back-scattering r.c.s. of an infinitely long conducting cylinder coated with a multi-layer of hexagonal ferrites is derived and the result modified to take account of the finite length of a monopole antenna. Computed results for layered coatings are presented to demonstrate the improvement in the microwave absorption bandwidth obtainable for a given coating thickness. It follows that the technique is best applied with all material and geometric parameters having a tapered distribution and the ferrimagnetic resonances staggered over the required frequency band. Finally, the theory is illustrated by the measurement of the back-scattering losses of a v.h.f. ferrite-coated antenna in the microwave frequency band (for both TM and TE polarizations of the incident waves) and its radiation performance at the v.h.f. range.

* *Department of Electrical and Electronic Engineering, Royal Military College of Science, Shrivenham, Swindon, Wiltshire SN6 8LA*
† *Formerly at the Royal Military College of Science; now with the Independent Broadcasting Authority, Crawley Court, Winchester, Hants, SO21 2QA.*

List of symbols

ψ	vector potential
∇	vector operator (del)
ω	angular frequency
$\mu_0, \varepsilon_0, k_0$	permeability, permittivity and wave number in free space
$\mu_i, \varepsilon_i, k_i$	permeability, permittivity and wave number of the material in the ith layer
μ_r', μ_r''	real and imaginary parts of relative permeability
n	number of layers
r, ϕ, z	cylindrical coordinates
t	time
J_p, J_p'	Bessel function of order p and its derivatives
$H_p^{(1)}, H_p^{(1)\prime}$	Hankel function of the first kind, order p and its derivatives
H^{sca}, H^{inc}	scattered and the incident magnetic fields
E^{sca}, E^{inc}	scattered and the incident electric fields
η_p	Neumann factor
l, F	length and the reduction factor of the monopole
σ_N, σ_B	back-scattering radar cross-sections in two-dimensional and three-dimensional cases
R	scattering loss factor

1 Introduction

A technique for the utilization of narrowband hexagonal ferrite materials to design wide bandwidth radar absorbers has been dealt with in part 1 of this paper.[1] The present paper considers the deployment of the materials on v.h.f. and h.f. wire antennas to reduce their radar cross section (r.c.s.) at microwave frequencies and the subsequent effect on the antenna efficiency within the communication band. Clearly, a reduction in r.c.s. at microwave frequencies could be achieved by cladding any absorbent material around the antenna, but this may impair the action of the antenna if the material retains its lossy behaviour over the lower frequency range of operation of the antenna. The novelty of the present method[2] is that the dispersive nature of the hexagonal-ferrites is used to bring about the frequency-conscious loss behaviour of the cladding material. The cladding increases the cross-sectional size of the antenna, but also reduces the length of the wire needed to bring the antenna to resonance at any given frequency.[3] Increasing the cross-sectional size increases the antenna r.c.s. whereas the reduction of the antenna length together with the absorption of incident microwaves within the cladding are factors which reduce the r.c.s. The combined effects are investigated here by first analysing the two-dimensional r.c.s. of an infinitely-long coated cylinder and then modifying the results to estimate the r.c.s. of an antenna of finite length. The r.c.s. are calculated in the back direction and the term back-scattering is referred to throughout the paper.

Dielectric and ferrite claddings have been investigated[3-6] in recent years for size reduction of v.h.f. and h.f. communication antennas. For these applications the cladding materials are arranged to be as loss-free as possible to achieve good antenna efficiencies over the communication bands. At microwave frequencies these clad antennas, though reduced in size, have significant r.c.s. due to the severe mismatch at their air/cladding boundaries. Ideally for low r.c.s. at microwave frequencies we require a lossy coating and a good match at the air/material interface which as previously noted[1] demands the existence of a material with significant permeability at microwave frequencies. Even if such a material existed, problems would occur when the antenna was operated in the intended communications wavebands since the presence of appreciable loss in the material would degrade the antenna efficiency.

Recent investigations[12, 13] have shown that hexagonal ferrites possess moderate values of magnetic permeability and permittivity with negligible loss tangents at v.h.f. and h.f. communication bands while at the higher u.h.f. range the relative permeability drops down to near unity though retaining the high values for permittivity with some increase in the loss tangents. However beyond u.h.f. at microwave frequencies they show a narrowband ferrimagnetic resonance, with relative permeability rising to a peak of up to 5 with an associated increase in the magnetic loss tangents, the exact frequency of resonance being dependent on the composition of the particular ferrite. Application of hexagonal ferrites in layers having individual narrow ferrimagnetic resonant band can reduce the back-scattering cross-section of the composite structure over a broad bandwidth at microwave frequencies.

The back-scattering r.c.s. of an infinitely long conducting cylinder coated with n layers of ferrites is derived in Section 2 and also the back-scattering reduction factor due to reduction in height of the communication antenna resulting from the ferrite coating is examined. In Section 3 analytical results are used to investigate the different design techniques and experimental results are presented where suitable materials are available. Discussions of the results and conclusions are presented in Section 4.

2 Theory

2.1 Radar Cross-section of a Multilayer Ferrite-coated Conducting Cylinder

An infinitely-long conducting cylinder of radius a_0 is coated with n concentric layers of homogeneous ferrites; the outer radius, permittivity and permeability of the ith layer are denoted by a_i, ε_i and μ_i respectively, (Fig. 1). μ_0 and ε_0 are respectively the permeability and the permittivity of the free space. The axis of the cylinder is oriented to lie along the z-axis and the incident wave is normal to it. It is convenient to treat the problem separately for two cases: (i) the transverse magnetic
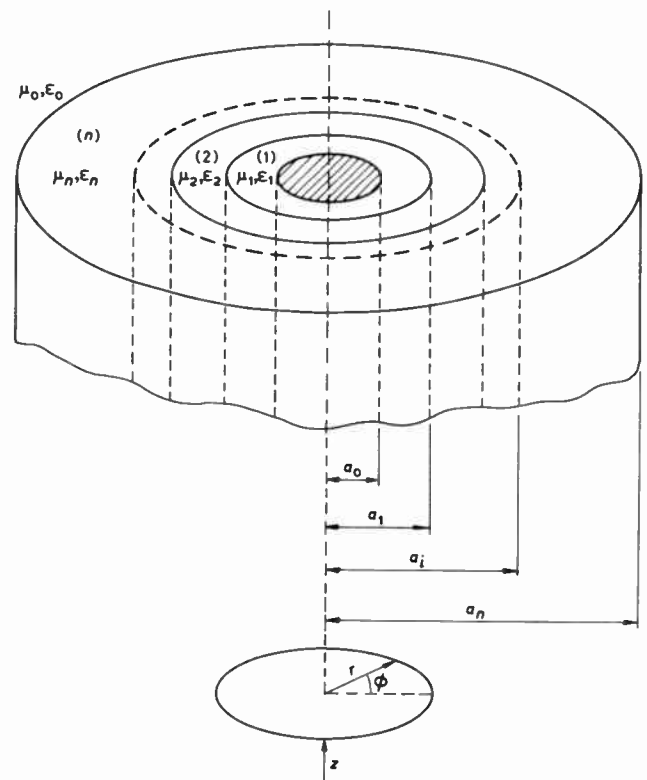
Fig. 1. A metal cylinder of infinite length coated with n layers of ferrites (cylindrical co-ordinates also shown).

(TM) case, in which the magnetic field is perpendicular to the axis of the cylinder, and (ii) the transverse electric (TE) case, where the magnetic field is parallel to the axis of the cylinder. The case of arbitrary polarization of the incident wave may be treated by a suitable combination of the TM and TE solutions.

The electric and the magnetic fields in each of the regions (1) to (n) and also in the free space can be derived from the wave function ψ, which must satisfy the Helmholtz equation $(\nabla^2 + k_i^2)\psi = 0$, where k_i is the wave number $(= \omega\sqrt{(\mu_i\varepsilon_i)})$ in the particular region.[8]

As the field is independent of the z-axis, the Helmholtz equation in cylindrical co-ordinates can be written as,

$$\frac{1}{r}\frac{\partial}{\partial r}\left(r\frac{\partial\psi_z}{\partial_r}\right) + \frac{1}{r^2}\frac{\partial^2\psi_z}{\partial\phi^2} + k^2\psi_z = 0. \tag{1}$$

An incident plane wave of unit amplitude which satisfies equation (1) in free space $(r \geqslant a_n)$ is

$$\psi_z = e^{j(k_0 r - \omega t)} \tag{2}$$

where r is the radius vector from the origin to the point of observation. Expressing the right-hand side of equation (2) in cylindrical co-ordinates at $r \geqslant a_n$:

$$\psi_z^{\text{inc}} = e^{-j\omega t}\sum_{p=-\infty}^{\infty} J_p(k_0 r)e^{jp\phi} \tag{3}$$

when $J_p(k_0 r)$ is the Bessel's function of the first kind of order p and argument $k_0 r$. The time dependence is omitted from the remainder of this paper.

220

The resulting scattered field in the free space ($r \geqslant a_n$) is of the form

$$\psi_z^{sca} = \sum_{p=-\infty}^{\infty} B_{p_0} H_p^{(1)}(k_0 r) e^{jp\phi}. \tag{4}$$

$H_p^{(1)}(kr)$ is the Hankel function of the first kind of order p and argument kr. The field in the ith region ($i = 1, 2, \ldots, n$) is the summation of the incident and the scattered field:

$$\psi_z = \sum_{p=-\infty}^{\infty} \{A_{p_i} J_p(k_i r) + B_{p_i} H_p^{(1)}(k_i r)\} e^{jp\phi}. \tag{5}$$

In equation (5), the first term involving A_{p_i} represents the incident field, while the second term involving B_{p_i} is the scattered field in any particular region. The field function ψ_z will be periodic with respect to ϕ and so the value of p is limited to integers only ($p = 0, \pm 1, \pm 2, \ldots$).

The wave function ψ_z which is assumed to be parallel to the z-axis is used to derive the tangential components of the electric and the magnetic fields for both the TM and TE cases.[8]

TM case:
$$\left. \begin{array}{l} E_z = k^2 \psi_z \\[2mm] H_\phi = j \dfrac{k^2}{\omega\mu} \dfrac{\partial \psi_z}{\partial r} \end{array} \right\} \tag{6}$$

TE case:
$$\left. \begin{array}{l} H_z = k^2 \psi_z \\[2mm] E_\phi = -j\mu\omega \dfrac{\partial \psi_z}{\partial r} \end{array} \right\} \tag{7}$$

The coefficients A_p and B_p in equations (4) and (5) are obtained by involving the boundary conditions for the tangential components of the electric fields (E_z, E_ϕ) and the magnetic fields (H_ϕ, H_z) at the interface between adjacent layers and at the conducting surface at $r = a_0$. Since only the scattered field outside the multilayer cylinder ($r \geqslant a_n$) is of interest, only B_{p_0} in equation (4) has been derived and is given by

$$B_{p_0} = \frac{Q_{p_n} J_p(k_0 a_n) - J_p'(k_0 a_n)}{H_p^{(1)\prime}(k_0 a_n) - Q_{p_n} H_p^{(1)}(k_0 a_n)} \tag{8}$$

J_p' and $H_p^{(1)\prime}$ are respectively the derivatives of J_p and $H_p^{(1)}$ with respect to their arguments. Q_{p_n} in equation (8) is obtained separately for TM and TE cases.

TM case:

$$T_{p_1} = \frac{J_p(k_1 a_0)}{H_p^{(1)}(k_1 a_0)} \tag{9}$$

$$Q_{p_i} = \frac{J_p'(k_i a_i) + T_{p_i} H_p^{(1)\prime}(k_i a_i)}{J_p(k_i a_i) + T_{p_i} H_p^{(1)}(k_i a_i)} \frac{\varepsilon_i k_{i+1}}{\varepsilon_{i+1} k_i} \tag{10}$$

$$T_{p_{i+1}} = \frac{Q_{p_i} J_p(k_{i+1} a_i) - J_p'(k_{i+1} a_i)}{H_p^{(1)\prime}(k_{i+1} a_i) - Q_{p_i} H_p^{(1)}(k_{i+1} a_i)} \tag{11}$$

$$i = 1, 2, \ldots, n.$$

TE case:

$$T_{p_1} = \frac{J_p'(k_1 a_0)}{H_p^{(1)\prime}(k_1 a_0)} \tag{12}$$

$$Q_{p_i} = \frac{J_p'(k_i a_i) + T_{p_i} H_p^{(1)\prime}(k_i a_i)}{J_p(k_i a_i) + T_{p_i} H_p^{(1)}(k_i a_i)} \frac{\mu_i k_{i+1}}{\mu_{i+1} k_i} \tag{13}$$

$$T_{p_{i+1}} = \frac{Q_{p_i} J_p(k_{i+1} a_i) - J_p'(k_{i+1} a_i)}{H_p^{(1)\prime}(k_{i+1} a_i) - Q_{p_i} H_p^{(1)}(k_{i+1} a_i)} \tag{14}$$

$$i = 1, 2, \ldots, n.$$

For both TM and TE cases, Q_{p_n} is obtained by following the sequence of successively computing T_{p_1} and Q_{p_1} and then T_{p_2} and Q_{p_2} and so on in an ascending order of the subscript of p until Q_{p_n} is reached by using the equations (9–11) or (12–14) above.

The back-scattering r.c.s. is defined[9] as the ratio of the total power scattered by a fictitious isotropic scatterer which scatters energy in all directions with intensity equal to that scattered directly back towards the source by the actual scattering object, to the incident power per unit area on the scatterer. In the two-dimensional case such as the infinitely long cylinder currently being discussed, the back-scattering r.c.s. is given by

$$\sigma_N = 2\pi r \left|\frac{E^{sca}}{E^{inc}}\right|^2 \quad \text{or} \quad 2\pi r \left|\frac{H^{sca}}{H^{inc}}\right|^2 \tag{15}$$
$$\scriptstyle r\to\infty \qquad\qquad\qquad r\to\infty$$

where E^{sca} and E^{inc} (or H^{sca} and H^{inc}) are respectively the scattered and the incident fields at a distance r from the axis of the cylinder in the direction of the source.

Using equations (2), (4), and (7), for TE mode of propagation, $k_0 r \gg 1$ and $\phi = 180°$:

$$|E_\phi^{inc}| = \omega k_0 \mu_0 \tag{16}$$

$$|E_\phi^{sca}| \simeq \omega\mu_0 \sqrt{\frac{2k_0}{\pi r}} \left| \sum_{p=-\infty}^{\infty} (-1)^p B_{p_0} \right|. \tag{17}$$

For TM mode, H^{inc} and H^{sca} at $k_0 r \gg 1$ and $\phi = 180°$ are obtained using equations (2), (4) and (6):

$$|H_\phi^{inc}| = \omega k_0 \varepsilon_0 \tag{18}$$

$$|H_\phi^{sca}| \simeq \omega\varepsilon_0 \sqrt{\frac{2k_0}{\pi r}} \left| \sum_{p=-\infty}^{\infty} (-1)^p B_{p_0} \right|. \tag{19}$$

It can be seen from equations (9–11) for TM mode or equations (12–14) for TE mode that $Q_{p_i} = Q_{-p_i}$, which when substituted in equation (8) gives $B_{p_0} = B_{-p_0}$. Using this condition and substituting equations (10) and (17) or equations (18) and (19) in equation (15), the two-dimensional r.c.s. σ_N is obtained.

$$\sigma_N = \frac{4}{k_0} \left| \sum_{p=0}^{\infty} \eta_p (-1)^p B_{p_0} \right|^2 \tag{20}$$

where η_p is the Neumann factor and is

$$\eta_p = 1, p = 0 \qquad \eta_p = 2, p \neq 0.$$

The scattering loss factor R, defined as the reduction in

the back-scattering r.c.s. (expressed in decibels) due to the application of the microwave absorbent coatings on the conducting cylinder, is

$$R = -20 \log_{10} \left| \frac{\sum_{p=0}^{\infty} \eta_p (-1)^p B_{p_0}^n}{\sum_{p=0}^{\infty} \eta_p (-1)^p B_{p_0}^0} \right| \text{dB} \quad (21)$$

where, $B_{p_0}^0$ and $B_{p_0}^n$ are the values of B_{p_0} for the cases when the number of coatings are 0 and n respectively and obtainable from equations (8)–(14). Although the final expression for σ_N and R, (eqns (20) and (21)) are same for both the TE and TM modes of polarization of the incident field, B_{p_0} will be different in the two separate cases.

2.2 Modification for a Finite Length Cylinder
For a thick cylinder of length l, the vector potential for the scattered field ψ^{sca} in the direction of the source is:[7]

$$\psi_y^{sca} = \frac{jk_0 l e^{-jk_0 r}}{r} \sum_{p=-\infty}^{\infty} (-1)^p B_{p_0} \quad (22)$$

$$E_y^{sca} = k_0^2 \psi_y^{sca} \quad (23)$$

$$|E_y^{inc}| = \omega \mu_0 k_0. \quad (24)$$

The above field equations are for TE polarization of the incident wave normal to the axis of the cylinder and ψ_y and E_y are same as ψ_ϕ and E_ϕ for $\phi = 0$ as used in Section 2.1. B_{p_0} is obtained as before using equations (8) and (12)–(14).

The radar cross-section due to a three-dimensional scatterer is given by

$$\sigma_B = 4\pi r^2 \left| \frac{E^{sca}}{E^{inc}} \right|^2_{r \to \infty}. \quad (25)$$

Using equations (23) and (24) in (25):

$$\sigma_B = \frac{4l^2}{\pi} \left| \sum_{p=0}^{\infty} \eta_p (-1)^p B_{p_0} \right|^2. \quad (26)$$

For TM polarization of the incident wave and for normal incidence, the expression for σ_B will again be same as in equation (25), but the value of B_{p_0} will be given by equations (8)–(11). Thus, it is apparent that inclusion of the term $(l^2 k_0/\pi)$ in equation (20) takes account of the effect of finite length thus allowing the back-scattering r.c.s. of a monopole antenna to be estimated.

Application of ferrite coatings causes a reduction of the resonant height of the communication antenna by a factor F ($F = l_2/l_1$, where l_1 is the uncoated resonant length and l_2 the length required for resonance after the application of the coatings), F depending on the thickness, the permittivity and the permeability of the material at the communication frequency band.[3] Thus from equation (26), the scattering loss factor R of a monopole antenna coated with n layers of ferrite is

$$R = -\{20 \log_{10} \left| \frac{\sum_{p=0}^{\infty} \eta_p (-1)^p B_{p_0}^n}{\sum_{p=0}^{\infty} \eta_p (-1)^p B_{p_0}^0} \right| + 20 \log_{10} F\} \text{dB} \quad (27)$$

where $B_{p_0}^0$ and $B_{p_0}^n$ are same as in equation (21). The first term in the right-hand side of equation (27) gives the change in the back-scattering r.c.s. of the antenna due to the application of the coating, while the second term takes account of the effect due to any reduction in the antenna height. If the coating is to provide a degree of invisibility then the R values of equations (21) and (27) must be positive.

3 Computed and Experimental Results
3.1 Computed Results
A computer program based on equation (20) was checked by computing the back-scattering r.c.s. of (i) an infinitely-long uncoated metal rod as a function of its radius a_0, and (ii) an infinitely-long metal rod of 4·71 mm in radius (a_0) coated with a single layer of dielectric ($k = \omega\sqrt{(2·54\varepsilon_0)}$) and outer radius of the coating $= a$) for TM polarization of the incident wave. The results given in Fig. 2 agree completely with those available in the literature.[9,10]
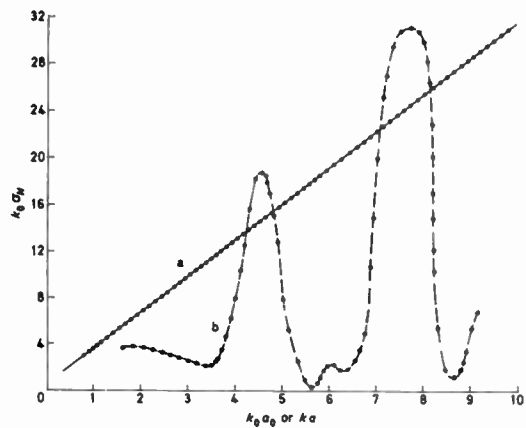

Fig. 2. Scattering cross-section as a function of the diameter of an infinitely long cylinder.
(a) ——— metal cylinder with no coating (Refs 9, 10)
(b) – – – metal cylinder (diameter = 9·42 mm) coated with single layer of dielectric ($\varepsilon_r = 2·54$) (Refs 9, 10)
(OOOO computed results, eqn. (20))

Figures 3–6 give the scattering loss factor, R, (eqn. (21)) plotted against frequency for a given layer thickness (2 mm) and number of layers in the coating. Figure 3 compares the relative improvements in the microwave absorptions obtained by coating a metal cyclinder (diameter = 1 cm) with a 2 mm thick layer of hexagonal ferrites as opposed to a dielectric having a permittivity value same as that of the ferrite. The zero-dB line, curve (a) gives the back-scattering loss factor for the uncoated cylinder for TM polarization of the incident wave and this will henceforth be taken as a reference to identify any
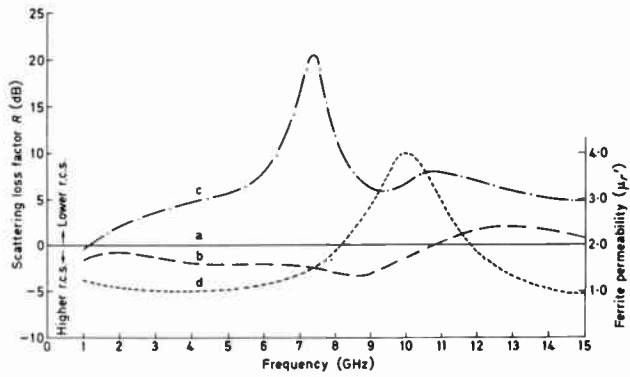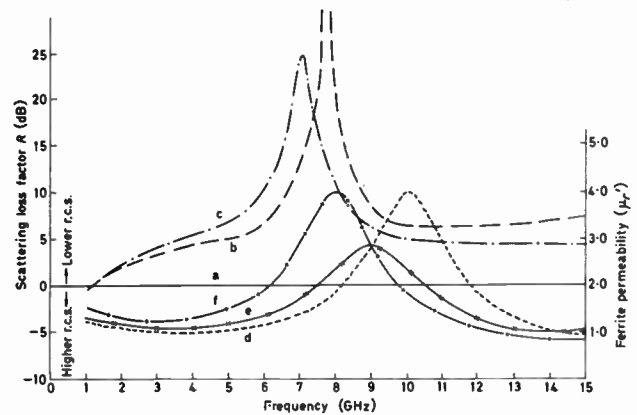
Fig. 3. Back-scattering power loss characteristics of ferrite and dielectric coated metal cylinder (diameter = 10 mm) of infinite length, overall coating thickness = 2 mm.
(a) ——— uncoated cylinder for reference.
(b) – – – cylinder coated with single layer dielectric, $\varepsilon_r = 10 - j\,1$.
(c) — · — · — cylinder coated with single layer of ferrite, permeability dispersion given by (d).

improvement in the microwave absorption due to the application of the coating. (b) shows the back-scattering losses by the same target when it is coated in a single layer with a 2 mm thick lossy dielectric having $\varepsilon_r = 10 - j1$. It is seen that by doing so the radar cross-section has increased with respect to the uncoated rod over almost the whole frequency range. This is due to the increase in the overall diameter of the scatterer without the provision of any impedance matching of the coating with the free space. (c) represents the scattering losses when the metal rod is coated with a layer of 2 mm thick hexagonal ferrites whose μ_r'-dispersion is given in (d). The μ_r''-dispersion curve of the ferrites has a frequency behaviour similar to the μ_r'-curve but shifted upwards in frequency by 1 GHz. A comparison of curves (a) and (c) illustrates the benefit in terms of higher scattering losses over a broad frequency range obtainable by coating an antenna-wire with hexagonal ferrites.
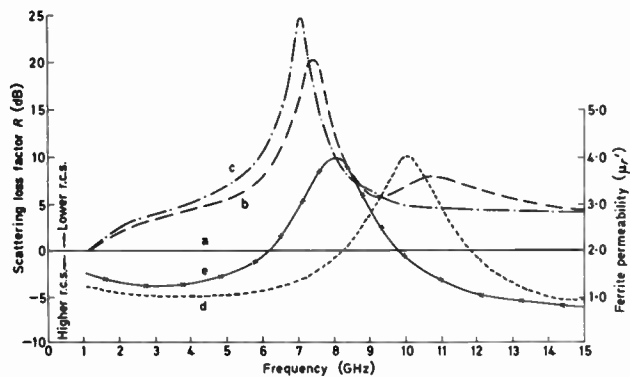
Fig. 4. Back-scattering power loss characteristics of ferrite coated metal cylinder (diameter = 10 mm) of infinite length, overall coating thickness = 2 mm.
(a) ——— uncoated cylinder for reference.
(b) – – – cylinder coated with a single layer ferrite, permeability dispersion given by (d).
(c) — · — · — cylinder coated with 2 layers of ferrites, permeability dispersions given by (d) adjacent to metal $i = 1$ and (e) adjacent to air $i = 2$

Figure 4 shows the relative merits in layering the ferrites in the coating in respect of the reduction of back-scattering. (b) represents the scattering loss factor when the metallic cylinder whose original scattering losses are given in (a) is coated with a single layer of hexagonal ferrites of 2 mm thick, while (c) for the same antenna when coated with 2 layers of ferrites, each of which is 1 mm thick. (d) shows the characteristics of ferrites used in (b); while (d) and (e) are the μ_r'-dispersions of ferrites used in (c). In both the cases (b) and (c), the ferrite material constants have not been diluted with a binder to improve the impedance matching at the layer interfaces. A comparison of their reflection losses does not suggest any noticeable improvement obtainable only by layering without paying any attention to the proper impedance matching of the coating with free space for a smooth transition of the electromagnetic waves at the interfaces.

Fig. 5. Back-scattering power loss characteristics of ferrite coated metal cylinder (diameter = 10 mm) of infinite length, total coating thickness = 2 mm.
(a) ——— uncoated metal cylinder for reference.
(b) – – – cylinder coated with 2 equal thickness layers of ferrites, top layer diluted for impedance matching and permeability dispersions given by (d) $i = 1$ and (e) $i = 2$.
(c) — · — · — cylinder coated with 2 equal thickness layers of ferrites none diluted and permeability dispersions given by (d) $i = 1$ and (f) $i = 2$

Figure 5 illustrates the improvement in the absorption bandwidth by diluting the top layer for the impedance matching in a two-layer coating. (a) as before is the reference curve and (b) shows the scattering losses due to a TM incident wave when the antenna is coated in two layers; the permeability dispersion of the first layer is given by (d) and that of the top layer by (e). As in practice, ferrites will be mixed with a dielectric binder having a relative permittivity very near to unity, a corresponding dilution of the permittivity values has been taken into account in the computation. (c) represents the scattering losses when the permeability characteristics of the two layers are given by (d) and (f); none of them is diluted for an impedance matching. It is seen that an improvement in the scattering losses in (d) (with respect to those given by (c)) has been achieved by
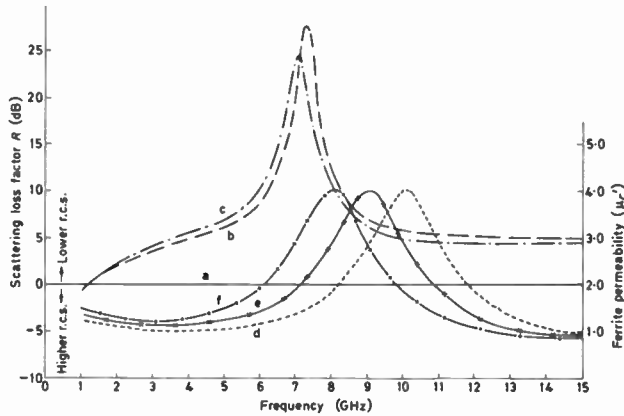
Fig. 6. Back-scattering power loss characteristics of ferrite coated metal cylinder (diameter = 10 mm) of infinite length, total coating thickness = 2 mm.
(a) ——— uncoated metal cylinder for reference.
(b) – – – cylinder coated with 2 equal thickness layers of ferrites, permeability dispersions given by (d) $i = 1$ and (e) $i = 2$.
(c) – · —ᴛ· – cylinder coated with 2 equal thickness layers of ferrites, permeability dispersions given by (d) $i = 1$ and (f) $i = 2$.

the process of dilution of the first layer.

Figure 6 compares the reflection losses from an antenna coated with two layers of undiluted ferrites of thickness 1 mm each; curve (b) is when the resonances of the materials in two layers are separated by 1 GHz and μ_r'-dispersions given by (d) and (e); while curve (c) is when the material resonances are separated by 2 GHz and their μ_r'-dispersions are given by (d) and (f). These two sets of results do not provide any conclusive evidence as to the advantage of the separation of the resonances of the materials in different layers. It is, however, envisaged that if proper impedance matching technique (such as dilution of the outer layer, control of the individual layer thicknesses, etc.) was adopted, some advantage can be achieved by varying the separation of the resonances in different layers as in the case of planar absorbers.[1]

3.2 Experimental Results

A number of ferrite-coated monopole antennas were constructed by encasing a cylindrical rod of 30 cm in length and 6·20 mm in diameter with annular rings of hexagonal ferrites whose inner diameter was same as that of the rod; the outer diameter of the rings is 14·15 mm. The conducting core of the antenna was attached to the inner conductor of an N-type coaxial connector whose outer fitted normal to a large plane metal sheet which formed the ground plane for the monopole. The reflection losses due to the ferrite cladding was obtained at X-band frequencies by comparing the reflected power due to the antenna with and without the coating and measured by adopting the technique described in Appendix 8.4, Part 1 of this paper.[1] The reflected power was measured by a sensitive detector by holding the antenna in front of the radiating horn at a fixed distance from its open end with orientation corresponding to

both the TE and the TM modes of polarization of the incident wave. Only a part of the whole length was illuminated to reduce the end effect which would otherwise affect the result for the finite length of the antenna and the error due to the slight spherical nature of the plane wave in the near field of the radiating horn was ignored. Among the coating materials tested, the ferrite-4 (as in Part 1 of this paper) which possesses a ferrimagnetic resonance in the X-band was found to be most promising in this frequency range. The measured electromagnetic properties of the above mentioned hexagonal ferrite at X-band frequencies were substituted in the equation (21) to compute the scattering loss factor R due to the single layer coating. Figure 7 (a and b) compares the experimental and theoretically predicted
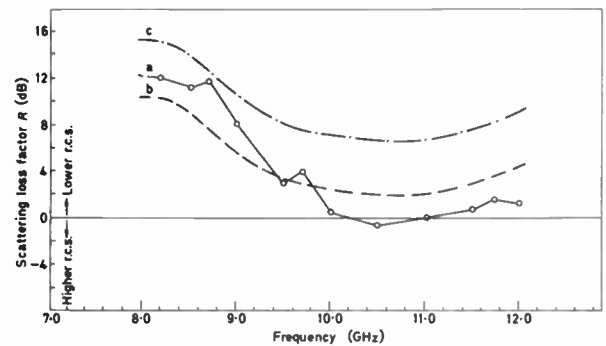

Fig. 7. Experimental and theoretical back-scattering losses of a ferrite coated antenna (wire diameter = 6·2 mm, coating thickness = 3·975 mm), TM mode.
(a) –O—O— experiment, two-dimensional.
(b) – – – theory, two-dimensional (eqn (27), first term).
(c) – · — · – theory, including reduction factor (eqn (27)).

reflection losses due to the application of the ferrite-coating on the antenna for TM-modes, while those for TE-mode of polarization of the incident wave are given in Fig. 8 (a and b). The zero-dB line in both the cases corresponds to the reflections when there is no coating on the antenna-wire. The experimental and the theoretical results agree fairly closely, at least in trend,
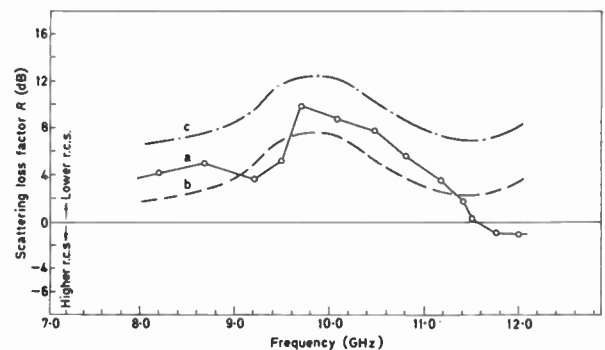

Fig. 8. Experimental and theoretical back-scattering losses of a ferrite coated antenna (wire diameter = 6·2 mm, coating thickness = 3·975 mm), TE mode.
(a) –O—O— experiment, two-dimensional.
(b) – – – theory, two-dimensional (eqn (27), first term).
(c) – · — · – theory, including height reduction (eqn (27)).

within the limits of the experimental errors. It is observed that in both the cases peaks of the reflection losses correspond as expected with the ferrimagnetic resonances of the cladding material.

3.3 Coated Antenna Performance at V.H.F.

The ferrite cladding technique[14] can be employed to reduce the height of h.f. and v.h.f. communications antennas. A 30 cm long monopole (diameter = 6·2 mm) having an unloaded quarter-wavelength resonance at 250 MHz resonated at 190 MHz, a height reduction factor $F = 0.76$ when coated with hexagonal ferrites of thickness 3·975 mm. The corresponding reduction factor computed using the theoretical analysis of James and Henderson[14] was $F = 0.6$; the discrepancy is attributed to a combination of effects due to measurement errors, the approximation postulated in the analysis and the uncertainty about the material parameters. No experimental result is available on the free-space measurement for the three-dimensional r.c.s. loss due to the coating on the antenna; the higher reduction factor F will, however, according to equation (27) contribute a further amount $20 \log_{10} F = -4.44$ dB (for $F = 0.6$) to be added to the r.c.s. in the two-dimensional case given by (b) in Figs 7 and 8. The combined theoretical reflection losses are illustrated by (c) in both the Figures. The efficiency of the monopole measured at the quarter-wavelength resonant frequency using Wheeler can method[11] was reduced to 92% due to the losses in the coating.

4 Conclusions

Equations have been derived for computing the microwave radar cross-sections of an infinitely-long conducting cylinder coated with n layers of ferrites for both TE and TM modes of polarizations of the incident wave. These with necessary modifications for the finite length have been applied to compute the scattering losses in the three-dimensional case of ferrite-coated antennas. Back-scattering at the microwave frequencies can be reduced significantly by coating the antenna-wire with layers of hexagonal ferrites. A single coating usually results in a narrow band absorption at the ferrimagnetic resonance of the materials in the coating, while broadband reflection losses can be obtained by applying the hexagonal ferrites in multi-layers, provided a proper care is taken for impedance matching at the layer-interfaces by tapering the layer thicknesses, diluting the materials in the outer layers and spreading the ferrimagnetic resonances of the constituent materials over the required frequency band. The hexagonal ferrite coatings by virtue of their high permittivity and permeability with negligible loss tangents at h.f. and v.h.f. bands reduce the physical height of the communication antenna, thus contributing further towards the reduction of r.c.s. at the microwave frequencies without significantly affecting the radiation efficiency at the communication band. Even when the advantage due to the height reduction is ignored, at least a 10 dB reflection loss is obtainable over a frequency band greater than 20% at the centre frequency by cladding the antenna with two layers of hexagonal ferrites of total thickness 2 mm. A further improvement in the microwave absorption is possible by optimizing the number of layers, layer-thicknesses and the controllable properties of the materials in the coating as discussed in Part 1.

Laboratory two-dimensional scattering measurements carried out on a ferrite-coated monopole demonstrate with good agreement the validity of the theoretical analysis. In practice the scattering from the antenna tip would modify the results somewhat but the overall advantage gained by the coating would be maintained; this can only really be checked with outdoor scattering measurements. The application of the technique to antennas radiating higher powers needs further measurements due to the slight loss of the antenna efficiency.

5 Acknowledgments

6 References

1 Amin, M. B. and James, J. R., 'Techniques for utilization of hexagonal ferrites in radar absorbers: Part 1, Broadband planar Coatings', *The Radio and Electronic Engineer*, **57**, no. 5, pp. 209–18, May 1981.

2 Amin, M. B., Henderson, A., James, J. R., Loyd, R. A. and Porter, G. B., British Patent Application.

3 James, J. R. and Henderson, A., 'Electrically short monopole antennas with dielectric or ferrite coatings', *Proc. Instn Elect. Engrs*, **125**, no. 9, pp. 793–803, September 1978.

4 James, J. R., Schuler, A. J. and Binham, R. F., 'Reduction of antenna dimension by dielectric loading', *Electronics Letters*, **10**, no. 10, pp. 263–5, 1974.

5 Richmond, J. H. and Newman, E. H., 'Dielectric coated wire antennas', *Radio Science*, **11**, no. 1, pp. 13–20, January 1976.

6 Smith, M., 'Properties of dielectrically loaded antennas', *Proc. Instn Elect. Engrs*, **124**, pp. 837–9, 1977.

7 Mentzer, J. R., 'Scattering and Diffraction of Radio Waves', pp. 94–108, (Pergamon Press, Oxford 1955).

8 Stratton, J. A., 'Electromagnetic Theory' (McGraw-Hill, New York, 1941).

9 Tang, C. C. H., 'Back-scattering from dielectric-coated infinite cylindrical obstacles', *J. Appl. Phys.*, **28**, no. 5, pp. 628–633, May 1957.

10 Rao, T. C. K. and Hamid, M. A. K., 'Scattering by a multi-layered dielectric coated conducting cylinder', *Intl J. Electronics*, **38**, no. 5, pp. 667–73, 1975.

11 Wheeler, H. A., 'The radian sphere around a small antenna', *Proc. IRE*, **47**, pp. 1325–31, August 1959.

12 Severin, H. and Stoll, P. J., *Z Angew Phys.*, **23**, no. 3, pp. 209–12, 1967.

13 Loyd, R. A. and Porter, G. B., Royal Military College of Science, Shrivenham, Unpublished report.

14 James, J. R. and Henderson, A., 'Investigation of electrically small v.h.f. and h.f. cavity-type antennas'. Proc. International Conf. on Antennas and Propagation, London, 1978, pp. 322–6. (IEE Conf. Proc. 169).

Developments in frequency-response determination using Schroeder-phased harmonic signals

Professor J. O. FLOWER,
B.Sc. (Eng.), Ph.D., C.Eng., F.I.E.E., F.I.Mar.E.*

and

S. C. FORGE, B.Sc., M.Sc., Ph.D.†

SUMMARY

A multi-frequency identification scheme employing Schroeder-specified relative phasing to achieve low-peak-factor excitation signals has been devised. These so-called Schroeder-phased harmonic signals have been proposed as a convenient multi-frequency signal for frequency-response testing offering high-power with low peak-factor and a flexible choice of test spectrum. In this paper the use of these signals is extended to obtain frequency-response information from multi-variable and sampled-data systems. Additionally there is a detailed discussion of the computational processes relevant to the use of these signals when the system output signals are contaminated significantly with noise.

* Department of Engineering Science, North Park Road, University of Exeter, EX4 4QF.
† Preece, Cardew and Rider, Consulting Engineers, Preston Park, Brighton.

1 Introduction

In previous papers[1,2] the authors have introduced Schroeder-phased harmonic signals (S-phs) as very straightforward practical multi-frequency test signals for obtaining the frequency-response characteristics of linear time-invariant systems. Indeed it is believed that this identification work was the first application of these signals. The usefulness of the S-phs stems mainly from the ease of signal design and modification, their efficiency, (i.e. power is injected at frequencies of interest only), and the facility with which these signals may be tailored to fit conveniently into digital-signal processing based on fast-Fourier transform (FFT) computational techniques.

The work reported here attempts to extend the range of applications of S-phs to the frequency-response testing of linear multi-variable systems and to sampled-data systems. Further the autocorrelation properties of these signals are exploited in attempting to reduce the effect that noise-contamination of system signals has on computed results. This is done by using these signals in a computational scheme based upon cross-power-spectral estimation.

2 S-phs and their Generation

S-phs are merely periodic signals composed of harmonics in which the relative phasing of these harmonics is arranged so that the *envelope* of a particular signal has a small variation of amplitude only. Signals of this form are said to have *low peak-factors*, i.e. the ratio of the maximum envelope excursion to the minimum approaches unity in the limit.[1,3]

A method of specifying the phases of the individual harmonics to achieve low-peak-factor signals has been suggested by Schroeder.[3] Although this method does not produce a mathematically-minimal peak-factor—indeed there is no known general way of producing the mathematical minimum—the variations in practice are quite small. Further the design of such signals is simple for the phasing prescription is simply related to the relative magnitudes of the harmonic components desired in the signal. For example, consider a signal of the form

$$r(t) = \sum_{k=1}^{N} (2p_k)^{\frac{1}{2}} \cos\left(\frac{2\pi kt}{T} + \phi_k\right),$$

where T is the periodic time and p_k is the relative power of the kth harmonic

$$\left(\text{i.e. } \sum_{k=1}^{N} p_k = 1\right)$$

and ϕ_k is the phase of this harmonic. For a S-phs the specification for the phases is given by the simple relation:[1]

$$\phi_k = 2\pi \sum_{i=1}^{k} i p_i \quad k = 1,2,\ldots,N.$$

Thus once the relative power of the harmonics has been decided the phase specification follows immediately, so that the S-phs can be generated quite easily and quickly via the inverse Fourier transform (or more conveniently in digital form by inverse Fast Fourier transform techniques) of the frequency-response amplitude profile.

3 Multi-variable Systems

In this Section the problem of using S-phs for measuring simultaneously the frequency-response for individual signal paths through a multi-input/multi-output system under test is considered. A major problem in this type of experiment is determining the proportion of each output signal that is due to each individual input-disturbance. Other workers have suggested the use of shifted pseudo-random binary sequences and pseudo-random tertiary sequences in such applications.[4] Here the approach is to excite simultaneously the inputs of the system with suitably designed S-phs and to identify the portion of each output signal (due to the corresponding input signal), as a gain- and phase-response curve either for some control-system design procedure,[5] or for use in system identification. The individual inputs are constructed to have mutually-exclusive harmonic components. It is assumed that the system under consideration is stable and may be specified in transfer-function form, and so will settle down to steady-state harmonic conditions some time after the excitation commences.

Each output signal, in general, will contain components of every harmonic which is present in all input signals. Thus if a harmonic analysis is performed on a particular output signal, then it is possible to assign each of the harmonics present as having arisen from a particular input. Provided enough harmonics are represented, a frequency response between each input and each output may be established from this procedure. The experiment may be repeated with the S-phs sets redistributed to different inputs, thus providing further data should this be desirable or necessary to give a sufficient number of points on individual frequency-response paths.

For example, consider a dual-input/dual-output system, then an experimental procedure might be to apply an S-phs composed entirely of the odd harmonics, of the basic frequency, at the first input and one composed entirely of the corresponding even harmonics at the other input. The harmonics should be closely enough spaced so that sufficient gain- and phase-points may be established.

An alternative scheme is to divide the spectral range of interest into bands of frequency and to rotate the inputs to build up the frequency response over the entire range of interest. The actual procedure to be adopted will depend upon consideration of the system being tested.

3.1 A Feedforward Example

The block diagram shown in Fig. 1 purports to represent a turbo-propeller system of an aircraft, described by Tou,[6] where the outputs are the engine speed and turbine-inlet temperature and the inputs are the deviations of the propeller-blade angle and of the fuel-rate flow. This system was simulated on an analogue computer and so analogue/digital effects are included in the results. It can be appreciated from the diagram that since the two inputs are directly linked to the output, i.e. no feedback paths are present, the technique discussed above reveals the frequency-response curves of the four blocks directly. A small computer system based upon a PDP11/20 digital computer was used to generate the two test-signals, to log the two responses, and to process the results.
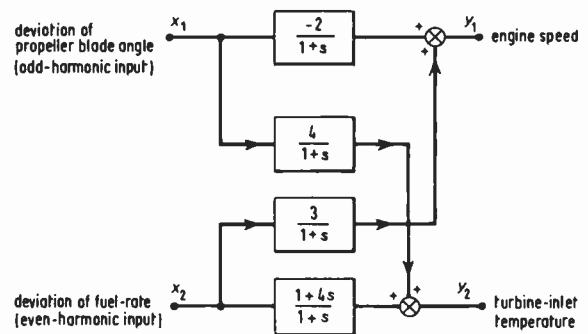

Fig. 1. Block diagram of propulsion system.

An odd-harmonic S-phs set was entered at input 1 and an even-harmonic S-phs set at input 2. The frequency response, i.e. the gain- and phase-functions, were computed for each input-output pair using only those harmonics that were common to each pair. The results obtained are shown in Fig. 2 together with the theoretically calculated values. The good correspondence is to be expected from such a simple experiment.

3.2 An Example Incorporating Feedback Elements

The block diagram of the system simulated in this application is shown in Fig. 3. This particular form was studied firstly because it does actually incorporate a feedback structure and, secondly, because it has the basic structure of a model, proposed by Morton,[7] for studying the dynamic relationships between forces and displacements existing as a shaft revolves in a journal bearing which was of particular interest to certain of the authors' mechanical engineering colleagues.

Examination of Fig. 3 reveals that four input/ouput frequency-responses may be written

$$\frac{Y_1(j\omega)}{X_1(j\omega)} = \frac{F_{11}(j\omega)}{F_T(j\omega)} \qquad \text{with } X_2(j\omega) = 0 \ (1)$$
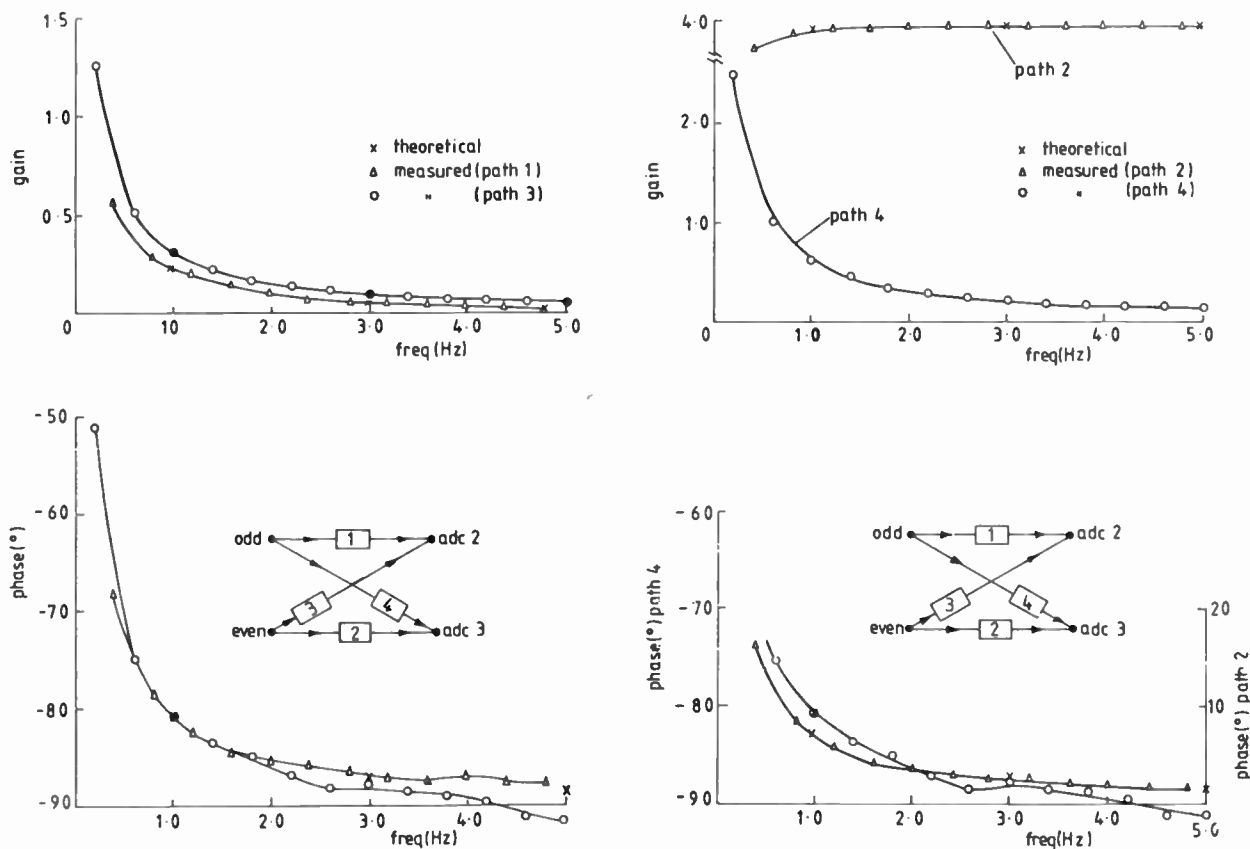
Fig. 2. Frequency-response diagrams for system shown in Fig. 1.

$$\frac{Y_1(j\omega)}{X_2(j\omega)} = \frac{F_{11}(j\omega)F_{21}(j\omega)F_{22}(j\omega)}{F_T(j\omega)} \text{ with } X_1(j\omega) = 0 \text{ (2)}$$

$$\frac{Y_2(j\omega)}{X_1(j\omega)} = \frac{F_{11}(j\omega)F_{12}(j\omega)F_{22}(j\omega)}{F_T(j\omega)} \text{ with } X_2(j\omega) = 0 \text{ (3)}$$

$$\frac{Y_2(j\omega)}{X_2(j\omega)} = \frac{F_{22}(j\omega)}{F_T(j\omega)} \qquad \text{with } X_1(j\omega) = 0 \text{ (4)}$$

where

$$F_T(j\omega) = 1 - F_{11}(j\omega)F_{12}(j\omega)F_{21}(j\omega)F_{22}(j\omega)$$

Now supposing the following experiment is performed on the system.

A S-phs composed of odd-harmonic terms only is entered at X_1 and simultaneously a S-phs composed of the complementary even-harmonic terms only is entered at X_2. If the steady-state ouput responses at Y_1 and Y_2 are logged and then Fourier analysed this would enable points on curves associated with equations (1) and (3) at the odd-harmonic frequencies to be established; similarly points on curves associated with (2) and (4) can be established at the even-harmonic frequencies.

Using these measured values the even-harmonic points corresponding to equations (1) and (3) can be established by interpolation and a similar process can be performed to obtain estimates at the odd-harmonic points corresponding to equations (2) and (4). All this

may be arranged easily within the computer including any smoothing of the data that may be necessary. Thus the frequency-response functions specified by equations (1), (2), (3) and (4) can be established at *all* harmonics of interest.

Further progress concerning the identification of the individual blocks $F_{ik}(j\omega)$ can only be made using approximations, on information based on experience, or from some analytical study of the system.

The approach adopted here is an iterative trial-and-error-type search to obtain estimates of $F_{ik}(j\omega)$. This technique which is greatly facilitated by the use of an
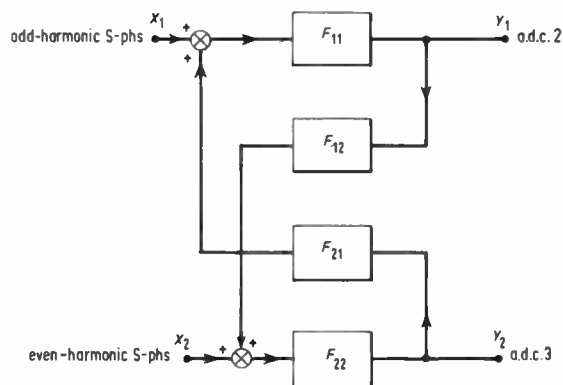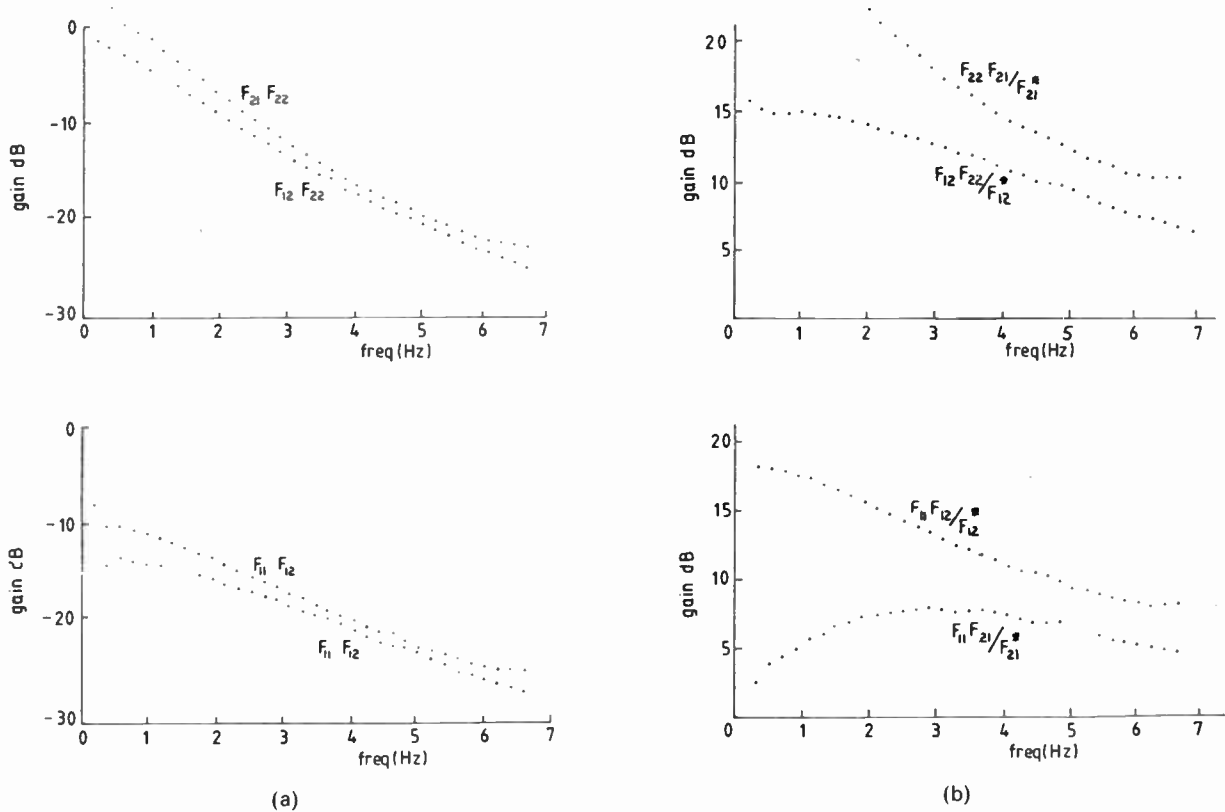

Fig. 3. Block-diagram of cross-coupled feedback system.

(a)

(b)

Fig. 4. Transcriptions of v.d.u. results for system shown in Fig. 3 (see equations (1)-(2) for interpretation of F_{11}, F_{12}, F_{21} and F_{22}). (a) Initial display (i.e. raw results). (b) Display using incorrect estimates of F_{12} and F_{21}. (c) Display using correct estimates of F_{12} and F_{21}, resulting in F_{11} and F_{22} being displayed.

interactive programme, in combination with a graphics-display unit, is based upon the following arguments.

Suppose that the points established previously corresponding to equations (1) and (4) are, in turn, each divided by the corresponding points associated with equations (2) and (3). The result would be four sets of points corresponding to

$$G_1(j\omega) = F_{21}(j\omega)F_{22}(j\omega) \tag{5}$$

$$G_2(j\omega) = F_{11}(j\omega)F_{12}(j\omega) \tag{6}$$

$$G_3(j\omega) = F_{12}(j\omega)F_{22}(j\omega) \tag{7}$$

$$G_4(j\omega) = F_{11}(j\omega)F_{21}(j\omega) \tag{8}$$

These four sets of points may be displayed on a v.d.u. (see Fig. 4(a)).

It may be possible at this stage to make further progress using any further known information about the system. Suppose that, for example, the cross-coupling terms F_{12} and F_{21} are known to be first-order lags but their time-constants are unknown. Then a guess is made of the break-points of these two expressions, i.e. estimates F_{12}^* and F_{21}^* are made of these quantities.

These estimates are divided into the expressions (6) and (7) and (5) and (8) respectively and the resultant

(c)
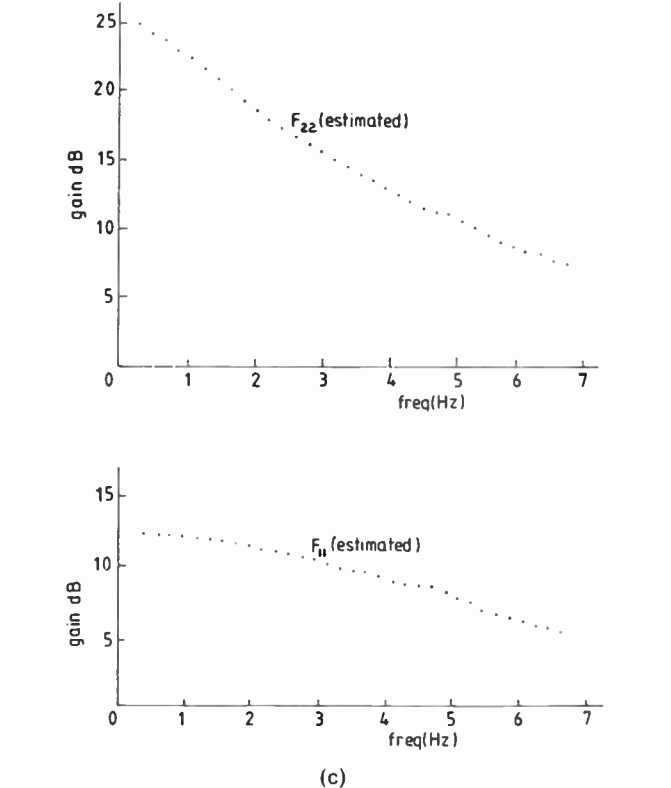
points displayed on the v.d.u. On the basis of the display produced one makes new estimates of F_{12} and F_{21} and goes through the process once more and so forth until satisfactory results are obtained.

This procedure is probably better appreciated by referring to Fig. 4. In Fig. 4(a) the display corresponding to expressions (5) to (8) is shown. Figure 4(b) displays a result obtained when the appropriate divisions are performed using incorrect estimates of F_{12} and F_{21}. Figure 4(c) shows the coalescence being sought when the correct estimates of F_{12} and F_{21} are used.

Thus the estimated frequency-responses F_{11} and F_{22} are left on the screen and the 'correct' estimates of F_{12} and F_{21} are available within the computer. This is just one simple approach but generally there is no systematic method after the curves corresponding to equations (5)-(8) have been established.

Obviously whether such procedures will be satisfactory depends on how much pre-knowledge of the system the investigator possesses.

4 Sampled-data Systems

Here we discuss briefly the use of S-phs for the frequency-response testing of sampled-data systems. Consider the sampled-data system shown in Fig. 5 where the continuous input, $x(t)$, is sampled before presentation to the continuous system represented by the transfer-function $G(s)$. The output is then $y(t)$; however, it is usual in sampled-data analysis that the output passes through a fictitious sampler to give the output $y^*(t)$.
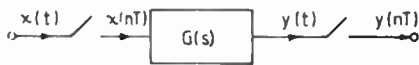
Fig. 5. Sampled-data system.

Considering the input $x(t)$ to be a S-phs it may be written in the form

$$x(t) = \sum_{i=N_1}^{N_2} a_i e^{j(\omega_i T + \phi_i)}$$

and the input sequence may be written

$$x(nT) = \sum_{i=N_1}^{N_2} a_i e^{j(n\omega_i T + \phi_i)}$$

Further the resulting output sequence becomes, by convolution theory,

$$y(nT) = \sum_{l=0}^{n} x[(n-l)T]g(lT)$$

where $g(lT)$ is the impulse-response sequence of the system and so

$$y(nT) = \sum_{l=0}^{n} \left[\sum_{i=N_1}^{N_2} a_i e^{j[\omega_i(n-l)T + \phi_i]} \right] g(lT)$$

and this may be rearranged in the form

$$y(nT) = \sum_{i=N_1}^{N_2} a_i e^{j(\omega_i nT + \phi_i)} \left[\sum_{l=0}^{n} e^{-j\omega_i lT} g(lT) \right]$$

Now since by definition $G^*(j\omega) = \sum_{l=0}^{\infty} g(lT) e^{-j\omega lT}$

then we may write

$$y(nT) = \sum_{i=N_1}^{N_2} a_i e^{j(\omega_i nT + \phi_i)} G^*(j\omega_i)$$

$$= \sum_{i=N_1}^{N_2} a_i e^{j(\omega_i nT + \phi_i)} M(\omega_i) e^{j\phi(\omega_i)}$$

where

$$|G^*(j\omega)| = M(\omega_i) \quad \text{and} \quad \underline{/\ } G^*(j\omega_i) = e^{j\phi(\omega_i)}$$

So in passing through the system the S-phs is modified by the modulus and phase of the sampled-frequency-response of the system and this may be determined by direct division as discussed in detail elsewhere.[1]

Thus the treatment for sampled-data single input/single output systems is a simple extension of the standard previously-described technique.

5 The Use of S-phs with Cross-power Spectral Estimation

One well-known procedure for obtaining noise-rejection in the frequency-response determination is to use the cross-correlation between the input and the output signal, with the input signal having a suitably noise-like autocorrelation function (a.c.f.). This has previously been exploited, largely in the time-domain, with the pseudo-random binary sequence (p.r.b.s.) as the input perturbation.[8]
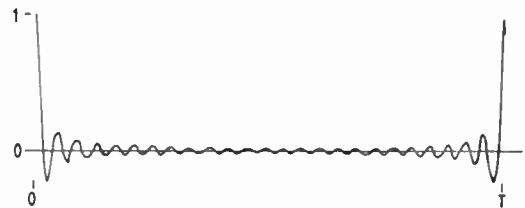

Fig. 6. Auto-correlation function of S-phs (containing 25 harmonics) over displacement corresponding to the periodic time of this signal.

However, a consideration of the a.c.f. of the S-phs (see Fig. 6) shows a similarly useful form as that employed in the p.r.b.s. estimation tests, i.e. a curve with a peak at intervals of the S-phs basic-period with rapid reduction between these peaks. This has been exploited, plus the facility of the S-phs to transform exactly into the frequency domain, (note the p.r.b.s. is not band-limited), to perform discrete correlation in the frequency domain. The complication of transforming from the time to the frequency domain pays off handsomely in computational time, i.e. it requires N^2 multiplications for a $2N$-length time-domain correlation but only $4N$ multiplications are required to form the power-spectrum. In fact, the actual reduction is not quite as efficient as this since multiple, over-lapped time-series blocks are used. Resolution is preserved when the data section for transformation is a subdivision of the total length available by extending it with zeros.

For example a 512-point set is considered as seven subsets of 128 with a 64-point overlap and each subset is extended with zeros to 512 points. This process is applied to both the input-perturbation and output-response time-series of the linear time-invariant system. The assumption is made that only the output time-series contains random-noise contamination.

The cross-power spectral function is then formed as

$$\phi_{xy(w)} = X(\omega)^* Y(\omega)$$

with $X(\omega)$ = input-signal Fourier transform; $Y(\omega)$ = output-signal Fourier transform including the noise contamination.

or,

$$\phi_{xy(w)} = X^*(\omega)H(\omega)X(\omega)$$

with

$$H(\omega) = \text{system frequency response}$$

and

$$\phi_{xy(w)} = |X(\omega)|^2 H(\omega)$$

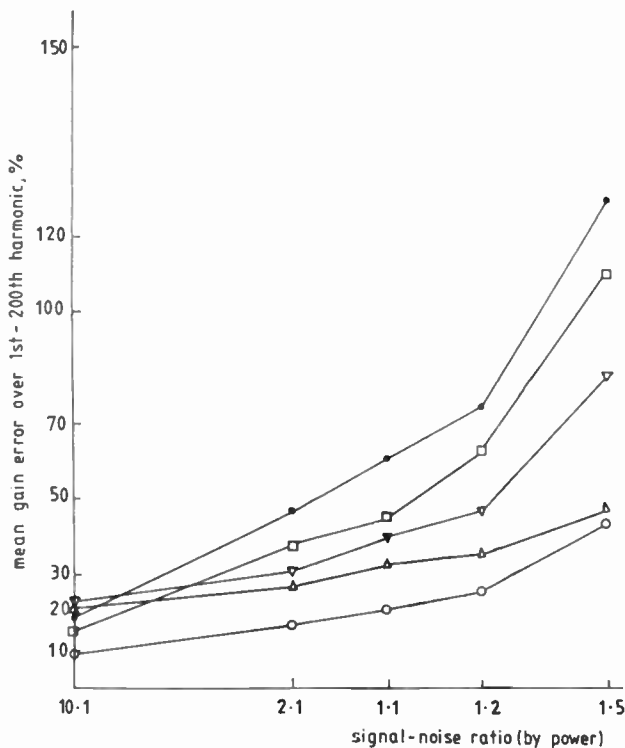Thus by rescaling by the square of the input-signal magnitude the system gain is obtained. (The phase is

Fig. 7. Mean of errors in gain-estimate of a second-order lag for various signal-to-noise ratios.
This is for 200 points with noise added to the output (noise magnitude characteristic having the same shape as the frequency-response of the system) for one block of data (i.e. 512 points). ●—direct division. ○—cross-power spectrum; window on input and output; 7 overlapped blocks. □—overlapped blocks with direct division; window on input and output. △—cross-power spectrum; window on output only. ▽—overlapped blocks with direct division; window on output only.

given immediately.) The payoff for all this extra computation, compared to direct division, is seen only when noise is present in the output signals. To demonstrate this, a random-noise signal was synthesized digitally and added, at required power ratios, to the response from a second-order lag, perturbed by a S-phs of flat spectrum having 200 components. The noise-power spectrum was an image of the response spectrum to maintain the same signal-to-noise ratio at all frequencies. The noise was restricted to the perturbations bandwidth; this is an extreme case as normally noise will have a bandwidth that is limited or far larger than the perturbation spectrum.
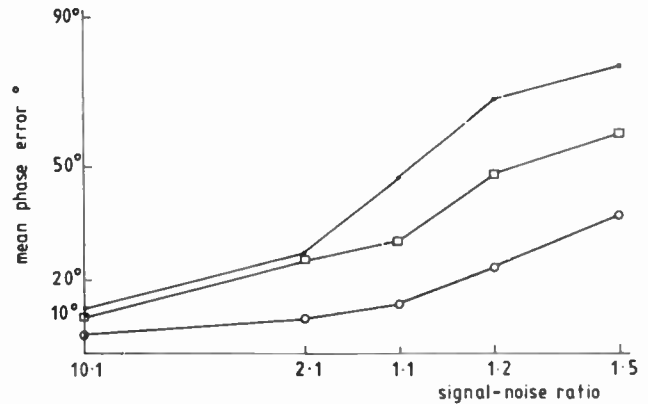

Fig. 8. Mean-error in phase-estimate. ●—direct division. ○—cross-power spectrum. □—overlapped blocks with direct division.

The graphs shown in Figs. 7 and 8 show the results comparing the 'direct-division' for one block of 512 time-data points with one 512-FFT, i.e. $H(\omega) = Y(\omega)/X(\omega)$ against the estimate using the average of the complex product formed from seven overlapped subsets of 128, with zeros extension to 512, i.e.

$$H(w) = \frac{X^*(\omega) . Y(\omega)}{|X(\omega)|^2}$$

and for the use of direct-division between the seven transforms for the overlapped subsets to show that it really is the cross-power spectrum calculation rather than just the averaging that is the source of the improvement seen in Figs. 7 and 8, for the various signal-to-noise ratios.

A decision that must be made in this form of processing is whether to use a data-window or not, since truncated subsections and heavy noise are being dealt with rather than only discrete harmonics of the FFT-length. If one is to be used, which sort should it be, and should it be applied to both input and output signals, since the input is presumably clean (although still truncated)? A consideration of the effect of a data-window on the cross-spectral estimate shows that

$$\phi_{xy(w)} = \frac{(X(\omega) . W(\omega))^* \cdot (Y(\omega) . W(\omega))}{|X(\omega) . W(\omega)|^2}$$

where $x.y$ indicates frequency-domain convolution. Since the input-perturbation is processed as a series of truncated subsets, then the use of a data-window is expected to be advantageous.[9] This was verified by experiment, as shown in Figs. 7 and 8 where the lowest mean-error at each signal-noise ratio was given by the cross-power-spectral (c.p.s.) estimate using a window on both the input and output-series.[10] The triangle window has been favoured as its convolution with the power spectrum gives an all-positive result.[10] This comes from earlier considerations for forming cross-spectral estimation from the cross-correlation function, rather than from multiplied 'periodograms', i.e. frequency-spectra.

A single block of 512 data points was used in the above example, but the same general principles apply to c.p.s. processing with longer time series. The decision on whether to accept estimates from multiple-block c.p.s. processing or from averaging the multiple blocks, and then c.p.s. processing the single (averaged) block can be made from the variances of the two results. The excellent noise rejecting properties of the S-phs perturbation can be enhanced when combined with the c.p.s. form of processing for analysis of noise contaminated data.

6 Discussion

Among the advantages of using S-phs is the fact that it is conceptually similar to single-frequency response testing, making the results easy to appreciate. Computational aspects are well catered for by commonly-available computer programs (e.g. FFT packages). The signal design is simple and allows the experimenter freely to specify at which frequencies and at what relative-power the system need be excited. It is easy to modify the signal in the light of experience.

So far as error-analysis is concerned there are no novel aspects arising. The signal may be generated to within the limits of the computer's accuracy and the inverse FFT will have corresponding accuracy. Distortion in the analogue-conversion process may be a problem but can be accommodated for in conventional ways.

Errors in the computation of system-gain and phase responses are governed by the usual signal-to-noise ratio considerations[11] and the computational accuracy is no different essentially from that for a multi-frequency signal applied to single-input/single-output systems using FFT techniques.

The effects of non-linearities occurring within the system are minimized to some extent by using a low-peak-factor signal anyway. It is, however, possible to achieve some degree of 'non-linear monitoring' by leaving particular harmonics out of the input excitation signal and monitoring the amplitude of these harmonics which appear in the output of the system.

Time-savings by going to multi-frequency testing can be considerable and this applies to both single-input/single-output and multi-input/multi-output systems. For example, Reference 1 reports experimental times for frequency-response testing of a particular system at particular conditions being reduced from 90 minutes to 6 minutes per run by using multi-frequency signals.

7 Conclusions

It has been shown that the S-phs is useful for frequency-response determination of multi-variable systems and we have described an example of its use in conjunction with an interactive-computer facility. The application of S-phs to sampled-data systems has also been discussed briefly.

Further we have pointed out that the S-phs has an auto-correlation function whose form may be advantageously employed in the estimation of frequency-response functions when the original signals are heavily contaminated with noise.

8 Acknowledgment

9 References

1 Flower, J. O., Knott, G. F. and Forge, S. C., 'Application of Schroeder-phased harmonic signals to practical identification', *Measurement and Control*, 11, pp. 69-73, February 1978.

2 Flower, J. O., Forge, S. C., Radcliff, N. G. and Roust, C. B., 'Dynamic measurements of a nuclear reactor using low-peak-factor excitation signals', *Nucl. Sci. & Engng*, 68, pp. 110-5, October 1978.

3 Schroeder, M. R., 'Synthesis of low-peak-factor signals and binary sequences of low auto-correlation', *IEEE Trans. on Information Theory*, IT-16, pp. 85-9, January 1970.

4 Briggs, P. A. N. and Godfrey, K. R., 'Pseudo-random signal for the dynamic analysis of multi-variable systems', *Proc. Instn Elect. Engrs*, 113, pp. 1259-64, 1966.

5 Rosenbrock, H. H., 'Design of multi-variable control systems using the inverse Nyquist-array', *Proc. Instn Elect. Engrs*, 116, pp. 1929-36.

6 Tou, J. T., 'Modern Control Theory' (McGraw-Hill, New York, 1964).

7 Morton, P. G., 'Dynamic characteristics of bearings', *GEC J. Sci. & Tech.*, 42, pp. 1-7, 1975.

8 Godfrey, K. R., 'Theory of the correlation method of dynamic analysis', *Measmt & Control*, 2, pp. T65-T72, 1969.

9 Burgess, J. C., 'On digital spectrum analysis of periodic signals', *J. Acoust. Soc. Am.*, 58, Sept. 1975, pp. 556-567.

10 Rabiner, L. R. and Gold, B., 'Theory and application of digital signal processing' (Prentice-Hall, Englewood Cliffs, N.J., 1975).

11 Flower, J. O. and Forge, S. C., 'Simple statistical assessment of system-frequency-response variance from time-domain data', *Proc. IEEE*, 67, pp. 1655-6, December 1979.

Voiced/unvoiced band-switching system for transmission of 6 kHz speech over 3·4 kHz telephone channels

P. J. PATRICK, B.Sc.*

R. STEELE, B.Sc., Ph.D., C.Eng., M.I.E.E.†

and

C. S. XYDEAS, M.Sc., Ph.D., M.I.O.A.*

SUMMARY

A voiced/unvoiced band switching system is described for the transmission of wide bandwidth speech (here 300 to 6000 Hz) over commercial telephone channels. Time waveforms and spectrograms are presented to demonstrate that the 6 kHz speech can be compressed into a 3·4 kHz telephone channel and yield improved speech quality at the receiver compared to current telephone quality speech. Informal listening experiences confirm these results. The system is conceptually simple and inexpensive to implement.

* *Department of Electronic and Electrical Engineering, University of Technology, Loughborough, Leicestershire LE11 3TU.*
† *Formerly at Loughborough University; now with Bell Laboratories, Crawford Hill, New Jersey 07753, USA.*

1 Introduction

Telephone speech channels are typically band-limited to between 300 and 3400 Hz. With many handsets, particularly those having carbon microphones, the band-limiting process of speech is complete even prior to transmission. We may, however, anticipate the introduction of wider bandwidth handsets if the telephone channels with their existing narrow bandwidths could be used to transmit wider bandwidth speech signals. The purpose of this paper is to propose a conceptually simple method for the transmission of relatively wide bandwidth speech, 300 to 6000 Hz, over the existing telephone voice channels.

Before describing the voiced/unvoiced band switching (VUBS) system we emphasize what is already known by every observant telephone user, namely that certain sounds that are generally associated with unvoiced speech[1] (i.e. where there is no vocal cord excitation) are frequently perceived incorrectly. This occurs in spite of the listener's syntax and semantic processing of the received message.

If isolated unvoiced sounds are transmitted the confusion to the listener may become acute, as in the case of deciding whether the received sound was /s/ or /f/. This difficulty in distinguishing unvoiced sounds is because most of their energy tends to be above the bandwidth of commercial telephone channels, and their reproduction at the receiver is consequently badly affected. Interestingly, and of use here, is that by suppressing the frequency components in unvoiced speech below 3 kHz the quality is only marginally altered.

In conversation, few isolated unvoiced sounds are uttered, and the effect of the band-limitation of the channel is to cause distortion in the received speech. This situation has been accepted, in addition to economic and social considerations, because voiced speech[1] (i.e. where there is vocal cord excitation) constitutes up to 80% of the speech and its significant frequency components are contained within the telephone channel bandwidth. However, if by an inexpensive method 6 kHz speech could be received, the subscriber would gain both in improved intelligibility and quality. Although 6 kHz speech cannot be conveyed over the network, an approximation of it can, and the VUBS method we propose here makes use of the two important facts mentioned above. First, if voiced speech is present 3·4 kHz is adequate, and secondly if unvoiced speech occurs, we only need to transmit frequency components from 3 to 6 kHz‡, i.e. a bandwidth of 3 kHz and one that can also be passed over the network.

2 VUBS System

At the transmitter the 6 kHz speech signal $x(t)$ is band-pass filtered to give a signal $x_1(t)$ having frequency

‡The edge frequencies f_{c1} and f_{c2} (here 3 and 6 kHz) are system parameters selected for quality of perception, where $f_{c2} - f_{c1} = 3$ kHz.
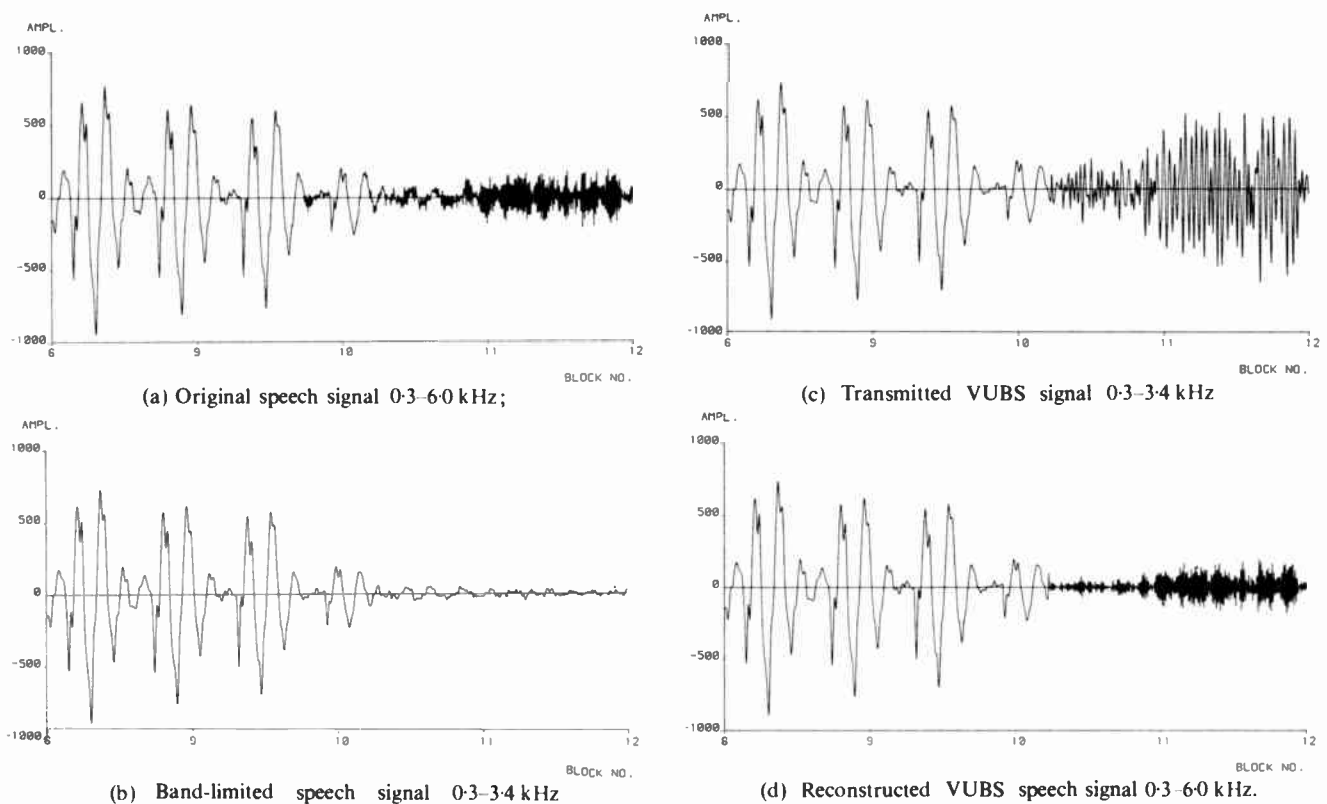
(a) Original speech signal 0·3–6·0 kHz;

(c) Transmitted VUBS signal 0·3–3·4 kHz

(b) Band-limited speech signal 0·3–3·4 kHz

(d) Reconstructed VUBS speech signal 0·3–6·0 kHz.

Fig. 1. Time waveforms for /ls/ in 'sister'.

components from 0·3 to 3·4 kHz. Another signal $x_2(t)$ is also derived from $x(t)$. This is produced by filtering $x(t)$ to extract frequency components between 3 and 6 kHz, which are then heterodyned down with the aid of a 6·3 kHz carrier. Thus $x_1(t)$ and $x_2(t)$ have frequency components in the same frequency band. The decision concerning whether $x_1(t)$ or $x_2(t)$ is to be transmitted is made by a voiced/unvoiced switch.[2] This switch filters $x(t)$ into two 1 kHz bands, 0 to 1 kHz, 5 to 6 kHz, and estimates the energy in each of these bands over 5 ms and 1 ms, respectively. These energy levels are compared and $x_1(t)$ is transmitted if the energy in the lower frequency band exceeds that in the higher frequency band, while $x_2(t)$ is transmitted if the energy in the higher band is the greater. Should the energies be comparable, as in the case of stop consonants and voice fricatives, $x_1(t)$ is selected. After the energy comparison, delays of 4 and 2 ms are incorporated depending on whether the switch is changing from voiced to unvoiced, or from unvoiced to voiced speech, respectively. These delays prevent spurious switching. In general, when voiced speech is present $x_1(t)$ is transmitted, while if unvoiced speech is detected $x_2(t)$ is transmitted.

The receiver must decide whether $x_1(t)$ or $x_2(t)$ was transmitted. This can be done in a number of ways. The most certain method, which involves some waveform distortion, is to insert a tone near the top of the speech band (say 2·6 kHz) whose phase or amplitude informs the receiver whether $x_1(t)$ or $x_2(t)$ was transmitted. A more elegant solution is not to transmit the decision of

whether $x_1(t)$ or $x_2(t)$ was transmitted, but for the receiver to deduce this information. Two measures are effective: the correlation coefficient (significantly lower for unvoiced than voiced speech) and the number of zero crossings which are much higher for unvoiced speech than voiced speech. If $x_1(t)$ is received it is passed to the loudspeaker, while if $x_2(t)$ occurs it must be heterodyned up to occupy its original band of 3 to 6 kHz before being passed to the loudspeaker. In the case of silence the $x_1(t)$ signal path is used, i.e. no heterodyning is employed.

The VUBS system does not recreate the original 6 kHz speech, but a signal that occupies the 6 kHz band, although never all of it at any instant. By arranging for voiced speech to reside in the conventional telephone band, and unvoiced speech in the higher band of 3 to 6 kHz, speech close in quality to the original 6 kHz speech is perceived.

3 Results

The system was investigated using computer simulation. An ideal telephone channel of 300 to 3400 Hz was assumed, and the following test words were used in the experiments: sister, father, S. K. Harvey, shift, thick, fist, talk, spent, vote.

Figure 1(a) shows a segment of the 6 kHz speech waveform for /ls/ in 'sister'. When this segment is subjected to the band-limiting effect of the telephone channel the waveform appears as in Fig. 1(b). The unvoiced /s/ is severely attenuated and distorted, whereas the voiced /l/ is only marginally effected. The
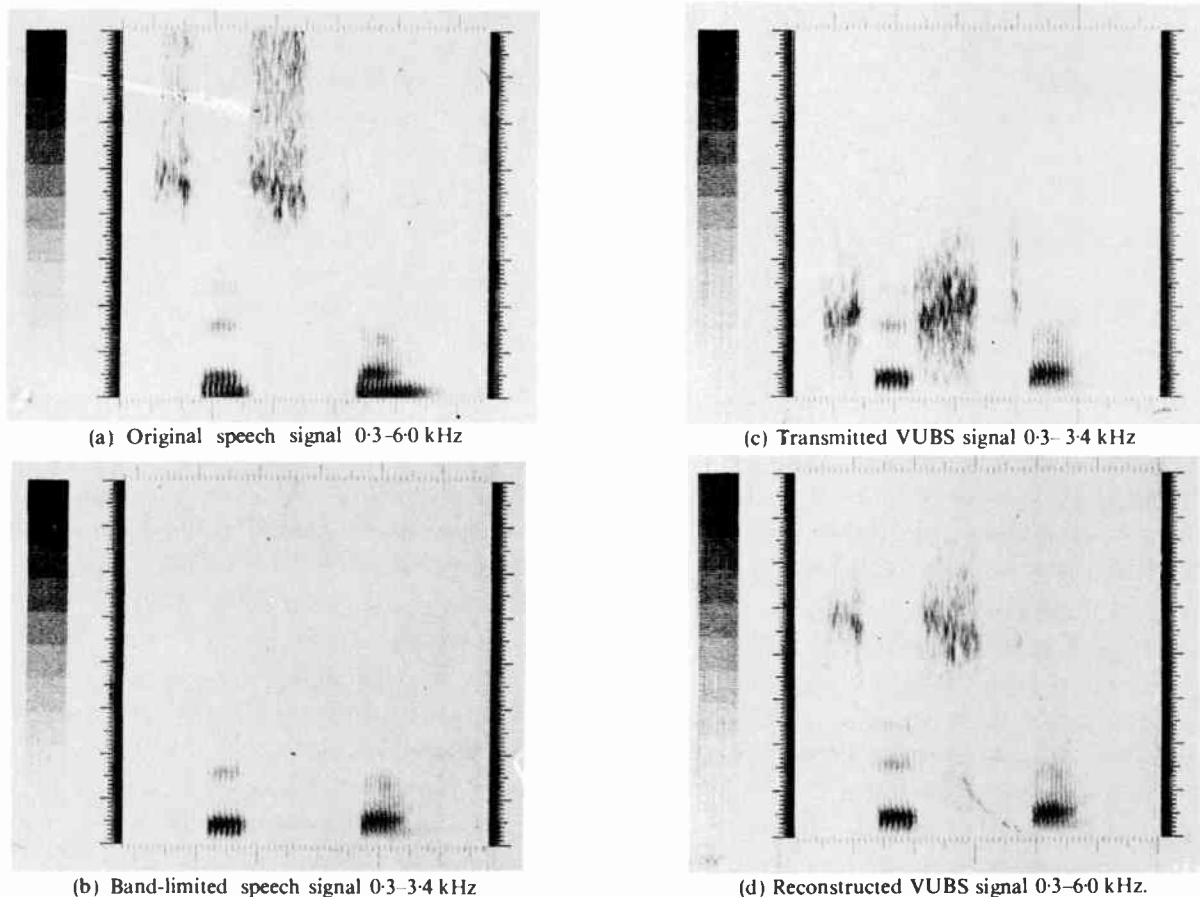
(a) Original speech signal 0·3–6·0 kHz

(c) Transmitted VUBS signal 0·3– 3·4 kHz

(b) Band-limited speech signal 0·3–3·4 kHz

(d) Reconstructed VUBS signal 0·3–6·0 kHz.

Fig. 2. Spectrograms for the utterance 'sister' (The marking depth = 40 dB)

Note.—The unvoiced transmitted signal in 1(c) was amplified by four times to emphasize the unvoiced signal in the spectrogram of 2(c). The unvoiced signal amplitude is divided by four at the receiver terminal.

VUBS system transmits the signal shown in Fig. 1(c), with an amplified unvoiced component. At the receiver, the VUBS demodulator produces the signal shown in Fig. 1(d), where the close correspondence with the 6 kHz speech of Fig. 1(a) is evident. The spectrograms for the complete utterance 'sister' are shown in Fig. 2 for, (a) original wideband speech, (b) telephonic speech, (c) transmitted VUBS signal and (d) the reconstructed VUBS speech. From Figs 1 and 2 we see the closer correspondence, both in the time and frequency domains, of the 6 kHz speech and the recovered VUBS signal transmitted over 3·4 kHz channel, compared to the conventional band-limited 3·4 kHz speech.

Informal listening experiences on this small sample of material seem to confirm the waveforms and spectograms in that the VUBS speech is preferable to telephonic speech although much more material needs to be processed so that formal subjective listening tests can be undertaken to fully evaluate the performance of the system.

4 Conclusions

This system has the prospects of allowing 'commentary-grade' speech to be conveyed over existing telephone channels at low additional cost. It may therefore be a useful adjunct to audio conferencing systems.[3] The VUBS system can also be used with digital coding techniques and thereby effect a reduction in the transmitted bit-rate, an approach we are currently pursuing. The VUBS systems is being constructed by British Telecom (Post Office Telecommunications) at Ipswich, England.

5 Acknowledgments

6 References

1 Flanagan, J. L., 'Speech Analysis, Synthesis and Perception', 2nd Ed. (Springer-Verlag, Berlin, 1972).
2 Knorr, S. G., 'Reliable voiced/unvoiced decision', *IEEE Trans on Acoustics, Speech and Signal Processing*, ASSP-27, no. 3, pp. 263–7, June 1979.
3 Groves, I. S., 'Orator—the Post Office audio teleconferencing system', 'Communications '80', IEE Conference Publication No. 184, April 1980, pp. 102–6.

Structured magnetic media for data security

J. S. T. CHARTERS,
B.Sc., Ph.D., C.Eng., M.I.E.E.*

and

J. HARRISON†

Based on a paper presented at the Conference on Video and Data Recording at Southampton in July 1979

SUMMARY

A method is described of structuring or 'freezing' digital encoding into a magnetic tape so that it is permanent and non-erasable. It is then shown how normal or 'soft' magnetic encoding can also be recorded on such a tape, and ensure the integrity of the normal encoding. It is further shown how structured tape may be fixed to the cards and documents to make them secure and machine readable.

* *Transducers (C.E.L.) Ltd., Reading; formerly with EMIDATA.*
† *EMIDATA, Alma Road, Windsor SL4 3JA.*

1 Introduction

Structured magnetic tape, invented by Dr R. R. Pearce and Mr C. A. Lee of EMI Central Research Laboratories, is of value in security applications because the encoding cannot be erased and cannot be altered without detection. Furthermore, it is manufactured by a unique and complex process and any attempt to duplicate the process would require the acquisition of a specialized high-level technology together with the investment of significant amounts of money in plant and equipment.

Once the discovery of structured magnetics had been made and the ability to produce the material proved, the question then arose as to the most suitable application for this product.

The plastic card has seen spectacular growth in the last 10 years. More recently an increasing number of cards have started to appear with magnetic stripes to facilitate data collection at the point of sale. Whilst the standard magnetic stripe is a most effective medium for carrying information about the card holder, the ease with which it can be recorded is at the same time one of its major drawbacks. The possibility of fraudulent alteration or complete re-encoding is very real and equipment can be obtained very easily to alter magnetic information. A workable duplication device has been produced in America for less than $50. It is against this background that EMI embarked on an acquisition programme in order to develop Watermark Magnetics as a practical system. The EMIDATA's worldwide card production is now in excess of 200 million cards per annum, of which some 30% contain magnetic stripes with this proportion increasing steadily year by year.

2 Standard Magnetic Tape

In order to explain Watermark tape it will be helpful to first look at standard magnetic tape. Most magnetic tape today is made from gamma ferric oxide $(-Fe_2O_3)$ magnetic material. These small magnetic oxide particles are acicular in shape, that is they are needle-like, and are about 0.5 to $0.8\,\mu m$ in length and 0.1 to $0.2\,\mu m$ in thickness and act like tiny bar magnets.

To make a magnetic tape, these small needle-like magnetic oxide particles are dispersed in a resinous dope containing solvents, wetting agents, and flow agents so that the mixture can be coated on to a film base.

The oxide layer while still wet is passed through a magnetic field which turns these particles into small bar magnets and align them with the long needle axes parallel along the length of the tape. The tape is then passed through a drying oven which exhausts the solvents, locking the oriented acicular particles in the binder.

The orientation of the particles is done so that during encoding of the magnetic tape, the digital write head, with its gap perpendicular to the tape direction, can

impart to the tape the maximum remanent magnetization and achieve the maximum encoded signal.

The binary bit pattern (in the case of the banking industry F2F encoding) is put down in such a way that each of these small acicular magnetic particles is magnetized along its length producing a flux reversal pattern that is parallel to the length of the tape. The acicular particles are left in a magnetized state (remanent magnetization) with the north and south poles facing left to right ($180°$ magnetization N—S) or right to left ($0°$ magnetization S—N). At the boundary between these alternating magnetization directions the flux changes direction by $180°$, hence the term flux reversal.

The binary zeros and ones of the F2F encoding are thus set into the spatial magnetization of the tape and are distinguished by the absence of a flux reversal (binary zero) within a given distance (clocking distance) or the presence of a flux reversal (binary one) within this clock distance.

The magnetic read head, which also has its gap perpendicular to the tape direction, is sensitive to a changing magnetic flux pattern. The magnetic flux pattern experiences its greatest rate of change at the transition from one remanent direction to the other remanent direction ($0°$ to $180°$) and a voltage pulse is derived from the read head at this flux reversal.

The voltage pulses define the edges of the bit pattern in the oxide and the spatial encoding in the oxide is converted into a temporal encoding, which can be decoded by electronic circuitry back into the binary zeros and ones of the F2F code.

Such an encoding method is referred to as longitudinal recording. This magnetic encoding can be erased by the application of a high frequency a.c. induced field from the write head, a decreasing mains frequency induced field from a bulk eraser, a d.c. induced field from the write head or a permanent magnet. The results of these fields are to leave no remanent magnetization in the tape in the case of the a.c. erase and no change in the

remanent magnetization, as in the d.c. field from the write head or permanent magnet. With no remanence or change in remanence, there is no change in the external flux for the read head to pick up and convert to a voltage output. Thus, there is no output and the tape is said to have been demagnetized. New information can now be encoded on this erased tape.

This relative ease of encoding and erasing information on magnetic tape is what makes it so attractive as a storage medium for information, and yet this is the very same property that makes magnetic tape so easy to duplicate, alter or counterfeit. Watermark magnetics, however, contains a permanent encoding that cannot be erased or altered.

3 Watermark Magnetic Tape

Structured magnetic tape is often referred to as Watermark Magnetics because of the parallel of incorporating a watermark into the structure of a paper sheet. In much the same way as standard magnetics, Watermark tape consists of γ-ferric oxide particles held in a resinous dope formulation.

While still wet the oxide film is subjected to a magnetic field system which aligns groups of the particles with their long axes either at $+45°$ or $-45°$ to the tape direction (Fig. 1). This pattern of particle orientation provides the distinguishing differences between the code bits. The film is then passed through a drying oven which exhausts the solvent, locking the oriented particles into the binder.

The techniques associated with the process have been acquired over a number of years of research and development and the equipment to manufacture Watermark tape is large and complex. It is beyond the scope of this paper to describe this technology.

A number of methods exist for reading $45°$ Watermark tape, and a particularly useful technique uses a two-gap reading head (Fig. 2). The first gap at $90°$ to the tape direction produced a steady magnetic field

1. The polyester base material
3. which produces a coating with randomly arranged needle-like particles
5. which produces a particle pattern at 45° to the tape axis to produce the encoded watermark pattern
7. and produces the permanent encoded watermark tape with the particles set in the alignment to which they were formed. This is known as 'hard' magnetics

2. is passed through a special resinous laquer of γ-Fe$_2$O$_3$ (iron oxide)
4. The tape passes through a magnetic encoder
6. The tape then passes through a hot air drier

CASTER   WATERMARK GENERATOR   DRIER

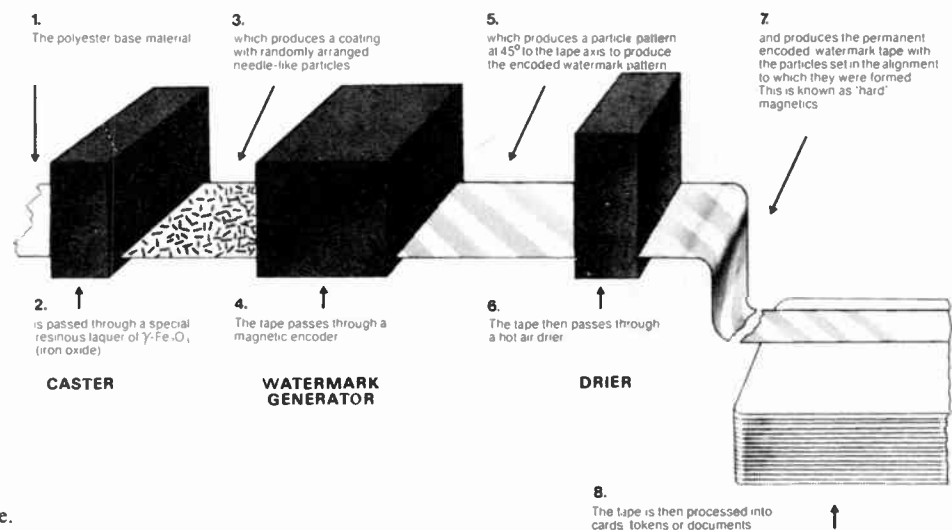8. The tape is then processed into cards, tokens or documents
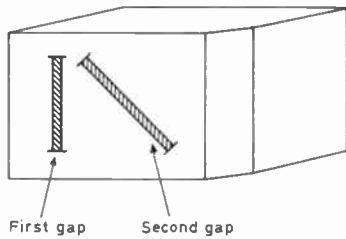
Fig. 1. Manufacture of Watermark tape.

Fig. 2. Watermark two-gap read head.

which magnetizes the tape with a remanent magnetization in the $+45°$ directions, and the second gap at $45°$ effects the reading process. A further function of the $90°$ gap is to saturate and remove any normal encoding on the tape so that the $45°$ gap only reads Watermark magnetics. Thus, normal tape with appropriate 'soft' encoding cannot be passed off as Watermark magnetics.

The reason for the $45°$ angles of the Watermark encoding is that this allows longitudinal recording of normal or 'soft' magnetic information onto Watermark tape without any interference from the Watermark encoding. This is because the component of remanence from the watermark (M) along the tape direction is the same in each code strip, i.e.

$$M \cos(+45°) = M \cos(-45°).$$

Thus a read head set to pick up the component of magnetization along the tape direction does not sense any signal from the Watermark encoding but will read normal longitudinal encoding.

cannot be altered or destroyed. The permanent unique encoding can be used in several ways to secure the integrity of the normal encoding.

4 Use of Watermark Tape

Watermark tape can be used to secure data in a number of ways such as the following:

(a) Recording the data directly in structured form.

It is possible to encode data directly in structured form but this requires the data to be given for encoding to the single company which has the method at its disposal (EMI). The process required large and expensive equipment and it is the intention of EMI to maintain its security by strictly controlling all aspects of its use. These reasons dictate that it is not an in-field process.

(b) Use of a sequence of Watermark numbers.

If a tape is Watermark encoded with a known sequence of numbers it is obvious that the removal of any section of tape can be detected.

A number of methods may be devised for protecting normal encoding from alteration by linking the data to the Watermark number sequence. This necessitates the encoding to be effected in blocks with one complete Watermark number per block. The normal data may then be algorithmically related to the Watermark number and the algorithm output recorded together with the data; any alteration to this data will cause the algorithmic relationship not to be satisfied. A further method is to record the data in encrypted form using the
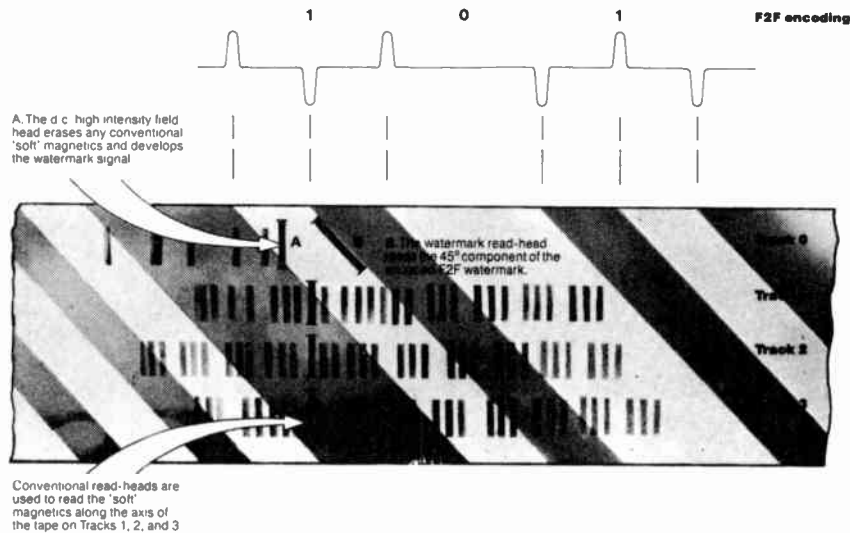

Fig. 3. Watermark tape with normal encoding.

Figure 3 shows a Watermark tape with three tracks of normal encoding and with the Watermark encoding being read at the top edge of the tape. The two encodings exist in the same Watermark tape; the normal encoding can be erased and re-encoded while the Watermark encoding is permanently structured into the tape and

Watermark number as the key (or part of the key) to the encryption algorithm.

5 Secure Cards and Documents

A requirement exists for a method of positively identifying and validating cards and documents as being

genuine and not counterfeit. Typical cards are bank cards and credit cards, identification cards of various types, and cards for use in electronic access control systems. Typical documents are tickets for various facilities, passports, driving licences, and social security documents.

Watermark tape can be attached to cards and documents to make them secure and machine readable. The fixing process depends on the materials involved and may be by lamination, by hot roll-on, by adhesive, or by insertion between the layers of layered substances such as paper.

A particular case which illustrates how Watermark magnetics can significantly improve the security of a complete system (and not just simply the security of a card) is that of the bank card. Many of the cards in use today use magnetic stripes together with normal magnetic encoding to access machine-oriented banking facilities such as automatic teller machines. A number of security threats exist with both on-line and off-line facilities which lead to the possibility of compromise to the banking system.

The data on a bank card stripe is encoded by the self-clocking Aitken F2F method in normal magnetics and each character is defined in 4-bit b.c.d. plus 1-bit odd parity. A Watermark magnetic stripe can also carry this data, but in addition can have a 12-character permanent decimal number (also in Aitken F2F). This number can be used in several ways but a particularly useful scheme involves splitting the number into three fields as follows:

```
*   *   *     *   *   *   *   *     *   *   *   *
```

Audit Number

Country/Bank Code   Card ID Number
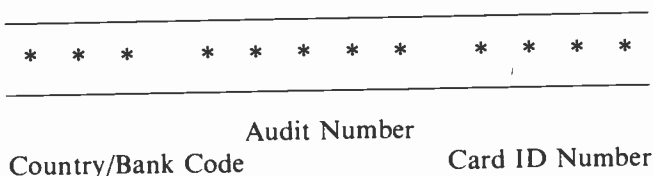
The Country/Bank Code is unique to a specific country or bank. The Audit Number is a fixed number for a particular roll of Watermark tape and provides a trace or audit function for tape and cards. The Card Identification Number varies from card to card so that the complete 12-character number is individual to each card. A hierarchy of security systems may be built up around the use of the three fields of the Watermark number and it is possible to devise a scheme which commences with a simple system and has the capability to be progressively enhanced in sophistication and security.

System 1: Read the Country/Bank Code to give anti-counterfeit protection

If the country/bank code is read and identified in an automatic teller machine this gives anti-counterfeit protection and defines that the card is specific to the particular institution.

System 2: Read the Country/Bank Code and Audit Number to give anti-counterfeit protection and validity verification.

If the first eight characters are read, then the first three can give anti-counterfeit protection and the next five are used to check validity. These five audit number characters represent batches of cards and establish an audit trail right back to the point of manufacture of the Watermark tape. The automatic teller machines must be programmed only with the valid system audit numbers and this gives protection against the illicit use of batches of cards or tape which have been stolen.

System 3: Read the Country/Bank Code, Audit Number, and Card Identification Number to protect other data.

If all twelve characters are read then anti-counterfeit protection and validity validation can be effected as above, and protection of other data such as that in normal magnetics can be obtained by linking that data to the Watermark number via a secure algorithm. This eliminates the possibility of card alteration or data duplication (often called 'skimming' in banking circles).

A further use of the 12-character number is for derivation of the key to be used with an encryption algorithm. A complete system of this type is shown in Fig. 4 and has the following features:

(1) The key for the encryption algorithm is set by algorithmically combining the customer Watermark number (WM), the customer primary account number (PAN), and the customer personal identification number (PIN).
(2) To enable look-up of the file at the central computer, the primary account number (PAN) is transmitted over the communication network in clear text (i.e. non-encrypted). There is no security reduction with this since the account number is not a secret.

6 Concluding Remarks

This paper has shown how Watermark magnetic tape can be used to protect data in tape form and in card/document form effectively against counterfeit, alteration, and illicit duplication, and how its use can also contribute to other aspects of total system security such as encryption key management.

Watermark Magnetics is now well established and is in use in a wide range of applications such as:

(1) Banking—the uses of Watermark Magnetics in this area have been the specific topic of this paper.
(2) Access Control—Watermark Magnetics is being used in all forms of control systems such as building access, flexitime, car parking, etc.
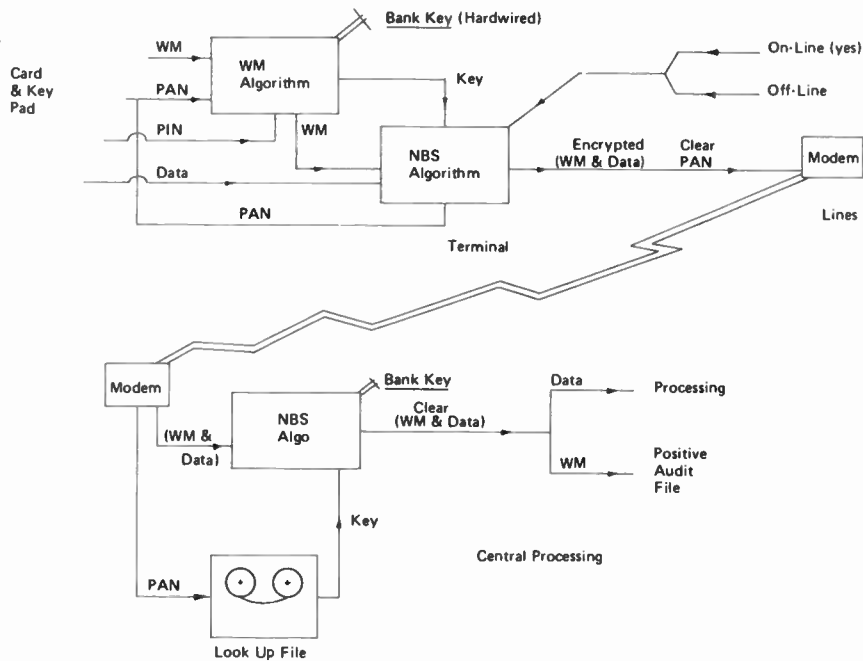(3) Telephones—A pre-encoded card for use in

Fig. 4. Watermark as encryption key.

telephones is now in the final stages of development and this derivative of Watermark technology will be tested by half-a-dozen European Telecommunications Authorities during 1981/82.

(4) Vending—Over the past few years there has been a substantial increase in the number of products supplied from vending machines. A Watermark Magnetics card enables a cashless system to be installed, which not only provides security for the machine operator as no money is required, but also by using a stored value card the customer has the potential for greater selection.

It can be seen by the above applications that Watermark Magnetics is being used wherever there is a requirement for a secure document that is also required to be machine readable.

The Authors

to industry as Engineering Manager of the Security Division of MESL. He joined Emidata in 1977. Dr Charters has published a number of papers on various aspects of electronic security techniques.

James Charters has been Managing Director of Transducers (C.E.L.) in Reading since July 1980. Prior to this he was Director of Engineering and Manufacturing with Emidata, and was concerned with the development and application of Watermark Magnetics. After graduating from Edinburgh University with a first-class honours degree in electronic engineering in 1962 he worked as a design engineer with Nuclear Enterprises before returning to University as a lecturer in 1966. He obtained a Ph.D. and a Diploma in Management Studies in 1970, and then went back

John Harrison completed an HND in printing technology at Watford College of Technology in 1971. He then worked in product development at a printing supply company, Cornerstone, before moving into Research and Development at McCorquodale & Co. in Basingstoke. While with McCorquodale's he developed a unique plastic card security system before moving to Emidata at Windsor in 1977, as Project Manager of the Access Control and Identification System Group. He has been Engineering Manager of Emidata since July 1980.

Some novel elements for delta-modulated signal processing

N. KOUVARAS, B.Sc.*

SUMMARY

New and interesting multipliers are proposed to use for the direct-multiplication of delta-modulated signals by constants. In addition to a non-recursive form, three recursive-form delta multipliers are given. The recursive multipliers are suitable for multiplication by periodic numbers or by non-periodic numbers which can be approached by periodic ones. A significantly smaller number of delta adders is needed for the realization of recursive delta multipliers, than for the non-recursive ones. In addition, an interconnecting method is suggested, if the outputs of the multipliers are to be added. With the method a significant reduction of the scaling-down is achieved as well as a reduction of the total number of the necessary adders for the realization of the multipliers. The combination of interconnecting multipliers and delta doublers gives very good results for the realization of digital filters.

* *Greek Atomic Energy Commission, Electronics Department, Aghia Paraskevi Attiki, Greece.*

1 Introduction

Delta modulation (d.m.)[1] is a simple encoding technique which appears to be very suitable for low-cost signal processing applications. The first papers, which describe methods for the application of d.m. in digital signal processing, have yielded interesting results.[2-7] None of them, however, has suggested a completely digital arithmetic method for direct processing of pure d.m. signals which will be also called from now on delta sequences (d.s.). Direct processing requires special digital circuits operating with d.m. signals. The delta adder is the first special circuit of this kind that has been developed.[8-10] Methods have also been suggested for the application of the delta adders in synthesizing digital filters[9-10] and a d.m./p.c.m. converter.[11]

The output signal of a delta adder is a delta sequence of the half sum of the analogue signals represented by the two input delta sequences. This scaling is a drawback which is enhanced whenever more than two d.s.s are to be added. This drawback can be removed, in general, as it is shown later in this paper. On the other hand, this adder is very suitable for the realization of the delta multiplier.[10] Such a multiplier delivers at its output a d.s. equal to the product of the input signal times a constant. In this paper some new interesting realizations of delta multipliers are given apart from the first delta multiplier circuit which was published.[10] More refined theoretical review of this basic delta multiplier was necessary in order to support the development of the new multipliers.

Primarily, a new multiplier has been developed which makes use of the idling sequence at only one position. Also, two new multipliers of recursive form are presented here which have the advantage that a reduced number of delta adders is necessary for their realization. Furthermore, the scaling-down of the outputs of the delta adders at the summing points of a digital filter can be removed by suitable interconnections of the multipliers.

To demonstrate the effectiveness the above multipliers interconnected method, two 2nd-order Butterworth digital filters, one non-recursive and one recursive were designed and tested. The results are given in the text. In the recursive filter a delta doubler[12] was used to correct the scaling-down of the addition.

In what follows the following assumptions are made.

(a) All d.s.s are generated from similar linear delta modulators, clocked by a clock generator which is common in the system and has a clock period equal to T. The pulse or level amplitude of the d.s.s is equal to -1 or $+1$ and the system's step magnitude is equal to δ.

(b) Each d.s. is symbolized by a capital letter and the corresponding decoded unfiltered analogue signal by the corresponding small letter. So, if, for example, $\{X_n\}$ is a d.s., then, $x(t)$ is the decoded signal. If now $\{X_n\}$ is of binary pulse form, then

$$x(t) = \delta \sum_{\kappa = -\infty}^{n} X_\kappa \qquad (1)$$

$$nT \leqslant t < (n+1)T$$

If $\{X_n\}$ is of binary level form, expression (1) is also valid, but for the end of the n-period.

2 The Delta Adder

Because the delta adder is the basic element for the realization of the delta multipliers, delta adder operation will be briefly considered.[3]

If $\{X_n\}$ and $\{Y_n\}$ are d.s.s of binary pulse form, a new sequence, $\{S_n\}$ is defined as follows:

$$\{S_n\} = \{(X_n, Y_n)\} \tag{2}$$

where

$$S_n = (X_n, Y_n) = 2^{-1}[X_n + Y_n - (C_n - C_{n-1})] \tag{3}$$

$$C_n = C_{n-1} X_n Y_n$$

$$C_{n-1} = 1 \text{ or } -1 \qquad n = \ldots, -1, 0, 1, \ldots$$

As it was shown in Ref. 10 the $\{S_n\}$, as defined above, is a d.s. of the half sum of the analogue signals represented in encoded form by $\{X_n\}$ and $\{Y_n\}$ plus an error. So, the decoded sum becomes now,

$$S(t) = 2^{-1}[x(t) + y(t)] + \varphi(t) \tag{4}$$

where

$$\varphi(t) = -2^{-1}\delta(C_n - \gamma) \tag{5}$$

$$nT \leqslant t < (n+1)T.$$

In equation (5), γ is constant equal to the initial value of C_n and, therefore, its value is either -1 or $+1$. So, $\varphi(t)$ is a binary level sequence with level amplitudes equal to 0 or $\gamma\delta$.
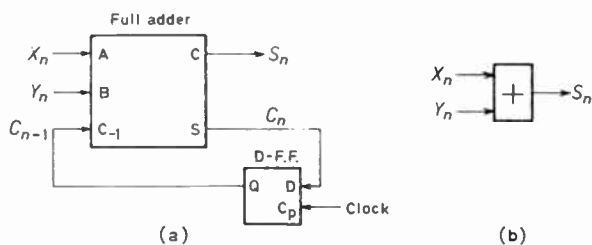

Fig. 1. (a) Delta adder; (b) delta adder block.

In Ref. 10 it was proved that a delta adder can be realized by using a conventional digital full adder wired in a serial form (Fig. 1). From the carry output of the full adder the sum d.s., $\{S_n\}$ is obtained, and from its sum output the carry sequence, $\{C_n\}$. The input–output d.s.s are of binary level form and the level amplitudes of -1 or $+1$ are taken as the logic values 0 or 1 accordingly.

3 Delta Multipliers

A circuit is defined here as a delta multiplier, if it can perform direct multiplication of a d.s. by a constant. Thus if α is the multiplication constant, $\{X_n\}$ the input d.s. and $\{P_n\}$ the output d.s. of such a delta multiplier, then $\{P_n\}$ is a d.s. of the product $a \cdot x(t)$, where $x(t)$ is the decoded signal of $\{X_n\}$. For the synthesis of the multipliers described in this Section, the constant a is always considered as a positive number not greater than unity, that is $0 \leqslant a \leqslant 1$. In the case that the multiplication constant a is a negative number of $-1 \leqslant a \leqslant 0$, then $|a|$ is employed as the constant for the synthesis of a delta multiplier and instead of the input sequence $\{X_n\}$ its inverted form is taken. Furthermore, if the multiplication constant a complies with the relation $2^{v-1} < |a| \leqslant 2^v$, $v = 1, 2, \ldots$, then for the synthesis of the delta multiplier, the constant $|a| \cdot 2^{-v} \leqslant 1$ is employed instead and the multiplication is completed by use of v delta doublers[12] in cascade.

The possibility of realizing delta multipliers has already been proved and a number of such multipliers has been proposed.[10] Some new interesting multiplier realizations are given in this Section to broaden the selection possibilities. Thus, for a given multiplication constant, one can select the multiplier introducing smaller error, the one that requires less delta adders for its synthesis or, finally, the one that meets both requirements.

The sequence $\{P_n\}$ is defined as follows.

$$P_n = (Z_n^{(1)}, (Z_n^{(2)}, (\ldots, (Z_n^{(q)}, W_n) \ldots))) \tag{6}$$

$$n = \ldots -1, 0, 1, \ldots.$$

where $\{Z_n^{(i)}\}$, $i = 1, 2, \ldots, q$ and $\{W_n\}$ are binary pulse d.s.s.

By repeated application of (2) and (3), into (6) the following relation is obtained,

$$P_n = \sum_{i=1}^{q} 2^{-i} Z_n^{(i)} + 2^{-q} W_n - (G_n - G_{n-1}) \tag{7}$$

$$n = \ldots -1, 0, 1 \ldots$$

where

$$G_n = \sum_{i=1}^{q} 2^{-i} C_n^{(i)} \tag{8}$$

and $C_n^{(i)}$ is the carry of this addition in which one of the addents is $Z_n^{(i)}$.

As will be proved further on, relation (6) leads directly to the synthesis of various types of delta multipliers, if the sequences $\{Z_n^{(i)}\}$, $i = 1, 2, \ldots, q$ and $\{W_n\}$ are properly defined. Relation (7) is also useful for the proof of some subsequent theorems. Relations (6) and (7) are very important for the realization of delta multipliers.

To reduce the complexity of some formulas to be used later, the following functions are defined

$$\zeta(t) = \delta \sum_{\kappa = -\infty}^{n} (G_\kappa - G_{\kappa-1}) \tag{9}$$

$$i(t) = \delta \sum_{\kappa = -\infty}^{n} I_\kappa \tag{10}$$

where $\{I_n\}$ is the zero signal sequence which is defined by

$$I_n = -I_{n-1}, \qquad n = \ldots, -1, 0, 1, \ldots \tag{11}$$

and

$$\tau(t) = \delta \cdot \sum_{\kappa = -\infty}^{n} (P_\kappa - P_{\kappa - 1}) \tag{12}$$

where

$$nT \leqslant t < (n+1)T.$$

Relations (9), (10) and (12) can be written, taking into consideration (8) and (11), as

$$\zeta(t) = \delta \cdot \sum_{i=1}^{q} 2^{-i}(C_n^{(i)} - \gamma_i) \tag{13}$$

$$i(t) = 2^{-1}\delta \cdot (I_n - \gamma_0) \tag{14}$$

$$\tau(t) = \delta \cdot (P_n - \gamma_P) \tag{15}$$

$$nT \leqslant t < (n+1)T$$

and γ_i, $i = 1, 2, \ldots, q$, γ_0 and γ_P are constants equal to the initial values of $C_n^{(i)}$, $i = 1, 2, \ldots, q$, I_n and P_n. Therefore, each constant takes the value -1 or $+1$.

3.1 The Basic Delta Multiplier

For the sake of completeness and for reason of comparison of the proposed new delta multipliers, a reconsideration of the first delta multiplier presented in an earlier paper[10] is considered necessary.

Let $\{X_n\}$ be the d.s. to be multiplied by the constant a where

$$a = \sum_{i=1}^{q} a_i 2^{-i} \tag{16}$$

$$a_i = 0 \text{ or } 1, \quad i = 1, 2, \ldots, q^{-1}$$

$$a_q = 1.$$

It will be proved that if in (7) $Z_n^{(i)}$ and W_n are replaced by

$$Z_n^{(i)} = \begin{cases} X_n & \text{if } a_i = 1 \\ I_n & \text{if } a_i = 0 \end{cases} \tag{17}$$

$$i = 1, 2, \ldots, q$$

and

$$W_n = I_n \tag{18}$$

then $\{P_n\}$ becomes a d.s. of the signal $ax(t)$ plus an error $\sigma(t)$.

Proof: Equation (17) can be written

$$Z_n^{(i)} = a_i X_n + (1 - a_i)I_n \tag{19}$$

$$i = 1, 2, \ldots, q.$$

Putting in (7) the values of $Z_n^{(i)}$ and W_n from (18), (19) and taking into account (16) we obtain,

$$P_n = aX_n + (1-a)I_n - (G_n - G_{n-1}) \tag{20}$$

It becomes obvious from (20) that the decoded signal $p(t)$ of $\{P_n\}$ is

$$p(t) = ax(t) + \sigma(t) \tag{21}$$

where $\sigma(t)$ is the error, and

$$\sigma(t) = (1-a)i(t) - \zeta(t) \tag{22}$$

and $\zeta(t)$ and $i(t)$ are obtained from the relations (13) and (14).

The maximum magnitude of the error $\sigma(t)$ is $(3 - a - 2^{-q+1})\delta$ and it is found as follows: let us consider the extreme case that $\sigma(t)$ is always positive in which case, from (13), (14) and (22), the following relation holds

$$-\gamma_0 = \gamma_1 = \gamma_2 = \ldots = \gamma_q = 1 \tag{23}$$

then, $\sigma(t)$ takes a finite number of values in the interval

$$0 \leqslant \sigma(t) \leqslant (3 - a - 2^{-q+1})\delta. \tag{24}$$

So, $\{P_n\}$ is the d.s. of $ax(t)$ plus the error $\sigma(t)$.

The realization of the multiplier becomes straightforward through the relations (6), (17), and (18).

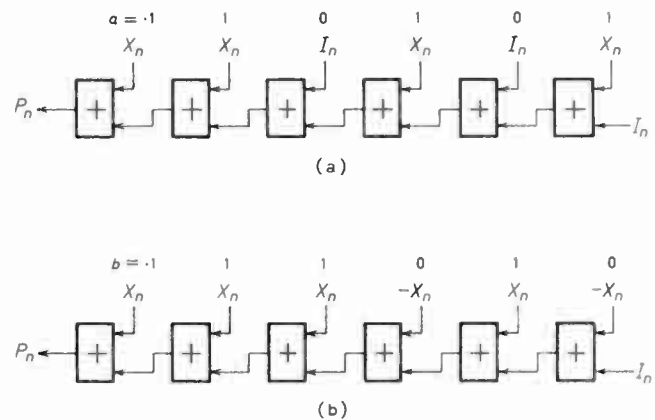The realized multiplier is shown in Fig. 2(a) for $a = (110101)_2$.

Fig. 2. Non-recursive delta multipliers. (a) Basic form for $a = (.110101)_2$; (b) modified form for the same a.

3.2 The Modified Delta Multiplier

The realization of this multiplier was achieved by using another binary constant b instead of a, derived from a through the transformation

$$b = 2^{-1}(1 + a - 2^{-q}) \tag{25}$$

with

$$b = \sum_{i=1}^{q} b_i 2^{-i} \tag{26}$$

The length of the binary constant b is always q bits even if some of the l.s.b.s are zero.

It will be shown now that if in (7), $Z_n^{(i)}$ and W_n are substituted by

$$Z_n^{(i)} = \begin{cases} X_n & \text{if } b_i = 1 \\ -X_n & \text{if } b_i = 0 \end{cases} \tag{27}$$

$$i = 1, 2, \ldots, q$$

and

$$W_n = I_n. \tag{28}$$

Then, $\{P_n\}$ is a d.s. of the product $ax(t)$ plus an error $\sigma(t)$.

Proof: Equation (27) can be written

$$Z_n^{(i)} = (2b_i - 1)X_n, \quad i = 1, 2, \ldots, q \tag{29}$$

by substituting W_n and $Z_n^{(i)}$ from (28) and (29) in (7) and taking into account (25) and (26), the following relation is obtained,

$$P_n = aX_n + 2^{-q}I_n - (G_n - G_{n-1}). \tag{30}$$

From (30), the corresponding decoded signal $p(t)$ is the same as in (21) except for the error $\sigma(t)$ which is given by

$$\sigma(t) = 2^{-q}i(t) - \zeta(t). \tag{31}$$

This error, under the same assumption as in the basic delta multiplier, satisfies the inequality:

$$0 \leqslant \sigma(t) \leqslant (2 - 2^{-q})\delta \tag{32}$$

with a maximum value $(2 - 2^{-q})\delta$ which is clearly smaller than the one in the basic multiplier.

The realization of this multiplier becomes straightforward through the relations (6), (27) and (28).

The realized multiplier is shown in Fig. 2(b) with $b = (.111010)_2$ which corresponds to the same a as in Fig. 2(a).

3.3 Type 1 Recursive Delta Multiplier

In this case the constant a must be periodic with a period of q bits. For the realization of this multiplier only q delta adders are needed, as will be shown later. For the case of a truncated non-periodic constant, it is possible to approximate it by a suitable periodic one. So, for example, if the binary number .10101001 is to be truncated to five bits, the periodical number .101010 ... with $q = 2$ is a good approximation and two delta adders are sufficient for the realization of the recursive multiplier. Thus by this technique a considerable reduction of the number of delta adders is possible.

Let a be a periodic constant:

$$a = \sum_{i=1}^{\infty} 2^{-i}a_i = \frac{a'}{1 - 2^{-q}} \tag{33}$$

and

$$a' = \sum_{i=1}^{q} 2^{-i}a_i. \tag{34}$$

It will be shown that, if in (7) $Z_n^{(i)}$ and W_n are substituted by

$$Z_n^{(i)} = \begin{cases} X_n & \text{if } a_i = 1 \\ I_n & \text{if } a_i = 0 \end{cases} \tag{35}$$

$$i = 1, 2, \ldots, q$$

and

$$W_n = P_{n-1} \tag{36}$$

then, $\{P_n\}$ will be a d.s. of the product $ax(t)$ plus an error $\sigma(t)$.

Proof: Equation (35) can be written in the same form as (19). By substituting (19) and (36) in (7) and taking

into account (33) and (34) P_n becomes

$$P_n = aX_n + (1-a)I_n - \frac{2^{-q}}{1 - 2^{-q}}$$
$$\times (P_n - P_{n-1}) - \frac{1}{1 - 2^{-q}}(G_n - G_{n-1}). \tag{37}$$

From (37) it can be seen that the decoded signal $p(t)$ is given again by the relation (21) except for the error which is given by

$$\sigma(t) = (1-a)i(t) - \frac{2^{-q}}{1 - 2^{-q}}\tau(t) - \frac{1}{1 - 2^{-q}}\zeta(t) \tag{38}$$

when $\zeta(t)$, $i(t)$ and $\tau(t)$ are given by (13), (14), and (15). In the extreme case that $\sigma(t)$ is always positive, $\sigma(t)$ satisfies the inequality:

$$0 \leqslant \sigma(t) < \left(3 - a + \frac{2^{-q+1}}{1 - 2^{-q}}\right)\delta. \tag{39}$$

This error, $\sigma(t)$ has the maximum value,

$$\left(3 - a + \frac{2^{-q+1}}{1 - 2^{-q}}\right)\delta$$

being a little larger than the error in the basic multiplier.
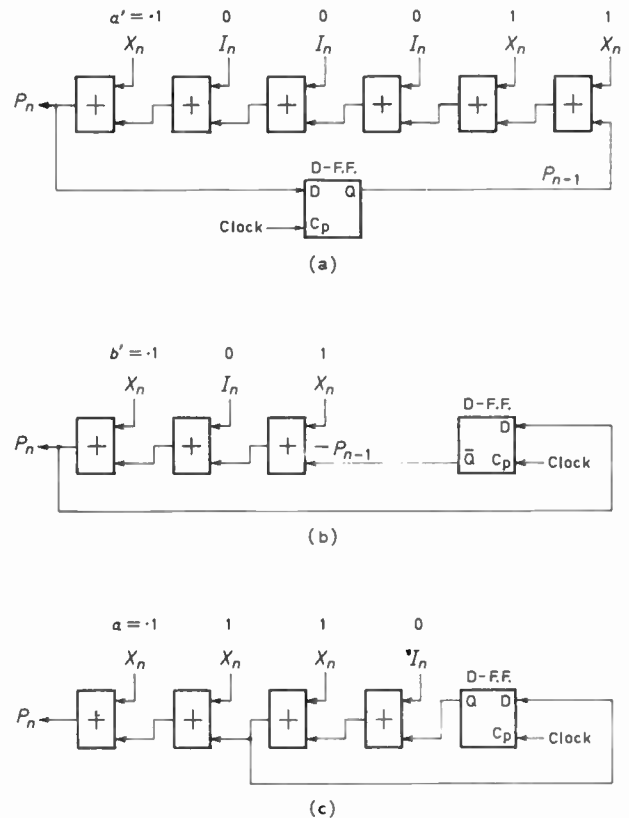

Fig. 3. Recursive delta multipliers.
(a) Type 1 for $a = (.100011100011\ldots)_2$
(b) Type 2 for the same a
(c) Type 3 for $a = (.11101010\ldots)_2$

The realization of the above multiplier is straightforward taking into account relations (6), (35) and (36).

In Fig. 3(a) such a multiplier is shown with

$$a = (.100011100011\ldots)_2$$

with $q = \sigma$ and $a' = (.100011)_2$.

3.4 Type 2 Recursive Delta Multiplier

In this case, the constant a is an even periodic number as in (33) and (34), but with $q = 2q'$, and the number of the q' l.s.b.s of a' is the complement of the q' m.s.b.s. Then, as it will be proved, it is possible to realize a multiplier comprising the half number of adders with respect to type 1 multiplier, and with a smaller error $\sigma(t)$. In this case, whatever was said in Section 3.3 holds for the truncated constants case, but with the possibility of further reducing the number of adders.

The constant a' can be rewritten

$$a' = a'' + (1 - 2^{-q'} - a'')2^{-q'} \qquad (40)$$

where

$$a'' = \sum_{i=1}^{q'} a_i 2^{-i} < 1 - 2^{-q'}. \qquad (41)$$

From (33), (34) and (40)

$$a = \frac{a'' + 2^{-q'}}{1 + 2^{-q'}} \qquad (42)$$

we define the number b' as follows

$$b' = \sum_{i=1}^{q'} b_i' 2^{-i} = a'' + 2^{-q'}. \qquad (43)$$

It will be shown that if in (7), $Z_n^{(i)}$ and W_n are substituted by

$$Z_n^{(i)} = \begin{cases} X_n & \text{if } b_i' = 1 \\ I_n & \text{if } b_i' = 0 \end{cases} \qquad (44)$$

$$i = 1, 2, \ldots, q'$$

where X_n the input d.s. and

$$W_n = -P_{n-1}. \qquad (45)$$

Then, $\{P_n\}$ is a d.s. of the product, $ax(t)$ plus an error $\sigma(t)$.

Proof: Relation (44) can be written

$$Z_n^{(i)} = b_i' X_n + (1 - b_i') I_n \qquad (46)$$

$i = 1, 2, \ldots, q'$.

Substituting (46) and (47) in (7) and taking into account (33), (34) and (43), P_n becomes,

$$P_n = aX_n + \left(\frac{1 - 2^{-q'}}{1 + 2^{-q'}} - a\right) I_n + \frac{2^{-q'}}{1 + 2^{-q'}} (P_n - P_{n-1}) -$$

$$- \frac{1}{1 + 2^{-q'}} (G_n - G_{n-1}). \qquad (47)$$

From (47), it can be seen that the decoded signal is

given again by (21), but with an error given by

$$\sigma(t) = \left(\frac{1 - 2^{-q'}}{1 + 2^{-q'}} - a\right) i(t)$$

$$+ \frac{2^{-q'}}{1 + 2^{-q'}} \tau(t) - \frac{1}{1 + 2^{-q}} \zeta(t). \qquad (48)$$

Here again for positive $\sigma(t)$ the inequality holds

$$0 \leqslant \sigma(t) \leqslant \left(\frac{3 - 2^{-q'}}{1 + 2^{-q'}} - a\right) \delta \qquad (49)$$

from which it can be seen that the maximum error is

$$\left(\frac{3 - 2^{-q'}}{1 + 2^{-q}} - a\right) \delta$$

which is smaller than that in type 1 and basic multiplier.

The realization of this multiplier can be done considering the relation (6), (44), and (45).

Such a multiplier is shown in Fig. 3(b) with the same constant a as in Fig. 3(a) and for $b' = (.101)_2$.

3.5 Type 3 Recursive Delta Multiplier

In this case the constant a consists out of two parts, one not periodic of q_1 bits and one periodic of type 1 or 2 of q_2 bits. It becomes obvious that it is possible to realize a partially recursive multiplier with $q_1 + q_2$ adders. This can be demonstrated with the following example.

Let

$$a = (.11101010\ldots)_2,$$

which can be written as the sum of one periodic and one non-periodic parts, or

$$a = (.11)_2 + 2^{-2}.(.1010\ldots)_2$$

leading to the realization of Fig. 3(c). It is easy to see that the error, $\sigma(t)$ is about the same as in the case of the basic delta multiplier.

From what has been presented so far it can be said that the three recursive delta multipliers considered here increase considerably the possibility of reducing the number of adders in the realization of multipliers according to the form of the constant and the required accuracy.

3.6 Remarks

From relations (22), (31), (38), and (48), the error $\sigma(t)$ is given, for each multiplier, by a polynomial function, the variables of which are the functions $\zeta(t)$, $i(t)$, and $\tau(t)$. These functions, however, include the constant terms

$$\delta \sum_{i=1}^{q} 2^{-i} \gamma_i, \quad -2^{-1} \delta \gamma_0 \quad \text{and} \quad -\delta \gamma_p$$

respectively, according to relations (13), (14), and (15). Consequently, $\sigma(t)$ always includes a constant term which expresses the offset error. This offset error can become even zero by proper presetting of the original

values of γ_i, $i = 1, 2, \ldots, q$ and γ_p. Assuming that the constant term in $\sigma(t)$ is zero, the maximum error, $|\sigma(t)|_{max}$, is now equal to the half of the maximum error given by relations (24), (32), (39), and (49) for the various types of multipliers. More specifically, the following conclusions can be drawn for $\sigma(t)$.

(1) For the basic delta multiplier the following relation holds:

$$|\sigma(t)| \leqslant \tfrac{1}{2}(3 - a - 2^{-q+1})\delta. \tag{50}$$

From equation (50) above it can be seen that the maximum error depends on the value of constant a and on the number of its q significant bits and the following relation holds:

$$\tfrac{3}{4}\delta \leqslant |\sigma(t)|_{max} < \tfrac{3}{2}\delta \tag{51}$$

where the maximum value occurs for $a \to 0$ and $q \to \infty$ and the minimum value for $a = \tfrac{1}{2}$ and $q = 1$.

(2) For the modified delta multiplier the following relation holds:

$$|\sigma(t)| \leqslant \tfrac{1}{2}(2 - 2^{-q})\delta. \tag{52}$$

The maximum error now depends only on the number of the q significant bits of the constant a and it holds that

$$\tfrac{3}{4}\delta \leqslant |\sigma(t)|_{max} < \delta \tag{53}$$

where the maximum value occurs for $q \to \infty$ and the minimum for $q = 1$.

(3) For the type-1 recursive multiplier the following relation holds:

$$|\sigma(t)| \leqslant \frac{1}{2}\left(3 - a + \frac{2^{-q+1}}{1 - 2^{-q}}\right)\delta \tag{54}$$

where $q \geqslant 2$, because when $q = 1$, then $a = 1$ or $a = 0$ (relations (33) and (34)) and the synthesis of a multiplier is meaningless. The maximum error now depends, according to (54), on the values of both the constant a and the period q and it holds that

$$\delta < |\sigma(t)|_{max} \leqslant \tfrac{5}{3}\delta \tag{55}$$

where the maximum value occurs when $a = \tfrac{1}{3}$ and $q = 2$ and the minimum value occurs when $a \to 1$ and $q \to \infty$.

(4) For the type-2 recursive multiplier the following relation holds:

$$|\sigma(t)| \leqslant \frac{1}{2}\left(\frac{3 - 2^{-q'}}{1 + 2^{-q'}} - a\right)\delta. \tag{56}$$

From (56) above it is inferred that the maximum error depends again on the values of a and q' and the following relation holds:

$$\tfrac{2}{3}\delta \leqslant |\sigma(t)|_{max} < \tfrac{3}{2}\delta \tag{57}$$

where the maximum value occurs for $a \to 0$ and $q' \to \infty$ and the minimum for $a = \tfrac{1}{3}$ and $q' = 1$.

A comparison of the relations of this Section leads to the conclusion that the proposed modified delta multiplier introduces the smallest error. This reduced error is due to the fact that in applying the method for the realization of the multiplier, the sequences $\{Z_n^{(i)}\}$, $i = 1, 2, \ldots, q$, in relation (6) are substituted by $\{X_n\}$ or $\{-X_n\}$ and never by the auxiliary sequence $\{I_n\}$, which always introduces its own error. On the other hand, although the recursive delta multipliers are realized with considerably fewer delta adders, they introduce greater error compared to that introduced by the modified type. It is, however, possible to reduce this error even in this case if the method of realizing the modified delta multipliers is also applied for the synthesis of the recursive delta multipliers. For such a case, the following relations hold for the type-1 recursive delta multiplier:

$$|\sigma(t)| \leqslant \frac{1}{1 - 2^{-q}}\delta \tag{58}$$

and

$$\delta < |\sigma(t)|_{max} \leqslant \tfrac{4}{3}\delta \tag{59}$$

while the following relations are valid for the type-2 recursive delta multipliers,

$$|\sigma(t)| \leqslant \frac{1}{1 + 2^{-q}}\delta \tag{60}$$

and

$$\tfrac{2}{3}\delta \leqslant |\sigma(t)|_{max} < \delta. \tag{61}$$

From the above analysis it is clear that a multiplier with the constant a given can be selected which combines both the least number of delta adders used and the smallest introduced error.

4 Interconnected Delta Multiplier

In the realization of digital filters, where the addition of several output d.s.s from the delta multipliers is necessary, the scaling down caused by the delta adders becomes a problem. Some methods for partial correction of the introduced scaling down have been already proposed.[10] The use of delta doublers to compensate for this scaling down has been proposed,[12] but this method increases the complexity and cost of the multipliers and introduces additional error. With the interconnected delta multiplier proposed here, the number of delta doublers is markedly reduced and in some cases it becomes zero. A realization method of such a multiplier has been suggested,[8] but it has limited uses because of the constraints imposed upon the form of the constants in contrast to the present method, which is applicable to any case.

The output $\{Y_n\}$ of the adder of a digital filter comprising multipliers is given by

$$Y_n = \sum_{\kappa=0}^{v-1} a^{(\kappa)} X_{n-\kappa m} \qquad (62)$$

where $a^{(\kappa)}$, $\kappa = 0, 1, \ldots, v-1$, are the coefficients of the filter, $\{X_{n-\kappa m}\}$ is the output sequence of the kth shift register and m is the number of stages of each shift register. The coefficients are here binary numbers of the form

$$a^{(\kappa)} = \sum_{i=1}^{q} a_i^{(\kappa)} 2^{-i}, \quad \kappa = 0, 1, \ldots, v-1 \qquad (63)$$

where

$$a_i^{(\kappa)} = 1 \text{ or } 0, \quad i = 1, 2, \ldots, q.$$

Relation (62), in conjunction with (63) can be written in the form

$$Y_n = \sum_{i=1}^{q} 2^{-i} \left(\sum_{\kappa=0}^{v-1} a_i^{(\kappa)} X_{n-\kappa m} \right). \qquad (64)$$

Relation (64) can also be written as

$$Y_n = \left(\left(\ldots \left(\left(\sum_{\kappa=0}^{v-1} a_q^{(\kappa)} X_{n-\kappa m} \right) 2^{-1} + \right. \right. \right.$$
$$\left. + \sum_{\kappa=0}^{v-1} a_{q-1}^{(\kappa)} X_{n-\kappa m} \right) 2^{-1} + \ldots \right) 2^{-1} +$$
$$\left. + \sum_{\kappa=0}^{v-1} a_1^{(\kappa)} X_{n-\kappa m} \right) 2^{-1}. \qquad (65)$$

It now results from relation (65) that Y_n can be found with step-by-step addition operations. More specifically, if $S^{(i)}$ is the sum at the jth step, then

$$S_n^{(i)} = \left(S_n^{(i-1)} + \sum_{\kappa=0}^{v-1} a_{q-i+1}^{(\kappa)} X_{n-\kappa m} \right) 2^{-1} \qquad (66)$$

where $S_n^{(0)} = 0$ and $S_n^{(q)} = Y_n$.

In (66), the coefficients $a_{q-i+1}^{(\kappa)}$, $\kappa = 0, 1, \ldots, v-1$ at the jth step represent the bits of the same order, $(q-i+1)$, of the coefficients of the filter and are valued 0 or 1. Thus, the sum

$$\sum_{\kappa=0}^{v-1} a_{q-i+1}^{(\kappa)} X_{n-\kappa m}$$

is a simple sum of those sequences $\{X_{n-\kappa m}\}$, $\kappa = 0, 1, \ldots, v-1$ for which the relation $a_{q-i+1}^{(\kappa)} = 1$ is satisfied.

A special method of performing the operation indicated in (66) is given now, in order to make use of the delta adders. Thus, if the number of the sequences to be added is even, they are separated in pairs. If their number is odd the zero signal sequence is added so that their number becomes even again. Then the sum or specifically the half sum, due to the factor 2^{-1} in (66), of each pair, is obtained. The sequences of these half sums are transferred as terms to be added to the next step and so on. Thus, the sequences $\{S_n^{(i)}\}$, $i = 1, 2, \ldots, q$, are now considered as polynomials. The terms of these polynomials are the sequences of the partial half sums, which result from the additions described above.

This analysis leads to the following steps for synthesizing an interconnected delta multiplier, taking, of course, into account the form (63) of the filter coefficients.

(1) For all bits of the coefficients with $i = q$ (l.s.b.), with value 1 the corresponding sequences are added through delta adders in pairs. If the number of 1's is odd the auxiliary zero signal sequence $\{I_n\}$ is added.

(2) The same procedure is adopted for the bits of the coefficients with $i = q-1$, but the output sequences of the adders from the previous step are also included.

(3) The same procedure continues until the m.s.b.s of each coefficient are reached, that is, until $i = 1$.

(4) If at the last step only one adder is necessary the procedure is considered completed and there will be no scaling down. If, however, several adders are required, the procedure continues until, finally, only one adder is necessary. In this latter case the use of doublers becomes necessary.[18] The number of the required doublers is equal to the number of the additional steps.

In applying the above procedure, it is useful to examine whether there are pairs of sequences which appear as addents in more than one step. Only one delta adder is required for such a pair. In this case, the output of this adder is considered as the sequence of the half sum of the sequences of the pair for all steps in which it appears.

It has been assumed up to now that the relation $0 \leqslant a^{(\kappa)} \leqslant 1$, $\kappa = 0, 1, \ldots, v-1$ holds. In realizing, however, various types of digital filters, multiplication coefficients having values greater than unity are often required. The procedure described above can be applied even in such cases as follows. Let $a^{(p)}$, $0 \leqslant p \leqslant v-1$, be the coefficient of the filter having the greatest value and that the relation $2^{\lambda-1} < a^{(p)} \leqslant 2^{\lambda}$, $\lambda = 1, 2, \ldots$, holds. The numbers $a^{(\kappa)} 2^{-\lambda}$, $\kappa = 0, 1, \ldots$, are taken as the new coefficients and the same procedure for the determination of the interconnected delta multiplier is applied again with the addition of λ delta doublers in cascade at the output of the multiplier.[12]

The case of negative coefficients is handled by taking the absolute values and inverting the corresponding sequences.

The method has been used for the realization of two second-order Butterworth filters,[13,14] one recursive and one non-recursive with the same cut-off frequency, $f_0 = 100 \text{ Hz}$, and p.c.m. sampling frequency $f_s = 1 \text{ kHz}$.

For the non-recursive filter the shift registers were of 128 bits each and the clock frequency was $f_c = 128 f_s = 128 \text{ kHz}$.
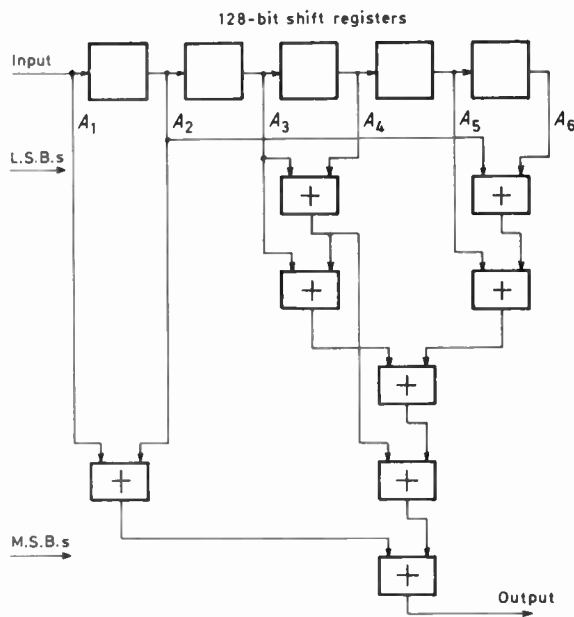
For the recursive filter, two shift registers were used,

Fig. 4. Second-order non-recursive Butterworth delta digital filter

Fig. 6. Second-order recursive Butterworth delta digital filter.

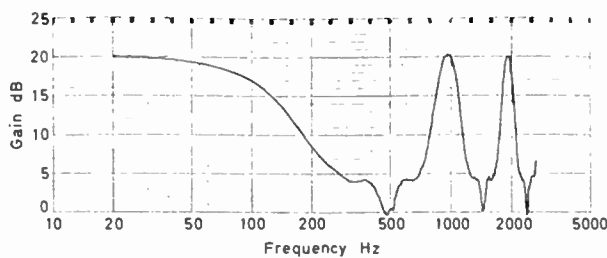Fig. 5. Output response of the d.f. shown in Fig. 4.

Fig. 7. Output response of the d.f. shown in Fig. 6.

one of 128 bits and the other with two more bits, that is of 130 bits, because the delta doubler which was used introduced a delay of two bits. The clock frequency was $f_c = 130 f_s = 130\,\text{kHz}$.

The coefficients of the filters were rounded off to 5 bits and for the non-recursive case were:

$$A_0 = 0, \quad A_1 = .01000, \quad A_2 = .01001, \quad A_3 = .00111,$$
$$A_4 = .00101, \quad A_5 = .00010, \quad A_6 = .00001$$

and for the recursive case:

$$A_0 = 0, \quad A_1 = .01000,$$
$$B_1 = -1.00101, \quad B_2 = .01101.$$

If the filters were realized with separate multipliers according to the conventional method, then two delta doublers would be required for each of the examples given above for elimination of the scaling down. It is therefore evident that the interconnected delta multipliers are superior for the realization of digital filters. Furthermore, the realization of filters by means of interconnected delta multipliers instead of separate multipliers requires less adders and, consequently, introduces smaller total error.
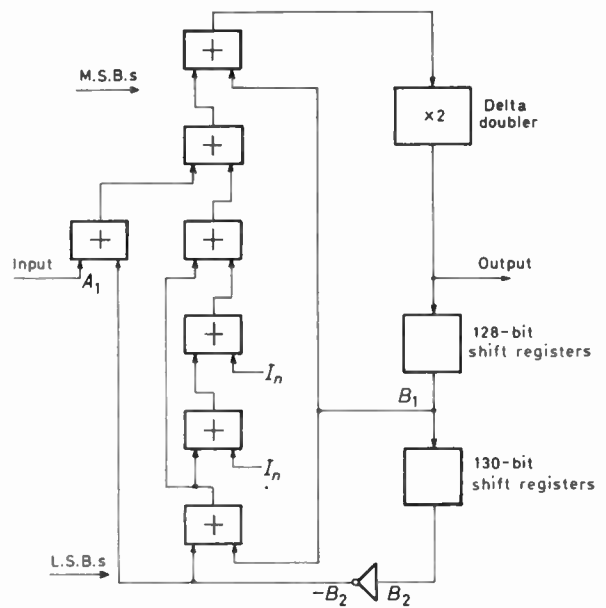
Figures 5 and 7 show the unfiltered response curves of the circuits shown in Figs 4 and 6 respectively. The higher noise appearing in the curve is due to the additional noise introduced by the delta doubler as well as to the recursive character of the filter of Fig. 6.

The experimental work has shown that if the d.m. encoder is an exponential one having a step magnitude in idling state equal to that of the above linear d.m. encoder, the filters yield the same results.

The circuit of the delta doubler is given in Fig. 8.[12] The part above the dotted line constitutes the simple delta doubler, the output $\{Y_n\}$ of which is a d.s. of the double amplitude input signal $\{X_n\}$, whereas both parts constitute an improved doubler. In this case clock-2 is the clock of the system and drives only the delta adder DA-3 and D-flip-flop-2, while clock-1 is of double frequency. The output $\{Y'_n\}$ gives a decoded signal with much reduced error. This improved version of the doubler was used in the recursive filter of Fig. 6.

5 Conclusions
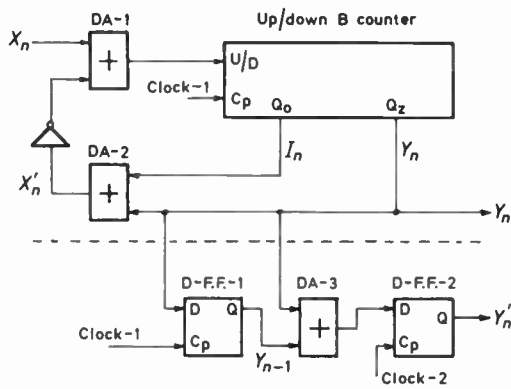The new recursive and non-recursive delta multipliers proposed here extend considerably the possibilities of

Fig. 8. Delta doubler.

6 References

1 Steel, R., 'Delta Modulation Systems' (Pentech Press, London, 1975).
2 Goodman, D. J., 'The application of delta modulation to analog-to-p.c.m. encoding', *Bell Syst. Tech. J.*, **48**, no. 12, pp. 321–42, February 1968.
3 Peled, A. and Liu, B., 'A new approach to the realization of nonrecursive digital filters', *IEEE Trans on Audio and Electro-acoustics*, **AU-21**, no. 6, pp. 477–84, December 1973.
4 Lockhart, G. B., 'A recursive section for filtering delta modulated signals', Proc. Florence Conference on Digital Signal Processing, September 1975.
5 Lockhart, G. B., 'Digital encoding and filtering using delta modulation', *The Radio and Electronic Engineer*, **42**, no. 12, pp. 547–51, December 1972.
6 Franks, L. E., 'Hybrid implementation of digital filters', IEEE Circuit Design Conference, London, July 1974.
7 Lo Cicero, J. L., Schiling, D. L. and Garodnick, J., 'Direct arithmetic processing of delta modulation encoded signals', National Telemetry Conference, pp. 392–7, 1974.
8 Engel, L. J. and Steenaart, W., 'Digital summation of delta modulation signals', Proc. Canadian Communication and Power Conference, Montreal, 1976.
9 Lockhart, G. B., 'Implementation of delta modulators for digital inputs, *IEEE Trans on Acoustics, Speech and Signal Processing*, **ASSP-22**, no. 6, pp. 453–6, December 1974.
10 Kouvaras, N., 'Operations of delta modulated signals and their application in the realization of digital filters', *The Radio and Electronic Engineer*, **48**, no. 9, pp. 431–8, September 1978.
11 Kouvaras, N., 'Delta-modulation/p.c.m. converter', *Electronics Letters*, **14**, no. 20, pp. 660–2, September 1978.
12 Kouvaras, N., 'A special purpose delta multiplier', *The Radio and Electronic Engineer*, **50**, no. 4, pp. 156–7, April 1980.
13 Temes, G. C. and Mitra, S. K., 'Modern Filter Theory and Design' (John Wiley and Sons, New York, 1973).
14 Bogner, R. E. and Constantinides, A. C., 'Introduction to Digital Filtering' (Wiley, New York, 1975).

delta signal processing hardware. With the new non-recursive multiplier the error is reduced, while with the recursive ones a large reduction of the number of adders needed for their realization becomes feasible.

The recursive multiplier can be realized for periodic as well as for non-periodic constants that can be approximated by periodic ones. Among them the type-2 recursive multiplier produces the smallest error.

The interconnected delta multipliers on the other hand, in connection with the delta doublers, compensate for the scaling down of the output at the summing points of the delta digital filters, reducing at the same time the necessary number of delta adders.

Furthermore, by proper choice of the variables in equation (7), new types of delta multipliers can be developed with special characteristics.

Book Review

Early Radio Wave Detectors

V. J. PHILLIPS (*University College of Swansea*). Peter Peregrinus, Stevenage, 1980. 14 × 22 cm. xv + 223 pages. £18.00 UK; $42.75 Americas; £19 elsewhere.

CONTENTS: Improved spark-gap detectors. Coherers. Electrolytic detectors. Magnetic detectors. Thin-film and capillary detectors. Thermal detectors. Tickers, tone-wheels and heterodynes. Miscellaneous detectors. And so to the modern era. Select bibliography.

It will probably come as a surprise to most radio and electronic engineers—even to those already interested in the history of radio—that so many different ideas were tried out for the detection of radio waves in the first few decades of radio from, say, 1880 to the beginning of the thermionic valve in 1904-6. Dr. Phillips describes and illustrates nearly two hundred detectors, many of which exploited little-known, and even less-understood, physical principles. He has attempted to explain how they worked, and has undertaken some experimental work himself to this end. It is a fascinating story, well told in an informal manner which makes the book very easy to read; yet it is, for all that, a scholarly work based on thorough research and with its sources properly referenced.

The longest chapter is, quite reasonably, that on coherers, and here we follow the variations in design of the devices which all exploited essentially the same basic principle; i.e. the change of resistance of loose contacts when subjected to a r.f. signal. The next longest is on magnetic detectors—the length again justified as they were so extensively and successfully used; but here there is a difference—numerous different underlying principles were exploited, and it is very difficult to understand how some of the devices worked. It is important to realize, as Dr. Phillips explains, that all these early devices were intended strictly to *detect* the presence of a signal; the extension of the term 'detector' to what were really demodulators came later.

Pity about the price—but recommended all the same.

D. G. TUCKER

Contributors to this issue

John Flower served an apprenticeship as a marine engine fitter and later, while working for the Naval Education Department, was awarded a Treasury Bursary enabling him to study at Queen Mary College where he gained a B.Sc.(Eng) in electrical engineering in 1965. After a further period with the Navy he became a Lecturer in Electrical Engineering at Queen Mary College and obtained a Ph.D. in 1969 for work on electric network theory. From 1969 to 79 he was in the School of Engineering, University of Sussex, firstly as a Lecturer and then as a Reader in Control Engineering. The academic year 1975–76 was spent as a Visiting Professor of Control Engineering, University of Witwatersrand. In October 1979 he became Professor of Engineering Science at the University of Exeter. Most of his research work in recent years has been devoted to the application of control, digital-processing techniques and instrumentation to systems having a marine flavour.

Simon Forge studied control engineering at the University of Sussex, obtaining his B.Sc. in 1968, followed by an M.Sc. two years later. His study for the Ph.D., which he was awarded in 1978, was devoted to aspects of system identification by digital methods. He has worked for Decca Navigator on R&D for aids to navigation, Sira on evaluation of process control equipment and for Honeywell-Bull, France, on design of a medium-level computer. Dr Forge joined Preece, Cardew and Rider, consulting engineers at Brighton in 1979 and is at present engaged on various projects involving digital intelligence such as radar data processing and minis/micros for control and communications. Concurrently, he is a Visiting Research Fellow at the University of Sussex, engaged on various signal processing problems.

'Nick' Kouvaras graduated first from the Athens Higher School of Electronics Engineering, after which he attended the Faculty of Mathematics of the University of Athens and obtained his B.Sc. degree in mathematics. In 1960 he joined the Electronics Department of the Demokritos Nuclear Research Centre, and he has done research and development work on digital systems which has led to several publications including previous papers in this Journal on delta modulation; he is also involved in a programme of work on digital processing systems for speech.

Peter Patrick was with the British Post Office from 1972 to 1977 and during this time he gained a scholarship to Loughborough University of Technology, where he received a first class honours B.Sc. in electronic and electrical engineering in 1976. He returned to the Post Office for a year and worked on frequency division multiplexing equipment at a trunk repeater station. In 1977 he returned to Loughborough University where he is currently undertaking research for a Ph.D. degree on the enhancement of band limited speech signals; this work is supported by the Science Research Council in collaboration with the Post Office Research Centre at Martlesham, Ipswich. His current interests include speech signal processing and telephone switching systems.

Raymond Steele was an indentured apprenticed radio engineer before going to Durham University, where he attained a bachelor's degree in electrical engineering in 1959. After research and development posts with E. K. Cole, Cossor Radar and Electronics, and the Marconi Company, he joined the lecturing staff at the Royal Naval College, Greenwich. Here he lectured on Telecommunications to the NATO and the External London University degree courses. As a Senior Lecturer in the Electronic and Electrical Engineering Department of Loughborough University of Technology, he directed a research group in digital encoding of speech and television signals. In 1975 he received his Ph.D. Dr. Steele was a consultant to the Acoustics Research Department at Bell Laboratories in the summer of 1975, 1977 and 1978 and in 1979 he joined the Company's Communications Methods Research Department. He is the author of the book, 'Delta Modulation Systems', has written over 50 papers relating to digital encoding and signal processing, and was awarded the Institution's Marconi Premium for 1978.

Costas Xydeas received his first degree in electronic engineering from Vranas Higher School of Electronics, Athens in 1972 and the M.Sc. and Ph.D. degree in electrical engineering from Loughborough University of Technology in 1974 and 1978 respectively. In 1977 he joined the Department of Electronic and Electrical Engineering of Loughborough University as a Research Fellow and has worked on low-bit rate digitization of speech signals. Dr Xydeas is at present a Lecturer in the Department where he is directing a research group in digital coding and processing of speech signals. His areas of interest include adaptive linear and non-linear prediction, adaptive quantization, low-bit coding of speech, suppression of acoustic noise in speech, enhancement of band-limited speech, and encryption of digitized speech signals.